MODELLING THE DYNAMICS OF PLUNGE MILLING

MODELLING THE DYNAMICS OF PLUNGE MILLING WITH WORKPIECE VIBRATIONS CONSIDERATION

BY

AHMED DAMIR

B.Sc., M.Sc.

A Thesis

Submitted to the School of Graduate Studies

In Partial Fulfillment of the Requirements

For the Degree of

Doctorate of Philosophy

McMaster University

DOCTORATE OF PHILOSOPHY (2010) McMaster University

(Mechanical Engineering) Hamilton, Ontario

TITLE: Modeling the dynamics of plunge milling with workpiece vibrations consideration.

AUTHOR: Ahmed Damir, B.Sc., M.Sc. with degree of Honor (Alexandria University)

SUPERVISOR: Professor M. A. Elbestawi

NUMBER OF PAGES: xv, 137

Abstract

Chatter vibrations in machining processes remain one of the major challenges that face the machining process planners to achieve high productivity and product quality. This is mainly due to its undesirable effect that leads to poor surface finish, low part dimensional accuracy, excessive tool wear and reduced productivity. Therefore, for high performance machining, it is extremely important to predict and model the process stability in order to be able to plan the process prior to machining. This will eliminate the need for trials and errors to select the optimum cutting conditions for each operation.

Plunge milling process is becoming an important rough machining operation for die cavities and aerospace parts. This is due to a higher removal rates when compared to other milling processes. This is mainly attributed to the fact that most of the cutting is performed in the axial direction, so that the process can benefit from the spindle rigidity to achieve higher metal removal rates. However, limited published research has been done to model the dynamics and stability of plunge milling and there is a need to study in depth the stability of this process while considering the effect of some parameters not studied in the literature on the process stability.

A time domain simulation model is developed in this research to study the dynamics of plunge milling process for systems with rigid and flexible workpiece. The model predicts the cutting forces, system vibration and process stability by considering the effect of workpiece and tool dynamics, tool setting errors and tool kinematics on chip area evaluation. The dynamic chip area is evaluated based on the interaction of the insert cutting edges (i.e. main and side edges) with the workpiece geometry determined by the pilot hole and surface left by the previous insert. A horizontal approach was used to model the insert geometry to be able to compute correctly the cutting area used in force prediction. This approach considers the contribution of both main and side edge in the cutting zone and is capable of dealing with any geometric shape of the insert. Mechanistic model is used to compute the cutting forces as a function of the dynamic chip area using instantaneous cutting coefficients for each insert to take into account the uneven chip

thickness removed by each insert as a result of system vibration and tool setting errors. For the case of a flexible workpiece, the dynamics of the workpiece and milling cutter in three directions, lateral and axial directions, as well as the tool torsional vibration, are considered in the model for accurate prediction of forces and stability limits. The variation of workpiece dynamics according to the hole location is considered in the simulation to model the process stability based on the actual system dynamics as a function of hole location. On the other hand, for a rigid workpiece, only the dynamics of the cutter is considered in the simulation.

Experimental cutting tests with single and double were carried out to check the validity of the simulation model for both cases of plunge milling of rigid and flexible workpiece. Experimental validation for single insert showed the ability of the simulation model to simulate the dynamics of plunge milling with single insert as well as the correctness of the cutting force model.

For case of plunge milling with double inserts, good agreement was found between the measured and the predicted cutting forces and vibration signals and power spectra for case of rigid and flexible workpiece. This indicates the ability of the model to accurately predict cutting forces, system vibration and process stability which makes it very reliable and effective to be used for process planning prior to machining. Both experimental and simulation results showed dominance of workpiece dynamics in the axial direction due to its flexibility as compared to the tool axial rigidity for systems with flexible workpiece. On the other hand, chatter behavior was found to occur due to tool lateral modes for case of rigid workpiece.

Acknowledgments

With all gratitude and respect, I would like to thank Dr. Mohamed Elbestawi for his great support, guidance and encouragement throughout this research.

Also, I would like to thank deeply Dr. Eu-Gene Ng for his encouragement and precious advices for technical matters throughout this research.

Special thanks to the members of the committee meeting for their continuing interest and priceless comments that helped me a lot throughout this research.

Many thanks to MMRI team for their support and help throughout the experiments. Special thanks to Warren for his endless support in carrying out the experiments. Deep appreciation goes to Terry for his help throughout the experiments.

I would like to thank my father, Dr. Nasr Damir, for his endless support and his valuable advises which helped me to deepen my thinking and expand my vision. Additionally, my deep gratitude to my family and my wife for their support and understanding.

TABLE OF CONTENT

LIST OF FIGURES

LIST OF TABLES

NOMENCLATURE

Ft, Fn, F	Tangential force, radial force and feed force (N)
T	Torque (Nm)
b	Elemental width of cut (mm)
Δz	Axial element elevation (mm)
R_{inner}	Radius of pilot hole (mm)
Φp	Pitch angle (degrees)
$\Delta\varphi$	Angular step (degree)
K_t, K_n, K_f	Tangential, normal and axial cutting coefficient (N/mm^2)
N	Spindle speed (rpm)
c	Feed per tooth (mm/tooth)
n	Time step index
m	Tooth index
l	Axial element index
n_m	Index of previous insert rotation angle
xt,yt,zt	Tool vibrations in x, y, z direction respectively (m)
θ	Tool vibrations in torsional direction (radian)
xw,yw,zw	Workpiece vibrations in x, y, z directions (m)
F_x, F_y, F_z	Cutting force in x, y, and z directions respectively (N)
e	Radial eccentricity (mm)
R_a	Axial Runout (mm)
r	Radial position of each element (mm)
rv	Radial position of each element considering system vibrations (mm)
Z_{ins}	Axial position of each element (mm)
r_o	Radial position of first element (mm)
Z_o	Axial position of first element (mm)
r_{edge}	Radial coordinate of the insert tip (mm)
Z_{edge}	Axial coordinate of the insert tip (mm)
$\varphi(n)$	Rotational angle (degrees)

h Chip thickness (mm)

β Entering angle

k, M, C Modal Stiffness (N/m), modal mass (Kg) and damping coefficient respectively

X_p, Y_p Position of each element in the x and y directions respectively (mm)

$b_{2\text{-}3}$ Maximum width of cut removed by main cutting edge (mm)

$b_{4\text{-}5}$ Width of cut by side edge (mm)

$h_{4\text{-}5}$ Chip thickness removed by side edge (mm)

Chapter 1: Introduction

Modern manufacturing is mainly characterized by high requirements on accuracy and productivity in an automated flexible manufacturing environment. Increased productivity has been achieved by employing high cutting speeds, feed rates and depth of cuts. However, one of the restrictions limiting large material removal rates and higher productivity is higher tendency of the machine tool to chatter. Chatter is an undesirable phenomenon because of its adverse effect on surface finish, part dimensional accuracy, machine tool elements (e.g. bearings) and tool life. Furthermore, chatter is responsible for reducing the productivity because, in some cases as a solution, metal removal rate has to be lowered until vibration-free performance is obtained. Thus, for high performance machining of precision components made of advanced materials, it is extremely important to adequately plan and control the machining process to ensure a stable operation with minimum vibrations and hence, high productivity. Chatter vibrations are mainly recognized by its characteristic noise associated with cutting marks on the machined surface and by the undulated and dissected chips.

The main characteristics of self excited chatter can be stated as follows:

- The vibration, once started, increases and grows continuously or stabilizes at constant amplitude due to non linearity in the system.
- The chatter frequency is equal or close to the dominant mode of the system.
- There is no external source of excitation; rather there is a steady energy source from which the system generates a periodic force through its vibration.

The modeling of dynamics and stability of machining processes is becoming increasingly important to be able to effectively plan and control the cutting operations to achieve higher productivity and part quality. Most of the efforts done in modeling have focused on selecting the optimum cutting conditions to achieve higher productivity within the stable conditions, and control or suppress the chatter vibration for different cutting parameters by considering the kinematics of each process and different factors that might affect the process stability such as the workpiece deflection.

Recently, the plunge milling operation has become very promising in roughing operations due to its higher productivity compared to conventional milling operations. It is used in automotive and aerospace industries for roughing cavities. However, more effort is required to better model and simulate the dynamics and stability of plunge milling by considering the effect of some parameters on the plunge milling process stability which were not covered by the previous research work.

1.1 Motivations:

- High requirements of accuracy and productivity in manufacturing processes. However, chatter is the major limiting factor to achieve high productivity, surface finish.
- Detrimental effects of chatter vibrations on surface integrity, productivity and tool life. The need for more accurate modeling of the chatter stability limit for plunge milling to accurately plan the cutting process and for more efficient chatter control.
- Plunge milling is a recently used process and it represents a promising process for roughing operations in different applications. However, limited literature has dealt with modeling its dynamics and majority of the published research did not include the effect of side edge cutting and workpiece dynamics in the stability of the process.
- Importance of workpiece dynamics in the stability analysis for machining process especially for flexible workpiece. Most studies in plunge milling have assumed a rigid workpiece and they simply focused on the dynamics of the cutting tool in the stability analysis. However, in practice, the workpiece may experience vibration as a result of the applied cutting force by the cutting tool. This deformation,

accompanied by tool deflection, changes the chip thickness and affects the stability limits of the cutting process.

1.2 Research Objectives

- Building a time domain simulation model to study the dynamics of the plunge milling process with a new approach to model the cutting area. The model should be capable of predicting cutting forces, system vibrations and process stability as a function of system dynamics, cutting conditions, insert geometry and tool setting errors.
- The model should include the effect of side edge as well as the main cutting edge to accurately model the actual cutting area during the plunge milling operation considering the effect of workpiece dynamics in the simulation model for accurate prediction of cutting forces and stability limits of the plunge milling process. This allows a better modeling of the process for cases where the workpiece dynamics is dominant (i.e. flexible workpiece).
- Consider the variation of workpiece dynamics according to the hole location in the simulation model to model the process dynamics based on the actual system dynamics.
- Accurate determination of cutting coefficient for better prediction of cutting force and hence, better modeling of plunge milling. Therefore, Full immersion plunge milling with a single insert was used to determine the cutting coefficients to realistically simulate the actual cutting action and avoid the influence of tool setting errors on the determination of the cutting coefficients. Considering the use of instantaneous cutting force coefficients for each insert based on the actual chip thickness cut by each insert and not the nominal feed value for better prediction of cutting forces and process stability.

1.3 Thesis Layout

This thesis contains 8 chapters. Each chapter is a step forward towards realizing the research objective stated in the previous section. The thesis outline is as follows:

- Chapter I briefly introduced the research topic and highlighted the motivation, the objectives and the contributions of the research.
- Chapter II presents a detailed review of the literature related to the chatter analysis, the different approaches used in modeling the dynamics and stability of machining operations, the available dynamic and force models for machining thin-walled structures and the work done to model the dynamics and stability of plunge milling process.
- Chapter III describes the proposed time domain simulation model used in the research. It highlights the modeling of the contribution of side edge into cutting actions as well as the parameters affecting its involvement in cutting.
- Chapter IV explains the experimental setup and the experimental design and parameters used in the experimental validation of the model.
- Chapter V presents the determination of cutting coefficient model as well as the experimental validation used to check the correctness of the coefficient model and the simulation model for the case of a single insert.
- Chapter VI highlights the experimental validation of plunge milling for a system with a rigid workpiece.
- Chapter VII presents the work done and the results of the experimental validation of plunge milling for a system with a flexible workpiece.
- Chapter VIII summarizes the outcome and the findings of the present research and highlights the potential areas for future research work.
- Appendix A describes the different approaches used to model the cutting area.

Chapter 2: Literature review

2.1 Introduction

Machine tool chatter is defined as self-excited vibration between the cutting tool and the workpiece at large metal removal rates [1]. Tobias [2-4], Merrit [5] and Tlusty [6] developed the fundamental chatter theory and recognized that the most powerful sources of self-excitation are associated with the structural dynamics of the machine tool, and the feedback between the subsequent cut that develop a build in mechanism in the system capable of generating a periodic force through the vibration in a way that it sustains the vibration [7]. The theory is based on a closed loop relationship that describes the mutual interdependence of the variation in cutting force and the structural dynamics. The main mechanisms of chatter are known as a regenerative mechanism, which is widely used in chatter modeling, and mode coupling, which occurs without undulations [8].

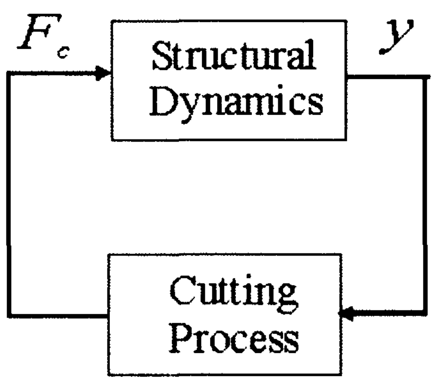

Figure 2-1 self-excited vibration built-in mechanism [8]

2.2 Chatter modeling and control

Chatter vibrations are considered as the main limiting factor for machine tool performance as it affects the surface quality of the part and decreases the machine and tool life significantly. It was found that chatter occurrence is determined by cutting dynamics which includes structure and cutting process dynamics [9]. Therefore, the modeling of dynamics of machining processes is becoming increasingly important to predict cutting forces, system vibrations and process stability limits. Such model could provide an effective and reliable planning of the machining operations for optimum productivity, quality and cost.

Different approaches and techniques were used to model and study the dynamics and stability limit of machining operations and especially milling operations [10]. This includes:

- Analytical approach (e.g. Frequency domain models)
- Time domain Simulation approach.
- Experimental approach [11-15].

Additionally, significant research was carried out to understand and control the chatter phenomenon in different cutting processes. Furthermore, different techniques were developed to suppress the chatter vibrations when they occurred and ensure stable cutting for high performance machining. This includes off-line or process planning techniques, where the cutting conditions are selected based on previously predicted stability lobes [16], on-line speed regulation techniques or sensor assisted, which are based on on-line monitoring of the cutting and the application of control action to move the cutting to a stable conditions [17-22], process and external damping [23-29], and the use of specially designed cutters [30].

2.2.1 Analytical approach

The analytical approach is widely used in modeling the dynamics and stability of cutting processes. It leads to the identification of chatter-free cutting conditions such as spindle speed, axial and radial depth of cut. In this approach, the limit width of cut is calculated from the specific cutting force, minimum real part of oriented transfer function between the tool and the workpiece and the number of teeth cutting simultaneously [31]. The approach is mainly based on the closed loop relationship between the tool vibration, chip modulation and the cutting force as shown in Figure 2-2. The stability limit of the cutting process is driven from the stability of the system closed loop. The analysis of the cutting process states that the limit width of cut that gives stable cutting condition, i.e. no dynamic component of chip thickness, depends on the real part of the oriented transfer function of the system, the cutting force coefficient and the phase shift between the waviness and the tool vibration.

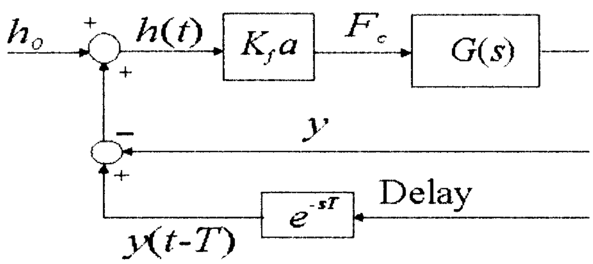

Figure 2-2 closed loop relationship between tool vibration, cutting forces and chip modulation [16]

Mathematical modeling of the dynamic milling process was first introduced by Tlusty [32]. The analysis was a one dimensional model by orienting the cutting forces from the directions of system degrees of freedom to the direction of the resultant force. The analysis was mainly based on the average directional factors as the directions of the cutting forces and chip generation were assumed to be time invariant. The critical borderline of stability was based on the fact that the vibrations between successive cuts do not decay nor increase exponentially from pass to pass (i.e. $y(s) = e^{-sT}y(s)$).

The effect of the time varying directional factors on the stability analysis was first studied in a two dimensional model by Altintas and Budak [33-35] in the feed and the normal directions. They presented a new model for the prediction of the chatter based on the identification of the transfer function of the cutting tool in the frequency domain. This method is mainly based on the formulation of dynamic milling with regeneration in the chip thickness, time varying directional factors and the interaction of the cutting forces with the machine tool structure. Fourier series expansion is used to approximate the time varying dynamic cutting force coefficients. The limit width of cut is modeled as a function of the oriented transfer function of the vibratory system, the number of teeth, and the static cutting force coefficients. The model was extended into 3-D configuration for milling operations by Altintas [36] as well as for turning and boring operations by Budak et al. [37]. The linear chatter analysis technique was extended to account for the force feed linearity by Landers et al. [38] to provide insight into the effect of feed on chatter behavior in milling operation. Other models were developed for the prediction of the onset of chatter for milling [39-50] as well as drilling operations [51, 52]. However, the analytical approach was found to be not inaccurate in the case of small radial immersions as the directional factors contain short impulse type wave forms. This requires either multi-frequency solution or time domain simulation of delayed differential equations [53-58]. Additionally, force or vibration signals cannot be extracted in order to check the severity of chatter.

2.2.2 Time domain simulation approach

Time domain simulation approach is known as a very attractive approach to be used in modeling the dynamics and stability of machining processes, specially for highly dynamic processes such as milling and drilling. It considers the true kinematics and mechanics of the cutting process, the effect of cutter geometry and the influence of inner and outer modulation. The model was found to be able to predict cutting forces, system vibrations and surface roughness of the finished part [59]

The Time domain simulation approach is widely used in modeling the dynamics and stability in milling operations as it takes into account the main aspects of milling operations such as the variation of orientation of the forces, chip thickness and tool deflection during the cutter rotation as well as non-linear effects during cutting such as tool jump phenomenon and process damping [59]. The model being used in the simulation is a regenerative force, dynamic deflection model. It was first developed by Tlusty in turning and later applied in milling [60]. The approach was based on digitizing the cutter rotation into equal small time steps and the cutting forces, system displacement in the direction of modes and the instantaneous chip thickness are computed at each time step. The force on any tooth in the cut depended not only on the feed per tooth and cutter deflection, but also on the surface left by the passage of previous teeth.

Several research efforts were done to use the concept of time domain simulation programs to study the chatter behavior and stability for different types of milling operations [10, 61-68]. Some of this work considered different tool geometries and effect of tool wear on chatter analysis by considering the effect of damping in tool-workpiece interface on the dynamics and stability of the process as studied by Elbestawi et al. [69] and Abrari et al. [70], as well as the effect of tool runout on the surface roughness and stability analysis in end milling processes [71-73]. Further models were developed to use time domain simulation to model dynamics and stability in drilling operations. Roukema et al. [74, 75] developed a time domain model of the torsional-axial chatter vibrations in drilling that considered the kinematics of the tool and the coupled torsional and axial vibrations of the drill. The model was able to predict the cutting forces, tool vibrations as well as the hole surface roughness. Arvajeh et al. [76] developed a time domain simulation model of drilling that combines both the effect of bending and torsion modes on the stability of drilling. The analysis was done for short and long drills and it was found that the bending mode was more susceptible to chatter for long drills while torsion modes were less stiff for short drills.

The Time domain simulation approach is capable of producing information about the severity of the resulting vibration, the surface quality left by the operation, the magnitudes and frequencies of the cutting forces and the vibration. This allows better modeling of the dynamics and stability of the cutting process especially for highly dynamic operations. However, in the time domain simulation, it is difficult to define the limit of stability clearly. Some of the research work dealt with the determination of chatter criterion in time domain milling simulations. The proposed criteria vary from the use of cutting force and vibrations peak to peak (PTP) diagrams [63], the ratio of the maximum predicted dynamic force to maximum static force [61], ratio of dynamic to static chip thickness [58], self-excitation damping ratio [77] and the relative roughness (i.e. ratio between the measured roughness and the kinematical roughness) [78].

2.2.3 Machining of flexible Structures

In machining processes, most studies have been mainly based on the assumption of rigid workpiece and they simply focused on the dynamics of the cutting tool in the stability analysis. However, in practice, the workpiece may experience vibration as a result of the applied cutting force which, accompanied by tool deflection, changes the chip thickness and affects the stability limits of the cutting process. This mainly appears in machining of flexible thin walled/ribbed workpiece, widely used in aerospace and automotive industry, as the deflection of the part to be machined is significant and dominant [79]. Several research work focused on modeling the variation of workpiece dynamics during cutting in stability limit determination, selecting the tool cutting path that relies on the support of unmachined workpiece, and modeling the variation of dominant modes of workpiece at different stages of milling of flexible workpiece. Anjanappa et al. [80, 81] developed an outline-optimal control to maximize the feed-rate for machining thin-webs while maintaining the dimensional accuracy. Techniques for high speed end milling of aluminum parts with thin, flexible webs were investigated by Smith et al. [82]. The study described the development of a strategy for the machining of thin webs and ribs based on selecting the tool path workpiece to obtain chatter-free machining. The main principle is to choose the tool path so that the area being machined is supported by the unmachined workpiece. This methodology was applied to the machining of thin webs (bottom floor of a pocket) and ribs (vertical side wall of a pocket), despite the difference in the direction of the most significant flexibility (i.e. axially for thin webs and radially for thin ribs). Chatter was found to occur due to the increase of the workpiece flexibility as the web thickness is reduced during machining. Several axial steps were suggested to machine the web to its desired thickness due to stability consideration in order to obtain chatter-free operation. Additionally, end mill cutter with zero corner radius was used to perform most of the machining in case of thin webs to minimize the axial force component that can excite the workpiece in its weakest direction. Tlusty et al. [83] considered the high speed milling of components with thin ribs. They proposed that the machining of thin ribs should be done using long slender end mills with relieved shanks, in a series of axial passes to avoid unnecessary contact between the tool and machined surface. As a result the machining action occurs at the base of the rib, which is stiff profiting of the stiffness of the unmachined workpiece without unintended contact between the rib and the cutter above the nominal cutting zone. Zhao et al. [84] proposed a stepped spiral-out tool path for machining of pockets with thin-webs in which the tool reaches the bottom of the pocket then spirals out such that the web is always supported by a bulk of material to minimize workpiece vibration.

Chen et al. [85] proposed a novel stability analysis method for the turning process in which the deflection of the workpiece is considered. It focused on the regenerative chatter generated during the cutting of a flexible workpiece supported with a tailstock. Two models were developed to study the interaction between the tool and the workpiece for rigid and flexible workpiece. It was found that in case of flexible workpiece, the transfer function of the workpiece is considered as a leading dynamics and affects the system stability. Sekar et al. [86] proposed an analytical approach for stability analysis in turning by considering the motion of the workpiece. Cutting force model was developed as a function of the relative motion between the tool and workpiece. They studied the variation of stability limits with and without considering the workpiece flexibility, workpiece dimensions and cutter position (Figure 2-3). Similar approach was used by Martinez et al. [87] as they developed a new analytical model for chatter prediction in turning by considering the compliance between the cutting tool and workpiece.

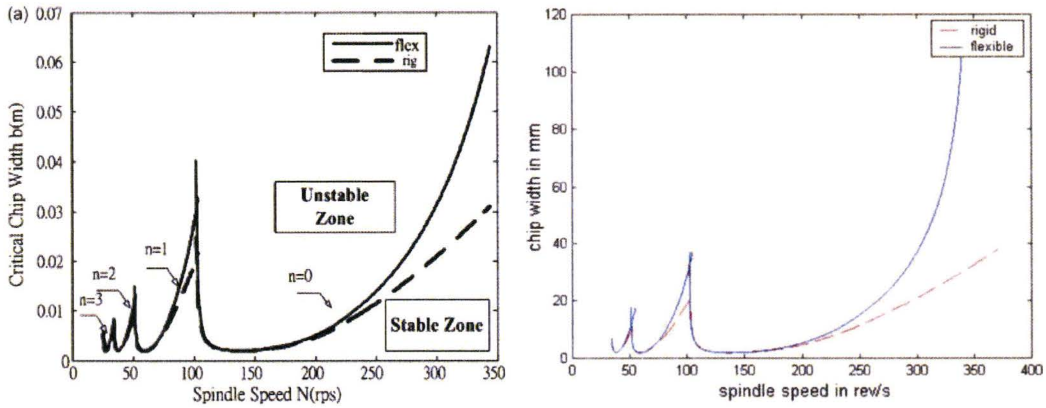

Figure 2-3 Variation of stability lobe for cases of rigid and flexible workpiece [85, 86]

Ismail et al. [88] implemented a combined off-line and on-line control scheme for chatter suppression in milling of flexible aluminum turbine blades in five-axis machine. This scheme included a spindle speed ramping controller for on-line control and feed scheduling as off-line control. Both methods were tested individually and combined to study the effectiveness of the proposed methods. Acoustic intensity signal was used for chatter detection and the spindle speed is changed accordingly until stable cut is achieved. The on-line method was found to be effective due to the fact that the stability lobes change during cutting and vary from point to point due to the variation of the workpiece flexibility during the cutting. Both off-line and on-line control schemes were found to be effective in chatter suppression as shown in Figure 2-4.

a)
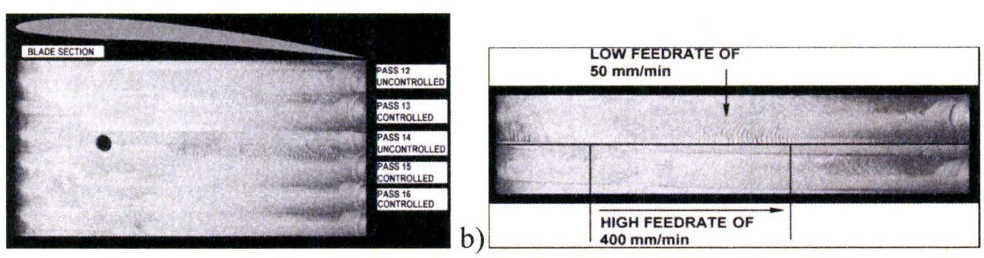

Figure 2-4 Effect of a) speed ramping, b) feed scheduling on surface texture [88].

A time domain simulation model for peripheral milling of very flexible plate type structures was proposed by Altintas et al. [89]. The study was based on modeling the structural dynamics of a cantilevered plate structure at the tool-workpiece contact zone using finite element method by considering the interaction of the flexible workpiece and rigid end mill. The structural dynamics of the plate was assumed to be constant. It was shown that the first bending mode is dominant at the top of the plate while the contributions of higher modes became significant towards the cantilevered bottom of the plate, where the plate is more rigid than at its tip. Similar observation was deducted by Davies et al. [90] as it was shown that the participation of different workpiece modes in the system dynamics changed at different cutting passes. Seguy et al. [91] studied the link between chatter instability and surface roughness evolution for milling of thin-walled structures. They took into account the coupling mode, modal shape and the ploughing effect on the prediction of the simulated 3D stability lobe as well as the surface roughness of the finished part. Mane et al. [92] developed 3D stability lobes for a thin-walled cantilever plate by modeling the workpiece, the tool and the spindle using a FE model. It was found that the dynamic behaviour of the coupled system greatly depends on the spindle-workpiece relative position and the spindle rotational speed. The effect of the change of spindle dynamics as a function of rotational speed was considered. However, the change of workpiece dynamics during machining was not taken into account. Same concept was applied by Thevenot at al. [93] as they generated 3D stability lobes for a thin cantilever plate model using FE model.

Herranz et al. [94] investigated both static and dynamic problems of the milling of low-rigidity parts. A global approach for the right selection of cutting conditions was presented. These include the optimization of the tool path to take advantage of rigidity of the uncut workpiece and generating tool paths with low cutting forces in the most flexible direction without decreasing the material removal rate. Two cutting strategies, "jump-to-jump" for thin walls and "two-level step" for thin webs, were presented and showed better surface roughness as compared to conventional strategies. Additionally, they suggested the use of large tool radii for the machining of ribs and small tool radii for the machining of webs. The stability of thin wall milling was studied by taking into account the relative displacement between the tool and the workpiece in the direction normal to the machined surface. Stability lobe diagram for each cutting step was predicted to take into account the changes of the workpiece dynamics during machining.

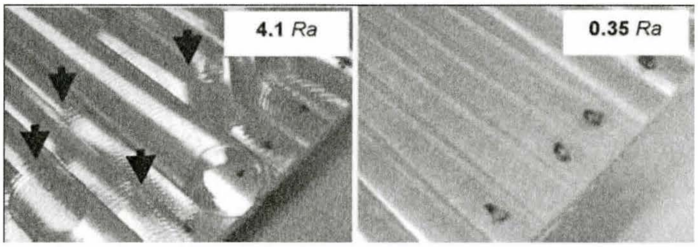

Figure 2-5 Influence of cutting strategies on surface roughness of thin floors a) Conventional strategy, b) "Two level step" strategy [94]

Bravo et al. [95] presented a method to obtain the stability lobes for high speed machining of low rigidity structures considering both the dynamics of machine structure and the machined workpiece using analytical approach. The relative displacement between the cutting tool and the flexible workpiece was considered. A three dimensional stability lobe diagram has been developed to account for the variation of the dynamics of flexible workpiece at milling stages as shown in Figure 2-6. The dynamics of the workpiece vary during the milling process as both mass and rigidity are reduced. The third axis describes the geometrical state of the workpiece during machining. They considered the discrimination of modes by means of finite element analysis to detect the modes without significant displacement in the milled zone to be rejected from the analysis.

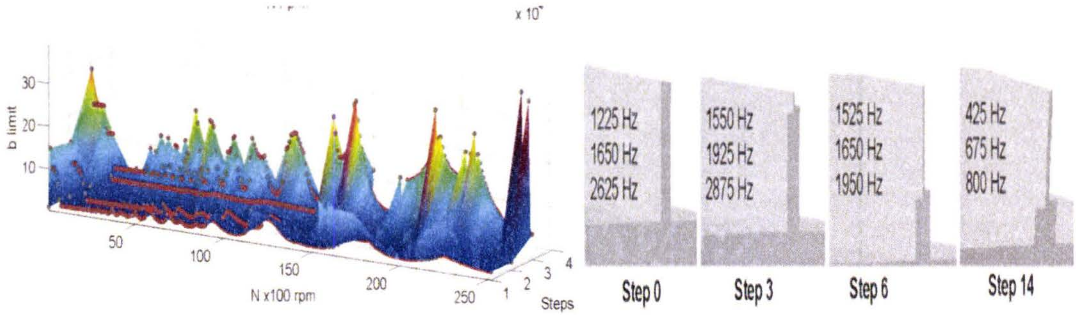

Figure 2-6 3D lobe diagram with speed, depth of cut and milling steps as coordinates [95]

2.2.4 Plunge milling process

Recently, plunge milling operation has gained attention as a roughing process. It is used in boring cylinders, roughing pockets, and aerospace parts made from hardened steel and thermally resistant alloys. In plunge milling, material is removed by feeding the tool in the axial direction towards and normal to workpiece surface. This aims to benefit from the high rigidity of the spindle in the axial direction where the main cutting action takes place leading to higher productivity compared to peripheral milling process [96]. It can be used to enlarge a hole or to remove parts of the material intermittently in axial direction from the periphery of a wall and can be plunged into a solid block with full immersion like a drill (Figure 2-7).

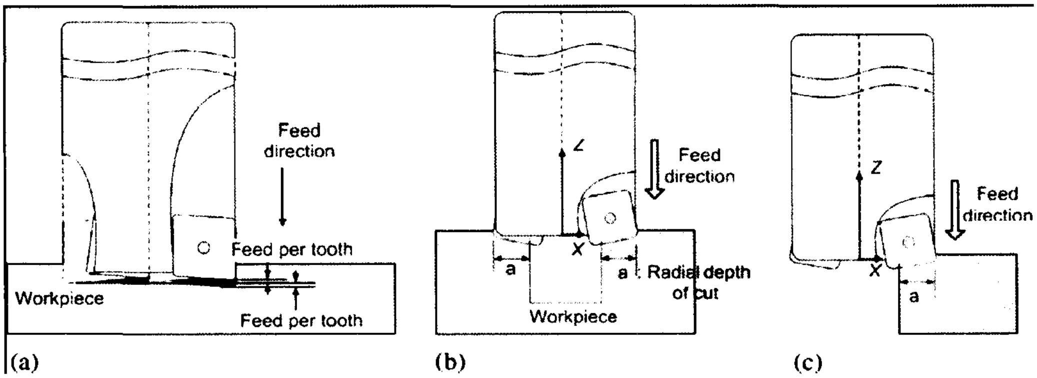

Figure 2-7 Plunge milling applications a) Making large holes, b) enlarging holes, c) intermittent cutting to make vertical walls [104]

Similar concept can be found for drilling with indexable drill. However, Limited published research was carried out to model the dynamics of indexable drilling with most of the work focusing on studying the performance of the process [97-99] and optimization of tool geometry to eliminate unbalanced radial force due to its asymmetrical point angle [100, 101]. There have been limited efforts to model and simulate the dynamics of plunge milling. Most of the efforts focused on the design of cutter geometry, tool motion [102] and estimation of the cutting forces while neglecting the dynamics of the system [103]. Recent work has dealt with the modeling of the dynamics and stability of plunge milling process using frequency domain approach [96] and time domain simulation approach [104, 105]. The dynamic chip thickness was computed along the main cutting edge as a function of cutter vibrations in lateral (x and y directions), axial and torsional directions, tool setting errors and the rigid body motion of the cutter as shown in Figure 2-8. Regenerative behaviour of chip thickness was considered by studying the surface waviness induced by the present and the previous main cutting edge. The main cutting edge is divided radially into elements along the edge and the chip load and cutting forces are calculated for each element. The cutting edge position for each element is computed and the corresponding chip thickness is computed as the difference between the position of the present and the previous main edge projected in the axial direction.

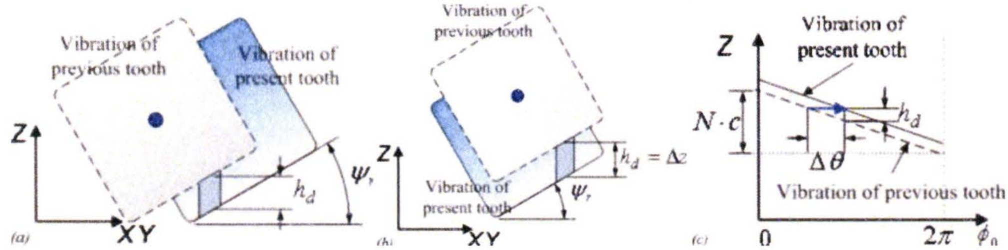

Figure 2-8 Effect of different vibration modes a) Lateral vibration, b) Axial vibration, c) Torsional vibration on chip thickness [105]

The cutting action was assumed to occur only at the main cutting edge with no consideration of the contribution of side edge into the cutting action and the workpiece was considered to be rigid as only the cutter dynamics was considered in previous studies. Additionally, an over prediction of the axial cutting forces of 18% was found for certain cutting conditions as shown in Figure 2-9. It was observed that torsional-axial coupled vibration mode is the dominant chatter mode due to strong coupling between the torque and axial vibrations as a result of the used cutter designed cavities for chip evacuation.

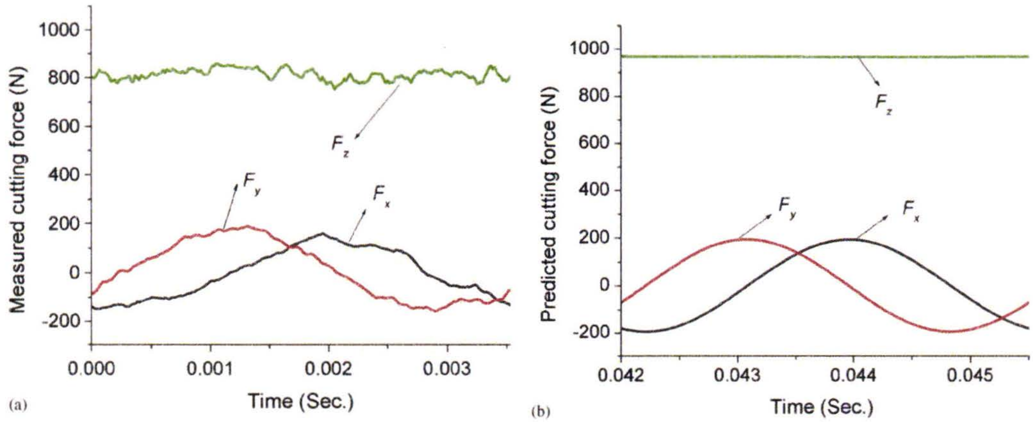

Figure 2-9 a) Measured and b) predicted cutting forces for stable cutting at 17142 rpm, 0.075 mm/tooth, 5 mm radial depth of cut [104]

2.3 Conclusion

In this chapter, a review of the literature is presented to describe the previous work done to study the chatter analysis in machining, especially for plunge milling process. This helps in shaping the objectives of the research by tackling the areas not considered in published research. This can be summarized as:

- High requirements of accuracy and productivity in manufacturing processes. However, chatter is the major limiting factor to achieve high productivity and surface finish. Therefore, there is an important need to accurately model the dynamics and stability of the cutting process for planning and control purposes by developing an effective and reliable method to plan and control the cutting process to improve productivity and product quality.
- Extensive work has been done to understand and model the dynamics and stability of machining, especially in milling, using analytical and time domain approaches. Most of the work focused on developing a reliable technique for planning of the cutting prior to machining by considering different parameters affecting the stability of the process.
- Workpiece dynamics can play an important role in the stability analysis of the machining process, especially for systems with a flexible workpiece. Recent work focused on modeling the effect of workpiece flexibility on the process dynamics for thin-walled structures by considering the relative motion between the tool and the workpiece as well as the variation of the workpiece dynamics during cutting due to thickness variation.
- Plunge milling is a promising process in roughing. However, limited work has dealt with modeling its stability and factors affecting it. Some of the points which were not considered in previous work for plunge milling can be summarized as follows:
    - Cutting action was assumed to occur only at the main cutting edge with no consideration of the contribution of the side edge in cutting.

- Workpiece was assumed to be rigid and only the cutter dynamics were considered in the modeling with now consideration of workpiece dynamics and its variation in the previous models.
- Over prediction of the cutting forces as compared to the measured forces was found. This can be attributed to the modeling approach (i.e. use of radial elements) used for evaluation of the chip area and/or the cutting coefficient model used in the mechanistic model.

Chapter 3: Simulation Model

3.1 Introduction

Modeling and simulation of a machining process is an interdisciplinary topic that involves many aspects: modeling of the cutting forces, geometric presentation of the workpiece and the cutting edges, considering tool setting errors and modeling of the process dynamics, which includes tool and workpiece dynamics. Therefore, the key element of the simulation model is to correctly compute the area cut by each insert, which affects the prediction of the cutting force and correspondingly the system vibrations, and hence, the validity of the model. Therefore, the accuracy of the simulation model depends mainly on the accuracy of the inputs, which include: system dynamics, tool setting errors and cutting coefficient model, as well as on the accuracy of the approach used in computing the cutting area by each insert. Preliminary study was carried out to investigate different approaches used for area calculation as described in Appendix A. This help at determining the best approach to be used in the time domain simulation for better modeling and prediction. The time domain model used in the simulation is then presented in the second section of the chapter. Finally, a detailed study is performed to model and analyze the effect of side edge contribution in cutting and understanding the factors affecting its involvement in cutting.

3.2 Simulation Model

Time domain simulation model is developed to study the dynamics of the plunge milling operation for systems with rigid as well as flexible workpiece. Simulation code was developed using commercially available software MATLAB. This model is used to predict the cutting forces, system vibrations and actual cut surface area which affect the cutting process stability. The model aims to accurately evaluate the area cut by each insert to be used in the mechanistic model for better process modeling and force prediction. For systems with rigid workpiece, system vibration is represented by the tool vibration only.

However, for case of systems with flexible workpiece, both the workpiece and the cutter vibrations are considered in the model and the system vibration is defined as the relative vibration between the tool and the flexible workpiece. The model considers both the cutter and workpiece vibrations in three directions, two lateral (x and y) and one axial (z direction), as well as the cutter torsional vibration. In the present model, both the workpiece and the milling cutter are modeled as 3-DOF vibratory system in x, y and z directions. However, for case of rigid workpiece, the system dynamics is represented by the tool dynamics only and the workpiece is considered rigid. Figure 3-1 shows the 3-DOF vibratory system for both cases of system with rigid and flexible workpiece. The model can consider any coupling between the vibrations modes depending on the geometry of the used plunge milling cutter. Additionally, the model can be applied to any number of inserts, whether it is plunge milling with single insert, which is the case for cutting coefficient model determination, or for multi-inserts plunge milling.

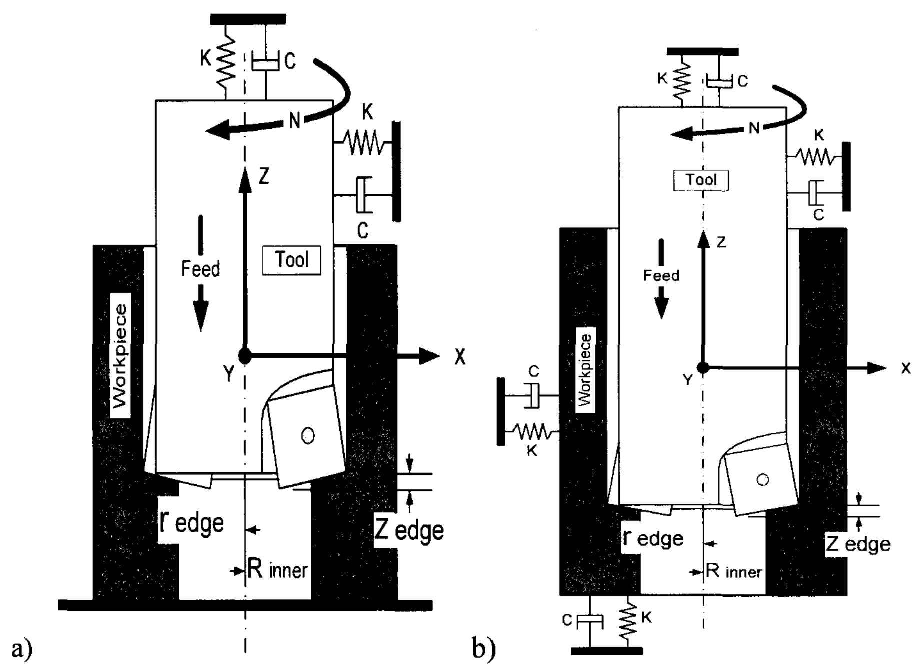

Figure 3-1 3-DOF vibratory system for a) Rigid workpiece, b) Flexible workpiece

The time domain model is based on discretizing the cutter rotation into small time step that corresponds to rotation step of $d\varphi$. The cutting forces on each insert, system displacements in the direction of the modes and chip area are then computed at each time step. The angular relation between successive teeth is given by:

$$\varphi_2 = \varphi_1 - \varphi_p \tag{3.1}$$

where, φ_p is the tooth spacing or cutter pitch angle and is given as $\varphi_p = \frac{2\pi}{m}$ where m is the number of teeth on the cutter. The increment in time that corresponds to each time step in seconds is given by:

$$dt = \frac{60 * d\varphi}{2\pi * N} \tag{3.2}$$

The model considers the regenerative mechanism that relates the cutting forces, system vibration and chip area modulation to simulate the dynamics of the process. Mechanistic model is used to calculate the cutting forces as a function of the dynamic chip area. The geometry and force distribution of plunge milling is shown in Figure 3-2.

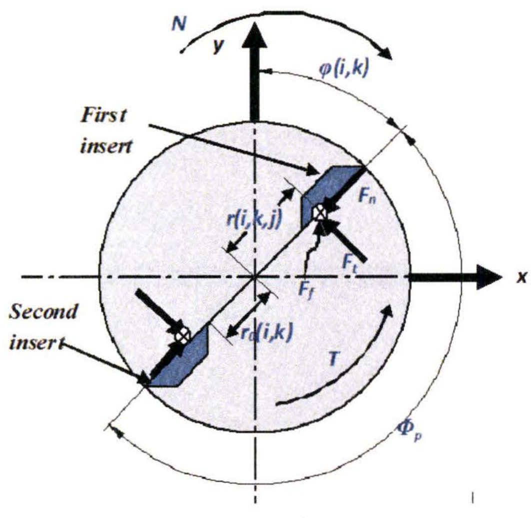

Figure 3-2 Configuration and force distribution in plunge milling process

The instantaneous dynamic chip area cut by each insert is evaluated by studying the interaction between the milling cutter inserts, the workpiece to be cut and the surface generated by the previous insert at same angular position. This is done by evaluating the resultant area from the intersection of the main and side edges of the present insert in contact with the workpiece, which is presented by the pilot hole to be enlarged and the surface cut by the previous insert. In the proposed model, the interaction of both main and side cutting edges of the insert with the workpiece is considered to realistically determine the area to be cut and hence, the cutting forces. The workpiece is determined by the diameter of the pilot hole to be enlarged. At each time step, the workpiece geometry is updated to consider the area removed by the cutting inserts. The insert profile is described by the geometry of the main and side edges that relates the radial position of each point on the edges to its axial elevation. Different modeling approaches to evaluate the cutting area were studied as described in Appendix A to select the best approach to be used in the simulation model. Based on the study, the horizontal approach was selected to model the cutting inserts and correspondingly, the cutting area as it showed the best results with the insert geometry. The modeling approach of inserts is based on dividing the main and side edges of the insert into equal axial elements of height Δz shown in Figure 3-3 width of cut evaluation at each axial element and the corresponding radial position is then determined as a function of insert geometry. The axial approach used makes the model capable of dealing with any shape of the insert based on its geometry and angles which can be effectively used in determining the surface profile, and hence, the surface roughness parameters of the workpiece.

The axial position of each insert is updated at each time step to consider the tool motion in the feed direction, system vibrations in the axial direction as well as axial runout as given by Equations (3.3), (3.4) and (3.5).

$$Zo(n,m) = \frac{-c*m*\varphi(n)}{2\pi} + zs(n) + Ra(n,m) \tag{3.3}$$

$$Z_{actual}(n,m,l) = Zo(n,m) + (l-1)*\Delta z \tag{3.4}$$

$$Z_{ins}(n,m,l) = Z_{actual}(n,m,l) - Zo(n,m) \tag{3.5}$$

Where *zs(n)* is the instantaneous system vibration in the axial direction which is defined as given in Equation (3.6) for rigid workpiece and Equation (3.7) for flexible workpiece.

$$z_s(n) = z_t(n) \qquad \text{For rigid workpiece} \qquad (3.6)$$

$$z_s(n) = z_t(n) + z_w(n) \qquad \text{For Flexible workpiece} \qquad (3.7)$$

Where $zt(n)$ and $zw(n)$ are the instantaneous tool and workpiece axial vibration respectively. Z_{actual} is the actual axial elevation of each element with respect to the workpiece reference surface, while, Z_{ins} is the normalized axial elevation of each element of the insert calculated at the workpiece reference surface and $Ra(n,m)$ is the axial runout. The corresponding instantaneous radial position $r(n, m, l)$ of the j^{th} element of the m^{th} insert at angular position n of the cutter is modeled as a function of the insert geometry as well as the radial runout and the system (i.e. tool and workpiece) vibrations in the radial direction as explained in Equations (3.8) and (3.9). Workpiece and cutter vibrations in lateral directions are projected radially to modify the insert's radial position as a function of system lateral vibration. This helps in computing the actual chip area cut by each insert as it depends on the actual penetration of the cutter inserts in the workpiece.

$$r(n, m, l) = rv(n, m) + \frac{Z_{ins}(n,m,l)}{\tan(\beta)} \qquad for\ Z_{ins}(n, m, l) \leq Z_{edge} \qquad (3.8)$$

$$r(n, m, l) = r_{edge} - \left(Z_{ins}(n, m, l) - Z_{edge}\right) * \tan(\beta) \qquad for\ Z_{ins}(n, m, l) > Z_{edge} \qquad (3.9)$$

Where, β is the entering angle of the inset, rv is the radius of the first element and is given in Equation (3.10) as a function of radial eccentricity and system vibration, r_{egde} and Z_{edge} are the radial and axial coordinates of the insert tip respectively as shown in Figure 3-1.

$$rv(n, m) = ro(n, m) + \frac{(xs(n))}{\sin(\varphi)} + \frac{(ys(n))}{\cos(\varphi)} \pm e \qquad (3.10)$$

Where $xs(n)$ and $ys(n)$ are the instantaneous system vibration in the lateral direction, x and y directions respectively, which is defined as given in Equation (3.11) for rigid workpiece and Equation (3.12) for flexible workpiece.

$$x_s(n) = x_t(n) \ \ and\ \ y_s(n) = y_t(n) \qquad \text{For rigid workpiece} \qquad (3.11)$$

$$x_s(n) = x_t(n) + x_w(n) \ \ and\ \ y_s(n) = y_t(n) + y_w(n) \qquad \text{For flexible workpiece} \qquad (3.12)$$

Where *xt(n)* and *yt(n)* are tool vibration in x and y respectively, *xw(n)* and *yw(n)* are workpiece vibrations respectively, *e* is the radial eccentricity and *ro(n,m)* is the initial radius of first element based on geometry only.

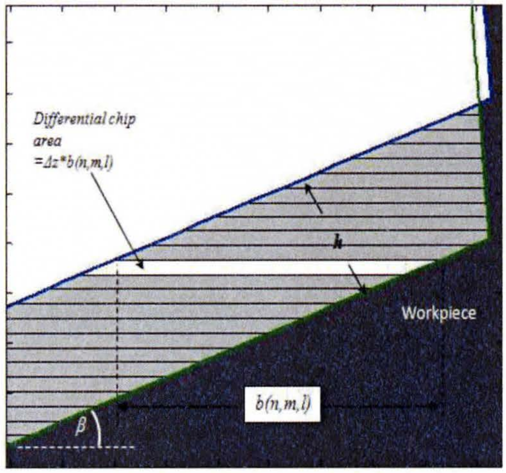

Figure 3-3 width of cut evaluation at each axial element

The effect of radial and axial runout is considered in the model to be able to simulate the actual cutting conditions and to accurately determine the chip area cut by each insert. In this case, one insert will penetrate deeper in the workpiece, either in the axial or the radial direction leading to uneven chip load removed by each insert as shown in Figure 3-4. This results in fluctuation in Fx and Fy due to tool setting errors. Additionally, higher portion of the side edge is involved in the cutting action due to radial runout. This demonstrates the importance of considering the effect of side edge cutting in the simulation to accurately evaluate the chip area and hence, the cutting forces. The instantaneous chip area removed by each insert is then evaluated by computing the width of cut at each axial element of the present insert within the cutting zone based on the penetration of main and side edge of the insert in the workpiece. This is done by comparing the radial position of each element of the present insert to the radial position of the element of the previous insert at the same axial level with respect to the workpiece at the same angular position as given in Equations (3.13) and (3.14).

$$b(n,m,l) = |rv(n,m,l)| - \max\left(rv(n-n_m, m-1, l-l_p), R_{inner}\right) \qquad for\ l > l_p \qquad (3.13)$$

$$b(n,m,l) = |rv(n,m,l)| - R_{inner} \qquad for\ l \leq l_p \tag{3.14}$$

Where l_p corresponds to the difference between the axial elements of same index (l) at two different insert due to tool motion and vibration in the z direction. Hence, $(l - l_p)$ is the index of the axial element of the previous insert located at the same axial level as the l^{th} element of the present insert. l_p is a function of the tool motion, axial runout and tool and workpiece vibration in the axial direction as given in Equation (3.15).

$$l_p = \frac{c + Ra(n,m) + zs(n)}{\Delta z} \tag{3.15}$$

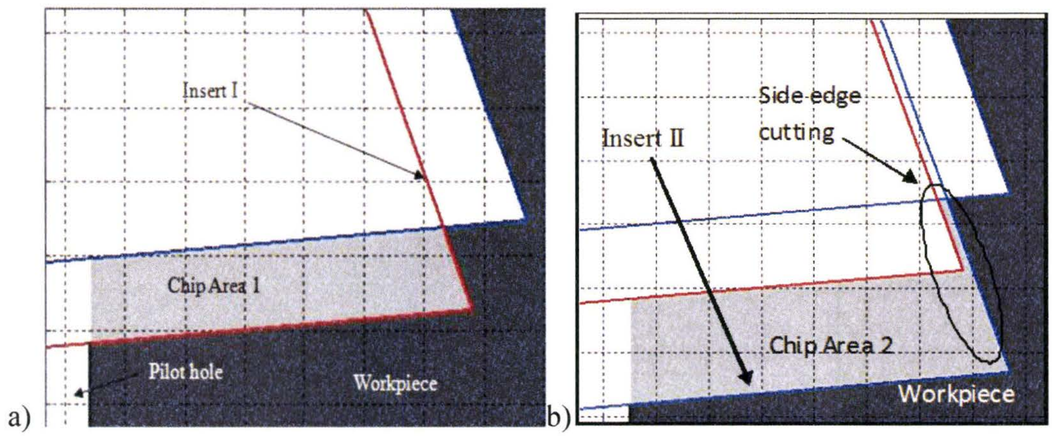

Figure 3-4 - Effect of radial and axial runout on chip area removed by a) 1st insert and b) 2nd insert

The area cut by each insert is then evaluated by calculating the width of cut at each element within the cutting zone and multiply their sum by the axial step as given in Equation (3.16).

$$area(n,m) = \left(\sum_1^{lend} b(n,m,l)\right) * \Delta z \tag{3.16}$$

Negative width of cut value is set to be zero to exclude the portion of the new insert that is out of the cutting zone as shown in Equation (3.17).

$$b(n,m,l) = 0 \qquad if\ b(n,m,l) \leq 0 \tag{3.17}$$

In the proposed model, the instantaneous width of cut at each element is then computed based on the penetration of the main and side edge of the insert in the workpiece which depends mainly on the insert geometry, tool motion, radial and axial runout and tool and workpiece vibrations in x, y, and z directions for better force prediction and process modeling. Figure 3-3 shows the width of cut evaluation at each axial element.

The cutting forces acting on each insert are computed in tangential (*Ft*), normal (*Fn*) and feed (*Ff*) direction as well as the torque (*T*) for each insert. The forces are calculated using mechanistic model as a function of the dynamic chip area cut by each insert as given in Equations (3.18) to (3.21).

$$F_t(n,m) = K_t(n,m) * area(n,m) \tag{3.18}$$

$$F_n(n,m) = K_n(n,m) * area(n,m) \tag{3.19}$$

$$F_f(n,m) = K_f(n,m) * area(n,m) \tag{3.20}$$

$$T(n,m) = K_t(n,m) * \Delta z * \sum_{l=1}^{l_{end}} (b(n,m,l) * rv(n,m,l)) \tag{3.21}$$

Where, *Kt(n,m)*, *Kn(n,m)* and *Kf(n,m)* are the instantaneous cutting coefficients in tangential, normal and feed directions respectively. The cutting coefficients are calculated instantaneously based on the actual chip thickness removed by each insert and not on the nominal feed to consider the variation in chip thickness at each time step due to tool and workpiece vibrations and tool setting errors as given in Equations (3.22) to (3.24).

$$Kt(n,m) = 325.17 * (h(n,m))^{-0.418} \tag{3.22}$$

$$Kn(n,m) = 202.85 * (h(n,m))^{-0.418} \tag{3.23}$$

$$Kf(n,m) = 130.33 * (h(n,m))^{-0.628} \tag{3.24}$$

Chip thickness is evaluated in the normal direction to the main edge as a function of the position of main edge of the present insert with respect to the main edge of previous insert as given in Equation (3.25).

$$h(n,m) = \max\big(b(n,m,l)\big) * \sin(\beta) \tag{3.25}$$

Figure 3-5 shows the flow chart demonstrating the main procedure used in the simulation model. A detailed flow chart is shown in Figure 3-6. The tangential, normal and axial cutting forces acting on each insert are then transformed into three perpendicular components in the X, Y (lateral) and Z (axial) directions. The total cutting forces *Fx* and *Fy, Fz* and torque acting on the cutter at each time step are given by summing the contributions of both inserts in cutting action as given in Equations (3.26) to (3.29).

$$F_x(n) = \sum_{m}^{m_{end}} -F_t(n,m)\cos\varphi(n,m) - F_n(n,m)\sin\varphi(n,m) \tag{3.26}$$

$$F_y(n) = \sum_{m=1}^{m_{end}} F_t(n,m)\sin\varphi(n,m) - F_n(n,m)\cos\varphi(n,m) \tag{3.27}$$

$$F_z(n) = \sum_{m=1}^{m_{end}} F_f(n,m) \tag{3.28}$$

$$T(n) = \sum_{m=1}^{m_{end}} T(n,m) \tag{3.29}$$

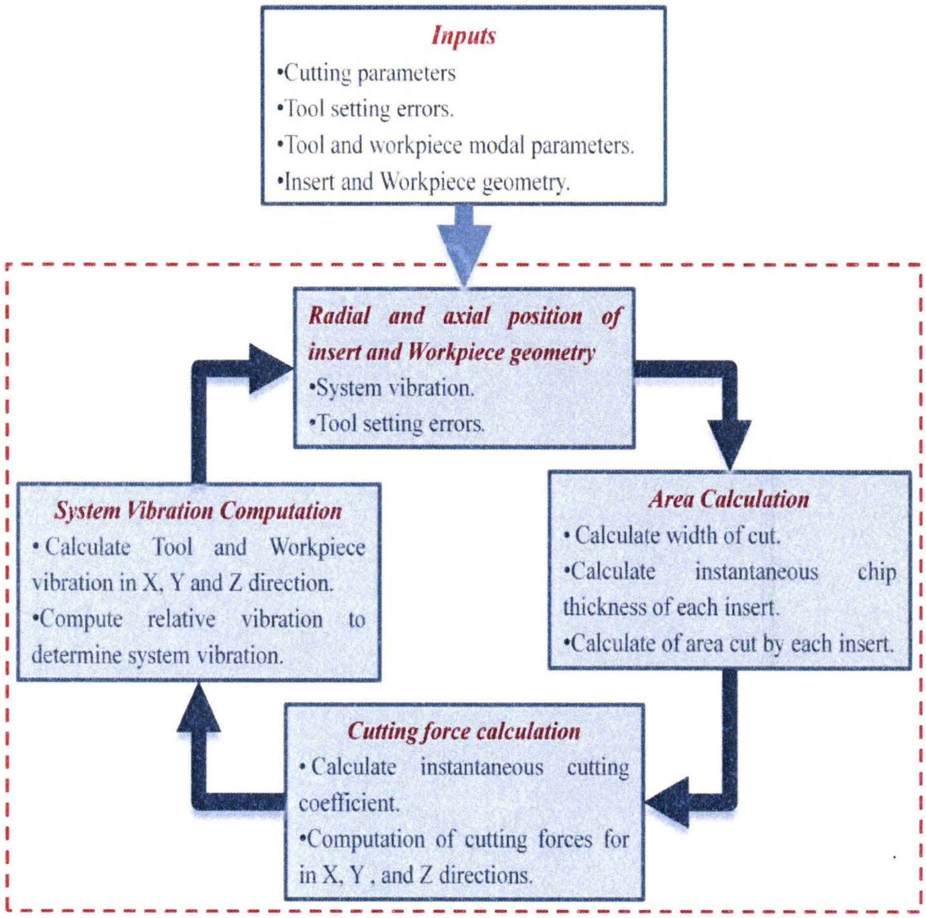

Figure 3-5 Flow chart of the model

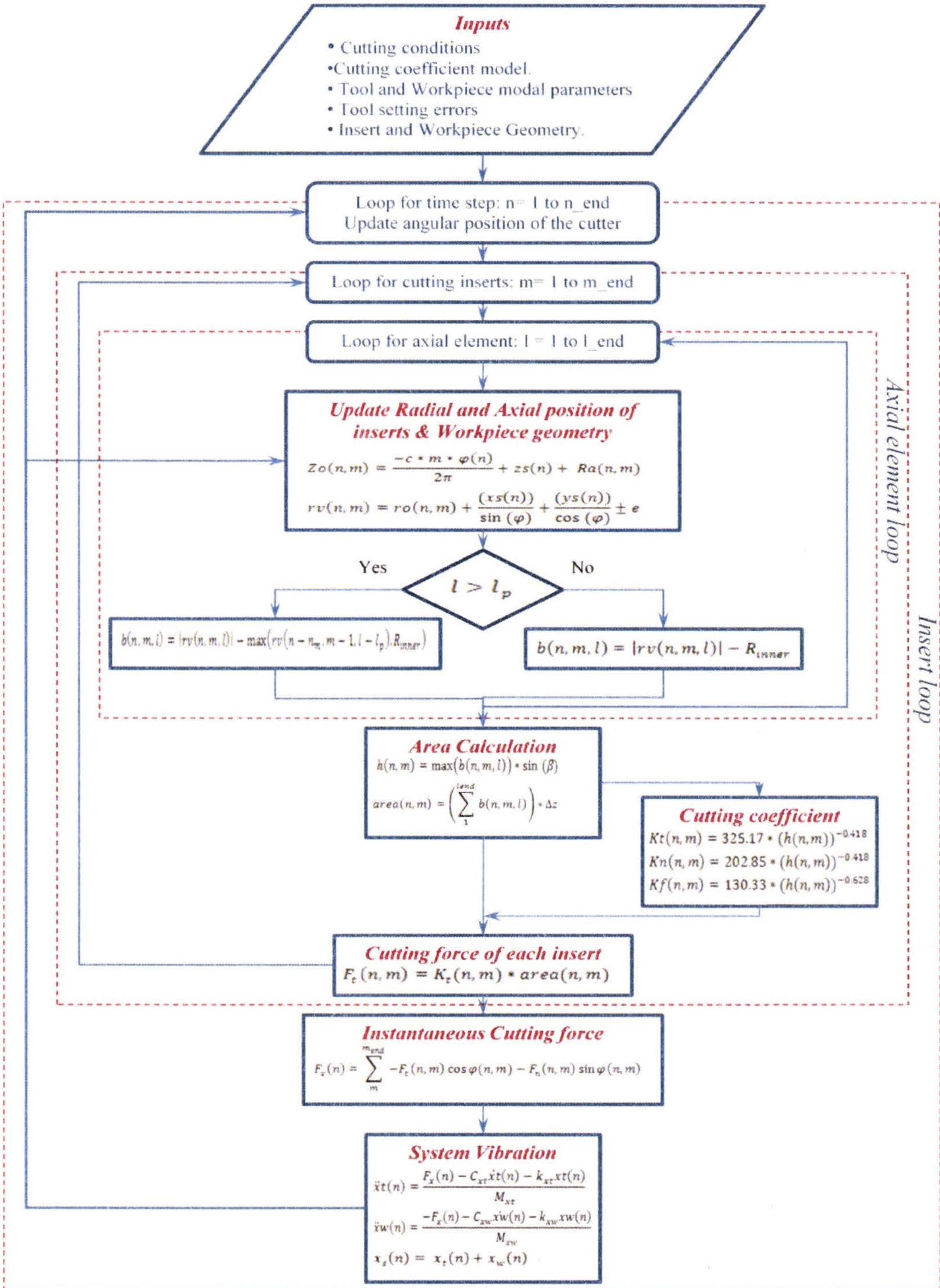

Figure 3-6 Detailed Flow chart of the developed simulation model

Both the cutter and workpiece vibrations are computed at each time step for all degrees of freedom based on the corresponding component of cutting forces. The dynamics at each mode are assumed to be a second-order damped vibration system. The accelerations are integrated twice using Euler integration to obtain the displacements used to get the deflection in axial and radial direction, which modifies consequently the chip area cut by each insert, and hence the cutting force. The equations of motion for each direction for the tool are given in Equations (3.30) to (3.33)

$$\ddot{x}t(n) = \frac{F_x(n) - C_{xt}\,\dot{x}t(n) - k_{xt}\,xt(n)}{M_{xt}} \tag{3.30}$$

$$\ddot{y}t(n) = \frac{F_y(n) - C_{yt}\,\dot{y}t(n) - k_{yt}\,yt(n)}{M_{yt}} \tag{3.31}$$

$$\ddot{z}t(n) = \frac{F_z(n) - C_{zt}\,\dot{z}t(n) - k_{zt}\,zt(n)}{M_{zt}} \tag{3.32}$$

$$\ddot{\theta}(n) = \frac{T(n) - C_\theta\,\dot{\theta}(n) - k_\theta\,\theta(n)}{M_\theta} \tag{3.33}$$

Similarly, Equations (3.34) to (3.36) give the equation of motion for the workpiece. It has to be noted that the used stiffness, damping and modal mass in simulation corresponds to the actual hole location studied.

$$\ddot{x}w(n) = \frac{-F_x(n) - C_{xw}\,\dot{x}w(n) - k_{xw}\,xw(n)}{M_{xw}} \tag{3.34}$$

$$\ddot{y}w(n) = \frac{-F_y(n) - C_{yw}\,\dot{y}w(n) - k_{yw}\,yw(n)}{M_{yw}} \tag{3.35}$$

$$\ddot{z}w(n) = \frac{-F_z(n) - C_{zw}\,\dot{z}w(n) - k_{zw}\,zw(n)}{M_{zw}} \tag{3.36}$$

3.3 Side edge cutting

As explained in the simulation model, the area removed by each insert is determined based on the position of both main and side edge of the insert with respect to the workpiece material defined by the pilot hole and surface cut by previous insert. The contribution of side edge in cutting is considered in the simulation model as it can affect the prediction of cutting forces as well as the determination of surface profile cut during plunge milling. Therefore, the influence of parameters affecting the side edge cutting is studied to understand and determine the conditions at which the contribution of side edge in cutting is significant. The studied parameters are 1) radial runout, 2) axial runout and 3) tool geometry (i.e. insert angles). Figure 3-7-a shows a detailed presentation of the area removed during plunge milling for case of radial and axial runout on the same insert demonstrating the area removed by the main edge (i.e. area OACD) and the area removed by side edge (i.e. area CDHGEC) of insert I which is enlarged in Figure 3-7-b and shows the width of cut and chip thickness h_{4-5} removed by side edge.

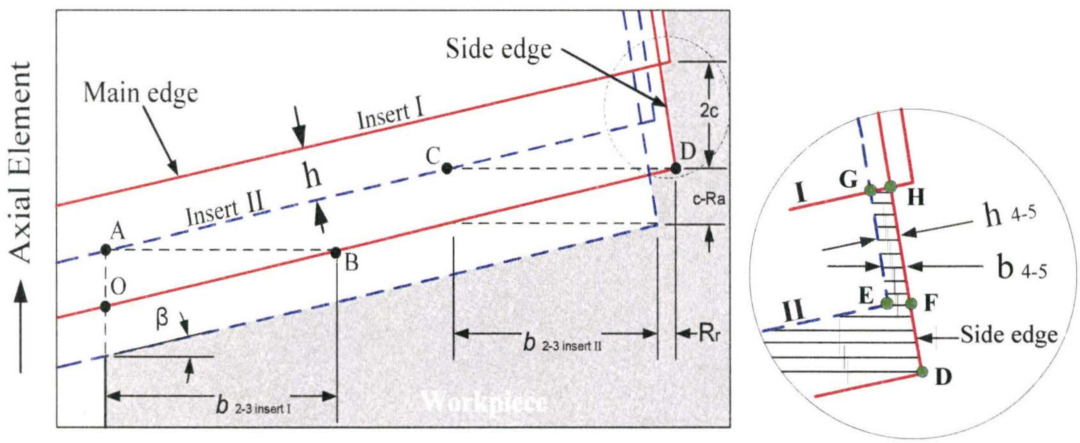

Figure 3-7 - a) Area removed by main and side edges of the insert, b) Detailed view of area removed by side edge.

The distribution of width of cut at each element within the chip area is shown in Figure 3-8 for speed of 14750 rpm and at 0.07 mm/tooth feed. It can be noticed from both figures that the distribution of width of cut can be categorized in four zones. With reference to Figure 3-7, first zone 1-2 or area (OAB), where the width of cut increases gradually from zero till it reaches its maximum value b_{2-3} which corresponds to distance AB. Second zone corresponds to zone ABCD at which the width of cut constant at its maximum value for each element in this zone. The third part corresponds to area CDEF cut by the side edge at which the width of cut decreases gradually until it reaches a value equals to b_{4-5}, corresponding to side edge width of cut that depends mainly on radial runout, axial runout, system vibrations and tool angles. It can be shown in Figure 3-8 that the value of side edge width of cut, $b_{4\text{-}5}$,is equal to the distance EF for Insert I while it is equal to zero for Insert II. This can be attributed to the effect of radial and axial runout which increases the penetration of side edge in the workpiece over the zone EFGH for insert I which is not involved in cutting for insert II. It can be noticed that area OACD represents the area cut by main edge of the insert, while area CDHGEC is the area cut by the side edge. Additionally, it can be noticed that the maximum width of cut (i.e. $b_{2\text{-}3}$) removed by the main edge of each insert is not equal due to the fact of uneven chip load due to radial and axial runout. This is demonstrated by the value of $b_{2\text{-}3}$ for insert 1 (i.e. 0.44 mm) compared to $b_{2\text{-}3}$ for the second insert (i.e. 0.35 mm) as shown in Figure 3-8. Equation (3.37) gives the maximum width of cut removed by main edge as a function of tool setting errors as well as system vibrations.

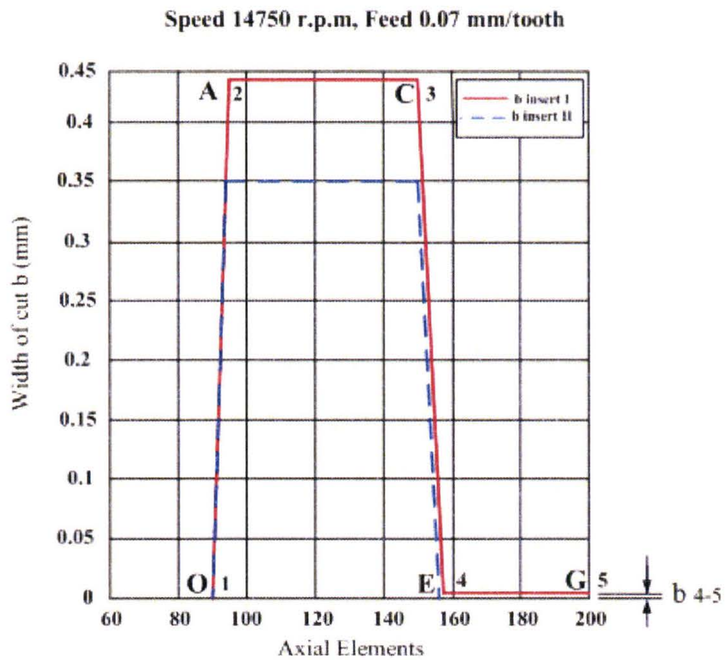

Figure 3-8 Width of cut distribution with respect to axial elements.

The effect of radial runout, axial runout and tool entering angle on the penetration of side edge in the cutting zone expressed by side edge width of cut $b_{4\text{-}5}$ was mathematically modeled. The width of cut distribution can be expressed as a function of tool setting errors and tool geometry as given by Equation (3.38).

$$b_{2-3\,insert\ I\,\&\,II} = (c \pm R_a + z_s(n)) * \tan\left(\frac{\pi}{2} - \beta\right) \pm (R_r + r_s(n)) \quad (3.37)$$

$$b_{4-5} = \left(R_r + r_s(n)\right) - \left(c + R_a + z_s(n)\right) * \tan(\beta) \quad (3.38)$$

Where β is the entering angle of the insert as shown in Figure 3-7-a and $z_s(n)$ and $r_s(n)$ are the relative vibration of tool and workpiece in the axial and radial directions respectively.

The side edge width of cut, $b_{4\text{-}5}$, is then used to compute the chip thickness cut by the side edge in the direction normal to the edge as shown in Figure 3-7-b. The chip thickness is used in the cutting coefficient model to compute the cutting forces due to side edge contribution in cutting. The chip thickness is given in Equation (3.39).

$$h_{4-5} = b_{4-5} * \cos(\beta) \quad (3.39)$$

The effect of radial and axial runout as well as the tool entering angle on the width of cut of side cutting is shown in Figure 3-9. It can be noticed that the width cut by the side edge increases with the increase of radial runout for constant axial runout and tool entering angle. The value of radial eccentricity at which side edge cutting occurs varies as a function of the entering angle of the insert. The area cut by the side edge was not found to be affected by the value of axial runout for a zero entering angle due to the fact that the side edge in this case is parallel to the workpiece surface and hence it is only affected by the radial runout and system vibrations. However, for a positive entering angle, an increase in axial runout will lead to a decrease in the side cutting width of cut. In this analysis, the axial and radial runout are acting on the same insert. The effect of axial runout will be reversed if the axial and radial runout were at different inserts. Additionally, an increase in the entering angle will lead to a decrease in the side cutting width of cut. Therefore, it can be concluded that the contribution of side edge into cutting action is mainly affected by radial and axial runout, tool geometry and system vibrations. Its effect can be significant for higher radial runout and radial vibrations, for higher axial runout acting on a different insert and smaller entering angle of the insert. Time domain simulation was performed to study the effect of side cutting on the cutting forces during plunge milling. The simulation was run with and without the contribution of side edge in cutting for radial eccentricity equals to 9 μm and axial runout equals to 5 μm acting on the same insert with an entering angle of 10° which is similar to the conditions used in cutting tests.

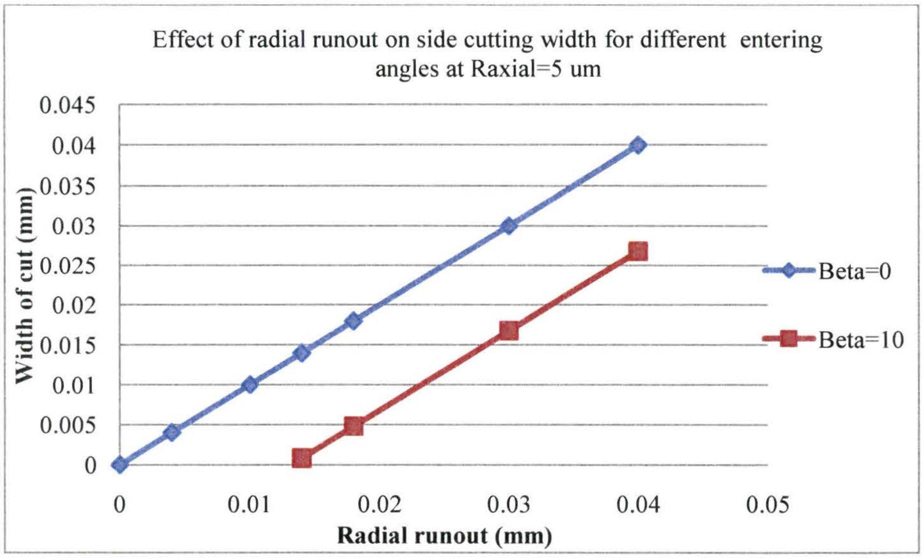

a)

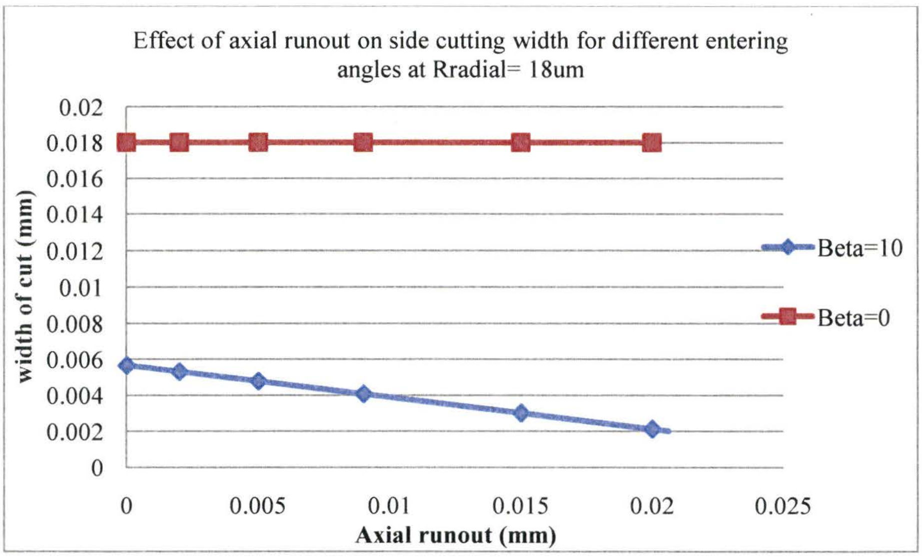

b)

Figure 3-9 - Effect of a) radial runout and b) axial runout on side edge width of cut at different entering angle (β)

In this simulation, both the tool and workpiece are assumed to be rigid and only the tool motion is considered in the simulation. Figure 3-10 shows the effect of consideration of side edge cutting on the predicted cutting forces. It can be shown that an increase in the cutting forces occurs with the consideration of side edge contribution in the cutting action. This is illustrated by the increase in lateral and axial forces compared to the case where no side cutting is considered. The increase in lateral forces is about 10% and around 6% in axial forces. Besides, the effect of side cutting was studied when the axial and radial runout are acting on different insert as shown in igure 3-11.

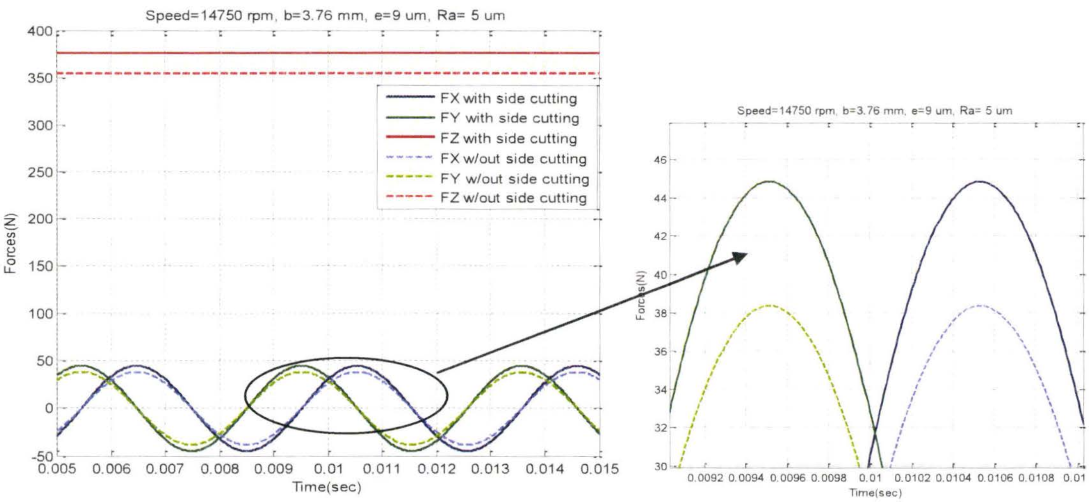

<u>Figure 3-10 - Effect of side edge cutting on cutting forces for axial and radial runout on same insert.</u>

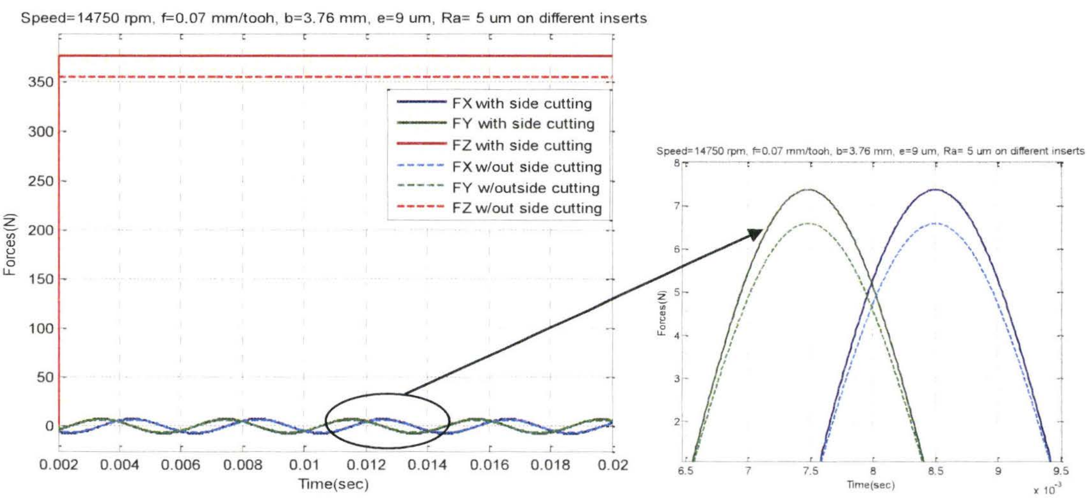

<u>igure 3-11 - Effect of side cutting on cutting forces for axial and radial runout on different insert.</u>

It can be noticed that no significant change in axial force, while the lateral forces decrease significantly as compared to Figure 3-10 . This is due to the fact that the axial and radial runout are acting on a different insert leading to a decrease in the difference between the area removed by each insert and hence a decrease in the resultant lateral forces. Additionally, an increase in axial and lateral forces occurs with the consideration of side cutting. The increase in axial force is about 6%, which is about the same when axial and radial runout act on same insert while it increases to 15 % in lateral forces and a 16% increase in side edge width of cut. It can be concluded that the direction of tool setting errors affect considerably the contribution of side edge in cutting. Figure 3-12 shows the values of the predicted cutting forces with and without the consideration of side edge cutting as compared to the corresponding measured cutting forces. It can be shown that better prediction of cutting force is achieved when considering the contribution of side edge leading to more accurate modeling of plunge milling process. Therefore, the effect of side edge cutting must be considered in the modeling of plunge milling process as it can play an important role in force prediction and the determination of surface profile produced during cutting.

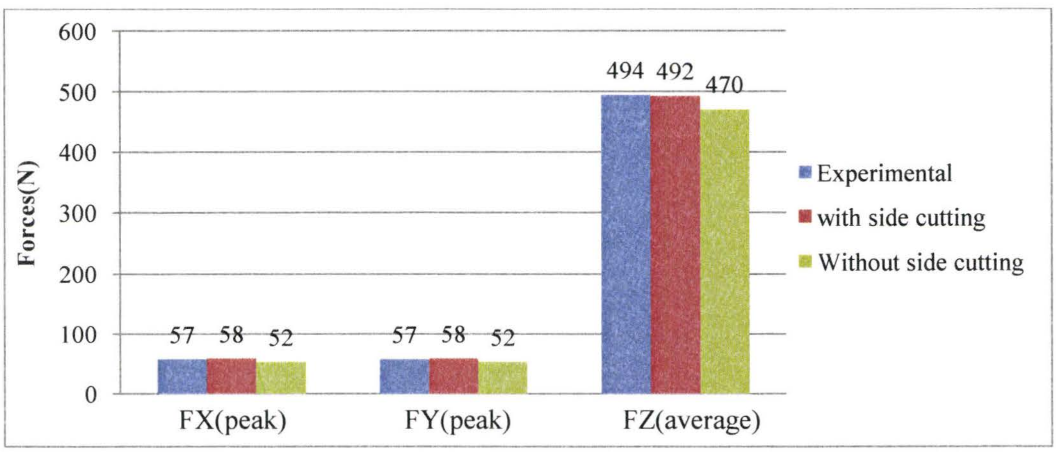

a)

b) 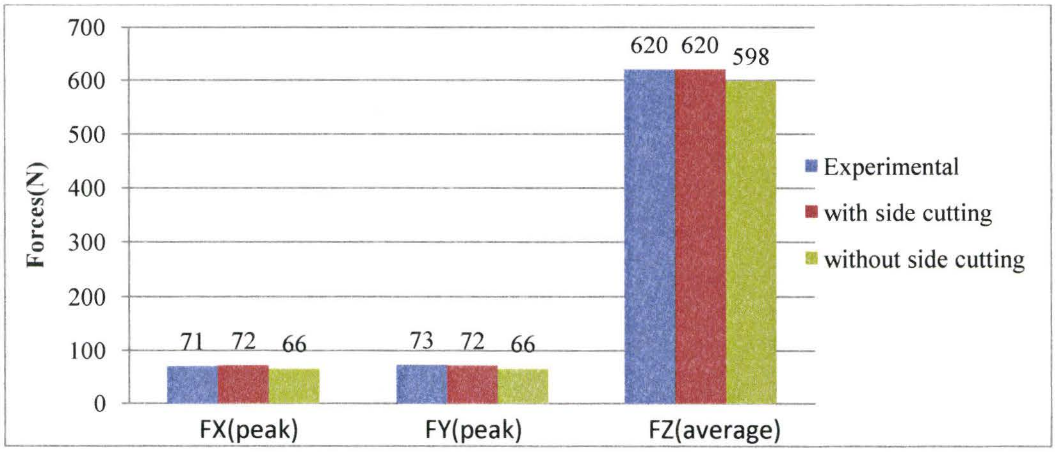

Figure 3-12 Predicted and measured cutting forces at 13500 rpm for a) 4.95mm and b)6.25 mm depth of cut

Chapter 4: Experimental Set Up

4.1 Introduction

Plunge milling tests were conducted to determine the cutting coefficient model to be used in the simulation as well as to validate the proposed model for plunge milling with single and double inserts for systems with rigid and flexible workpiece. In this chapter, the experimental set up used in plunge milling is described and the test matrix is given for each set of experiments. The experimental setup was comprised of machining centre, and force and displacement measurement systems as explained in the following subsections.

4.2 Experimental Set up

The cutting tests were performed on Matsuura FX-5G vertical milling machine using plunge milling cutter sandvik R210-025A20-09M of 25 mm diameter using PVD coated carbide inserts. The 3-axis high speed vertical milling machine, with 27 HP spindle power, 25 mm/min feed rate and a maximum spindle speed of 27000 rpm, has the capability to machine medium size components due to its large machining envelope (1020 mm X 560 mm X 400 mm). Coolant was used to avoid chip jamming and overheating in the hole that can lead to tool damage.

Cutting force and vibration signals in three directions (x, y, z) were measured using a three component dynamometer and three piezoelectric accelerometers respectively to be compared to the simulated results to check the ability of the proposed model to predict cutting force and vibration. The 3-component force measurement dynamometer (Kistler 9255B) was fixed on the moving table of the machine to measure three orthogonal components of the cutting force. The dynamometer has high rigidity (> 2 kN/μm in x and y directions and > 3 kN/μm) and high natural frequency (~ 3 KHz in x, y and z direction) which make it very efficient for cutting force measurements for milling and grinding applications.. The vibration of the system (i.e. tool and workpiece) in three directions was measured using three low impedance, voltage mode, piezoelectric accelerometers (Kistler 8702B) mounted on the workpiece in the x, y and z direction using threaded 10-32 UNF studs. The acceleration measuring range is of 50 g with a sensitivity of 98.9 mV/g and a frequency response of 10 kHz to cover the frequency range of system dynamics. The measured cutting force charge signal was converted into proportionally controlled voltage using Kistler 5010 charge amplifier. Both signals were amplified and filtered and acquired using an 8 channel data acquisition card and a PC software application developed in LabView. Force and vibration measurement was triggered using the developed 6 channel LabView software and recorded for further study and analysis. All signals were recorded with a sampling frequency of 10000 Hz to minimize the possibility of aliasing and to capture small variations in both signals to obtain better measurement results.

Experimental cutting tests were conducted on a 290 x 290 x 30 mm Al 356 rectangle block used for die and mold making. The aluminum block was mounted on the dynamometer by means of four bolts. The plunge milling tool was balanced before cutting to minimize the tool unbalance at high rotational speed which can affect the validation of the model. The cutter was balanced up to 20000 rpm, which is acceptable for the range of speeds used in the cutting tests to be performed. Axial and radial runout (i.e. tool eccentricity) were measured and it was found that the tool has 9 μm of radial eccentricity and 5 μm of axial runout on the same insert. Experimental modal analysis was performed on both the plunge milling cutter and the workpiece to determine their dynamic properties to be used in the simulation model for validation. Experimental validation of the model were carried out using one insert as well as plunge milling tests using two inserts. This aimed to elaborate the ability of the proposed model to simulate the dynamics of plunge milling with different number of inserts. Figure 4-1 shows the equipment used in experimental work with a detailed view of setup used in plunge milling tests in Figure 4-2.

Figure 4-1 Equipment used in Experimental work.

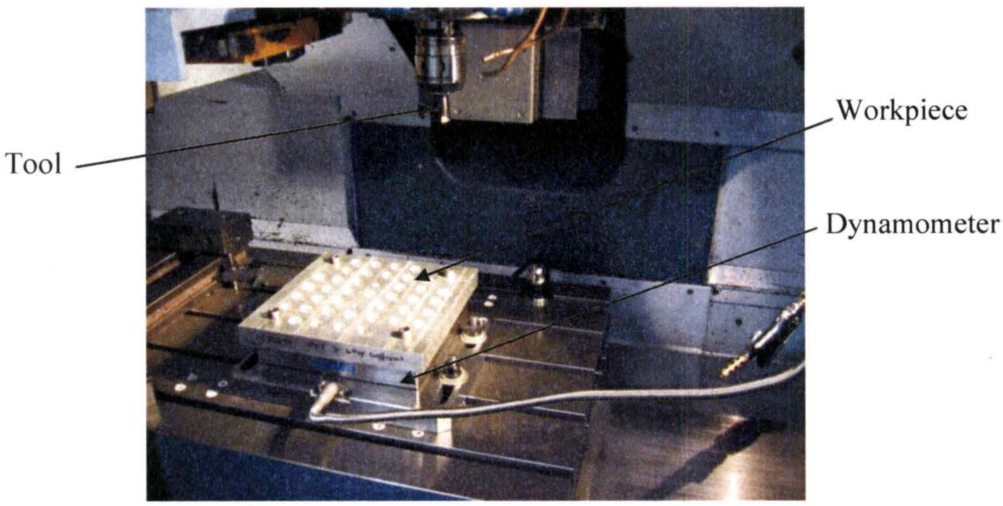

Figure 4-2 Setup used for plunge milling tests.

4.2.1 Balancing

The plunge milling tool is balanced when mounted in the tool holder before performing cutting in order to reduce the tool unbalance when cutting at high rotation speed. The balancing of the tool is done using Best Balancing 2000-2000 Plus, which determines the amount and location of unbalance and recommends corrections. The balancing method used was balancing with weight displacement which requires two weights with the same mass mounted on the tool holder. The two weights are moved and located along a guide at specific angular position determined by the balancing machine based on a specific unbalanced amount. Figure 4-3shows a view of the balancing machine used with the panel showing the output of the test and the location of unbalance. After balancing, the plunge milling cutters used for cutting coefficients determination and plunge milling tests were shown to be able to achieve 20000 rpm of rotational speed. The achievable speed limit is acceptable for the cutting tests to be performed as the maximum operational speed of the plunge milling cutter is set to be 17000 rpm.

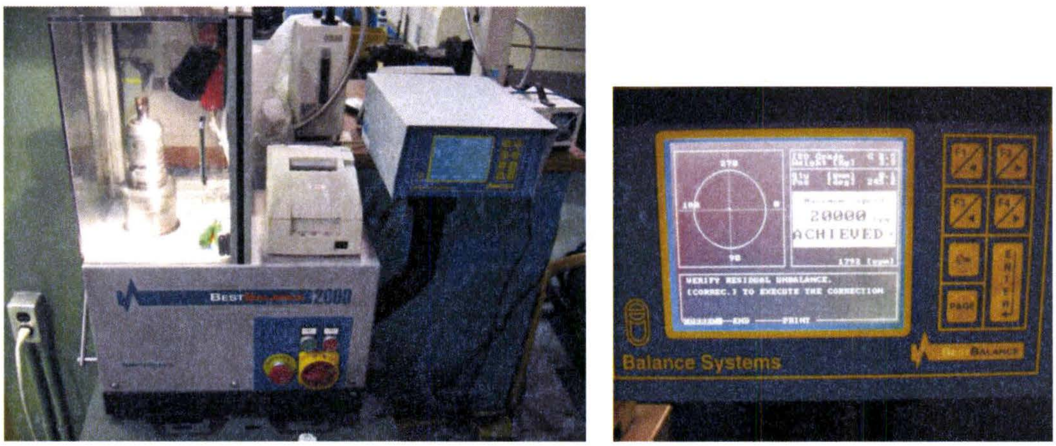

Figure 4-3 View of the used balancing machine.

4.2.2 Radial and Axial runout

Axial and Radial runout (i.e. tool eccentricity) were measured in order to account for their effect on the measured cutting forces and vibrations. The measured values of radial and axial runout are used in the simulation model for comparison with the measured data to validate the model. Mechanical comparator was used in the measurements with a scale value of 1 μinch. The eccentricity between the tool centre and spindle axis of rotation was measured in the radial direction while the tool is mounted on the machine spindle. Readings of the radial position of each insert were taken using the dial gague at specific angular position and the difference between the two readings corresponds to the double of tool eccentricity, which is equivalent to the radial runout. On the other hand, the axial runout was determined by measuring the relative axial position of the two inserts at a specific angular position of the mounted tool. It was found that the tool has a 9 μm of radial runout and 5 μm of axial runout.

4.2.3 Modal analysis

Experimental modal analysis was performed to extract the modal parameters of the plunge milling cutter as well as the workpiece and fixture in order to study the structural parameters that can affect the dynamics of the process. The FRF of both the tool and the workpiece were identified through impact modal tests. Kistler 9726A hammer was used to induce an impact force to the tested structure. Force transducer Kistler 9726A5000 was connected to the hammer to measure the force signal used to compute the FRF. Kistler type 8778A500 accelerometer was used to measure the induced response to compute the FRF. HP 35670A dynamic signal analyzer was used for signal conditioning and analysis in order to obtain both the response and excitation signals as well as the computed FRF of the measured system. A coherence function is used to ensure the validity of the measured FRF. The coherence function is used to check the accuracy of the measurement. A high value of coherence function (i.e. almost unity) demonstrates low noise level and that the measured vibration signal is due to the applied input force. The measurements were considered acceptable at a coherence function higher than 0.90 at a frequency corresponding to FRF peak. Averaging of the measured FRF is used to attenuate the noise and smooth the measurements. An average of ten measurements was used which shown to be sufficient to obtain a reliable FRF of the measured structure. Impact test was performed to measure the workpiece and tool modes in x, y and z directions. Additionally, the torsional and coupled torsional axial modes of the tool were measured. The torsional mode is measured by attaching the accelerometer on one tooth and applying the impact on the other tooth tangentially. On the other hand, the effect of bending mode was minimized by selecting a small overhang length of the cutting tool during machining. Additionally, most of the cutting tests were carried out using a milling cutter with two symmetrical equidistant inserts. This will lead to force cancellation in the radial direction, and hence, minimizing the effect of bending vibration of the tool. The coupled torsional-axial mode is measured by attaching the accelerometer axially on one tooth and applying the impact on the other tooth tangentially. However, based on the configuration of the cutting tool (i.e. solid cylinder), torsional-axial coupling would not be remarkable. This fact is backed up by the high rigidity of the measured coupled torsional-axial mode. Table 4-1 and Table 4-2 give the measured modal parameters of both the tool and the workpiece at the location of highest flexibility respectively. Figure 4-4 shows the equipment used in the modal testing. A close up of the measurement of tool mode in the x direction is shown in Figure 4-5.

Figure 4-4 Setup of experimental modal testing

Figure 4-5 Modal testing measurement of X mode of the tool

Table 4-1 - Measured modes of the cutting tool.

Mode	*Natural frequency (Hz)*	*Damping ratio (ξ)*	*Stiffness(K)* $*10^6$
X	1600	0.1	25 N/m
	2050	0.0207	20 N/m
Y	1530	0.097	25 N/m
	2100	0.016	22 N/m
Z	2960	0.03	332 N/m
	6918	0.023	517 N/m
Z-θ	5102	0.045	209 N/m
θ	3900	0.0558	$9.9 * 10^{-2}$ Nm/rad
	5151	0.015	$12 * 10^{-2}$ Nm/rad

Table 4-2 - Measured natural modes of the workpiece.

Mode	*Natural frequency (Hz)*	*Damping ratio (ξ)*	*Stiffness(K)* $*10^6$
X	1950	0.02	90 N/m
	6643	0.0142	300 N/m
Y	2117	0.016	95 N/m
	3520	0.041	200 N/m
Z	1750	0.02	70 N/m
	2027	0.023	90 N/m

4.3 Experimental Design and parameters

Experimental work can be categorized as shown in Figure 4-6 which describes briefly the different phases of experiments carried out. Detailed description of each phase is provided in the corresponding subsections.

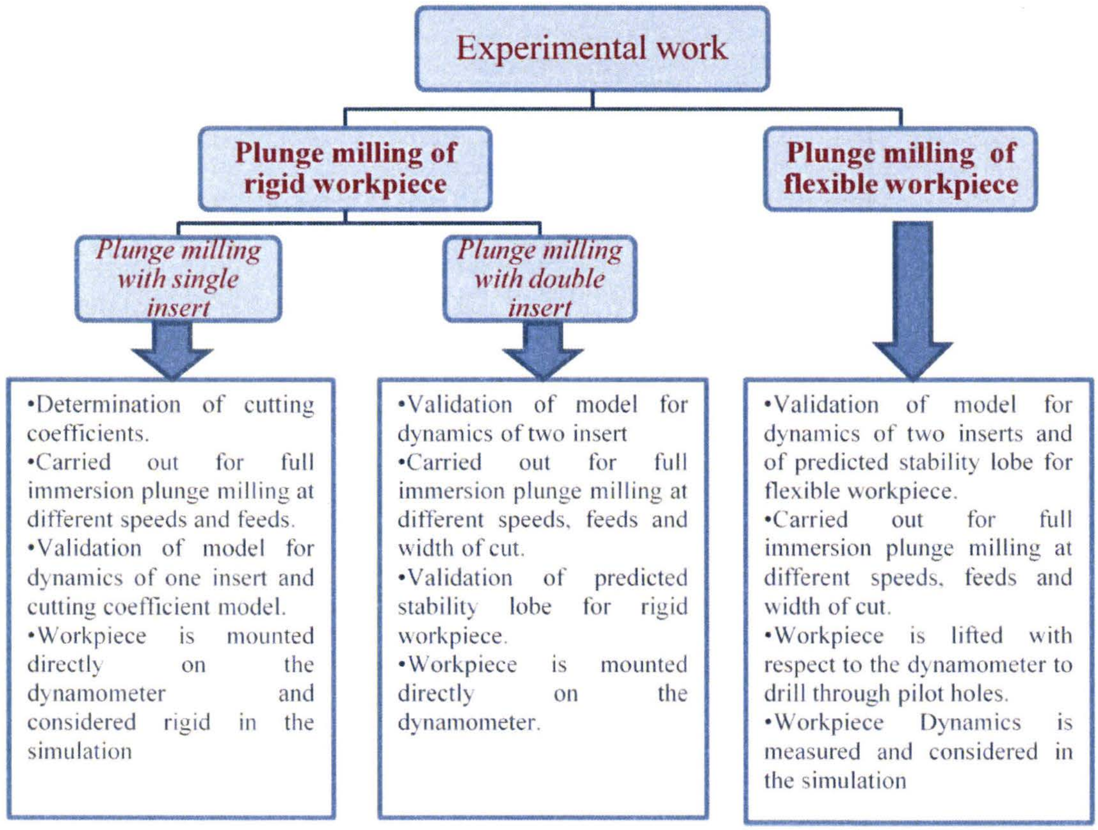

Figure 4-6 Layout of experimental work.

4.3.1 Plunge milling with single insert

Experimental cutting tests were carried out in order to validate the proposed time domain simulation of the plunge milling process as well as to identify the cutting coefficients. Cutting tests were performed in two sets of experiments. In the first group (*Phase I*), plunge milling tests with one insert were carried out to evaluate the cutting force coefficients and validate the coefficient model used in the mechanistic model for accurate prediction of the cutting forces in the simulation model. The tests were carried out at different feeds and speeds with a constant width of cut on a rigid workpiece mounted directly on the dynamometer, which was mounted on the machine table. Table 4-3 describes the cutting conditions used to calibrate and determine the cutting coefficients. The cutting conditions used for calibration were selected to cover the speed and feed ranges used in plunge milling cutting tests. The range of feed rate used for coefficient determination is selected to cover the expected value of uncut chip thickness to be cut by main and side edges. Additionally, plunge milling tests with one insert were conducted at different cutting conditions used for cutting coefficient determination to validate the extracted coefficients and to check the ability of the model to simulate the dynamics of plunge milling with a single insert.

Table 4-4 shows the test matrix used to validate the cutting coefficient model.

Table 4-3 Test matrix for cutting coefficient determination tests

Experiment index	Speed (rpm)	Feed (mm/tooth)	Width of cut (mm)	Number of tests
1	11000	0.005	2.5	3
2	17000	0.005	2.5	3
3	11000	0.01	2.5	3
4	17000	0.01	2.5	3
5	11000	0.05	2.5	3
6	17000	0.05	2.5	3
7	11000	0.07	2.5	3
8	17000	0.07	2.5	3
9	11000	0.1	2.5	3
10	17000	0.1	2.5	3

Table 4-4 - Test Matrix for cutting coefficient model validation

Experiments number	Speed (rpm)	Feed (mm/tooth)	Width of cut (mm)
1	11000	0.03	2.5
2	15000	0.03	2.5
3	17000	0.03	2.5
4	11000	0.085	2.5
5	15000	0.085	2.5
6	17000	0.085	2.5

4.3.2 Plunge milling with double inserts

In the second phase (*Phase II*), experiments were carried out using a plunge milling cutter with two inserts at different cutting speeds, width of cut and axial feed. In this phase, experiments were carried out for rigid and flexible workpiece to validate the predicted stability lobe as well the simulation model for both systems. The cutting conditions used in experimental validation were selected to cover a wide range of speeds, feeds and width of cuts to test the correctness of the model as well as its limitations. Additionally, the combination of speed, feed and width of cut was selected to cover various cases of stable and unstable cutting for both cases of rigid and flexible workpiece at different locations of the stability lobe. For case of system with rigid workpiece, the setup was similar to the one used for *Phase I*, at which the workpiece was directly mounted on the dynamometer and hence, considered rigid. However, for system with flexible workpiece, the workpiece was lifted using two rectangular parallels on two of the four edges of the plate to be able to generate through pilot holes. This arrangement leads to a dominance of workpiece dynamics in the axial direction compared to the cutter and hence, workpiece dynamics is considered in this phase. Table 4-5 show the test matrix for experiments used model validation for systems with a rigid and flexible workpiece with plunge milling with double inserts.

Table 4-5 Test matrix for plunge milling tests for rigid and flexible workpiece.

Experiment number	Speed (rpm)	Feed (mm/tooth)	Width of cut (mm)
1	11500	0.07	3.76
2	11500	0.07	4.95
3	11500	0.07	6.25
4	12000	0.086	7.5
5	12600	0.07	3.76
6	12600	0.07	4.95
7	12600	0.07	6.25
8	12750	0.0809	7.5
9	13000	0.0795	7.5
10	13500	0.07	3.76
11	13500	0.07	4.95
12	13500	0.07	6.25
13	14750	0.07	3.76
14	14750	0.07	4.95
15	14750	0.07	6.25
16	16000	0.07	3.76
17	16000	0.07	4.95
18	16000	0.07	6.25

Chapter 5: Plunge Milling with Single Insert

5.1 Introduction

The accurate determination of cutting coefficients is of a great importance in the simulation and modeling of cutting processes. Cutting coefficient models are very important in computing and predicting the cutting forces, which are very crucial to the success of any simulation model to be able to simulate the cutting process. Experiment cutting tests were carried out to determine the specific cutting coefficients as well as to validate the cutting coefficient model to be used in the simulation model. Additionally, the validity of the simulation model for case of plunge milling with single insert was checked to determine the ability of the model to simulate the process dynamics when only a single insert is cutting, which is similar to the case of intermittent plunge milling. Cutting tests were performed for full immersion plunge milling with the same combination of milling cutter and workpiece used in actual cutting.

5.2 Cutting Coefficient Model Determination

5.2.1 Experimental work

The key issue in the mechanistic model is the accurate determination of cutting coefficients, which correlate the cutting force to the chip load for specific tool/workpiece material and geometry combination. The cutting force coefficients were identified by series of chatter-free plunge milling cuts performed on 20 mm diameter pilot holes to achieve constant width of cut. The pilot holes were enlarged to 25 mm diameter using the plunge milling cutter with single insert. A single insert was used to introduce a theoretical variation in the cutting forces in x and y directions to determine tangential and normal cutting coefficients for the case of plunge milling with full immersion. The cutting tests were performed on the same workpiece material and geometry and the same milling machine used in plunge milling tests. This eliminates any variability due to workpiece and spindle rigidity on the measured results that could affect the analysis and hence, the accuracy of coefficients determination. Tests were carried out at different feeds and speeds to determine the effect of process parameters on cutting force coefficients. Pilot holes were drilled to a diameter of 20 mm using an end mill drill for better surface finish when compared to those produced by a centre drill. The workpiece in this group of experiment is considered rigid as it is clamped directly on the force dynamometer, which is mounted directly to the machine table. The actual depth of cut of each test is considered by comparing the measured diameter of the enlarged hole to the pilot hole. This aims to consider any possible effect of the bending mode of the tool.

The cutting force coefficients dependency on cutting conditions (i.e. speed and feed per tooth) was studied statistically from the experimental results. Two-way analysis of variance (ANOVA) was performed to study the dependency of cutting coefficients on both variables (i.e. speed and feed rate). F-test is applied to determine the most significant parameter(s) that affect the response (i.e. cutting coefficient) to avoid the effect of non significant parameter on the cutting coefficient mode. Statistical significance is tested by comparing the F-test statistic to the value of F-distribution table with L-1 and n-1 degrees of freedom where L and n are the experiments levels of the independent variables feed and speed respectively. The levels used for cutting coefficient determination were 5 levels of feed rate (0.005, 0.01, 0.07, and 0.1 mm/tooth) and 2 levels of speed (11000 and 17000 rpm). Therefore, the degrees of freedom used in the F-test were 4 DOF for feed and 1 DOF for speed. A confidence level of 95 % was used in the analysis which corresponds a significance level α of 0.05. From the F-distribution tables, for a significance level of 0.05 for 4 degrees of freedom in the numerator and 1 degree of freedom in the denominator, it was found that the critical F value is 224.6. Therefore, an independent variable is considered statistically significant if its value of F-test statistic is higher than 224.6 which corresponds to the critical F value found from the F-distribution tables. Table 5-1, Table 5-2 and Table 5-3 show the F-test results for Kt, Kn and Kf respectively as dependent variables with respect to the feed and speed.

Table 5-1 F-test results for Kt vs feed and speed

Source	DF	SS	MS	F	P
Feed	4	18221687	4555422	53776.53	0.000
Speed	1	85	85	1.00	0.374
Error	4	339	85		
Total	9	18222110			

Table 5-2 F-test results for Kn Vs feed and speed

Source	DF	SS	MS	F	P
Feed	4	7091012	1772753	53776.53	0.000
Speed	1	33	33	1.00	0.374
Error	4	132	33		
Total	9	7091177			

Table 5-3 F-test results for Kf Vs. feed and speed

Source	DF	SS	MS	F	P
Feed	4	33837366	8459342	15105.97	0.000
Speed	1	2560	2560	4.57	0.099
Error	4	2240	560		
Total	9	33842166			

It was found based on the test results that cutting force coefficients vary significantly as a function of feed per tooth for the studied range of cutting conditions whereas, cutting coefficients were not found to be affected by the variation of cutting speed which can be shown in Figure 5-1. This observation is in accordance with the fact that Aluminum is not speed sensitive as it does not strain harden during machining. The relation between cutting force coefficients and feed per tooth was determined by fitting the experimental data using the best fitted curve using least square error as shown in Figure 5-2. The cutting force coefficients were better expressed as a nonlinear function of the uncut chip thickness (i.e. feed per tooth (mm/tooth)) which showed the better fit with the experimental result with a coefficient of correlation R^2 ranging from 95.54% to 98.35 % where the proportionality constant (p) and the power (q) can be determined from the experimental results. The cutting coefficients are given as a function of the feed per tooth (i.e. chip thickness) by the power function:

$$K = p * h^{-q} \tag{5.1}$$

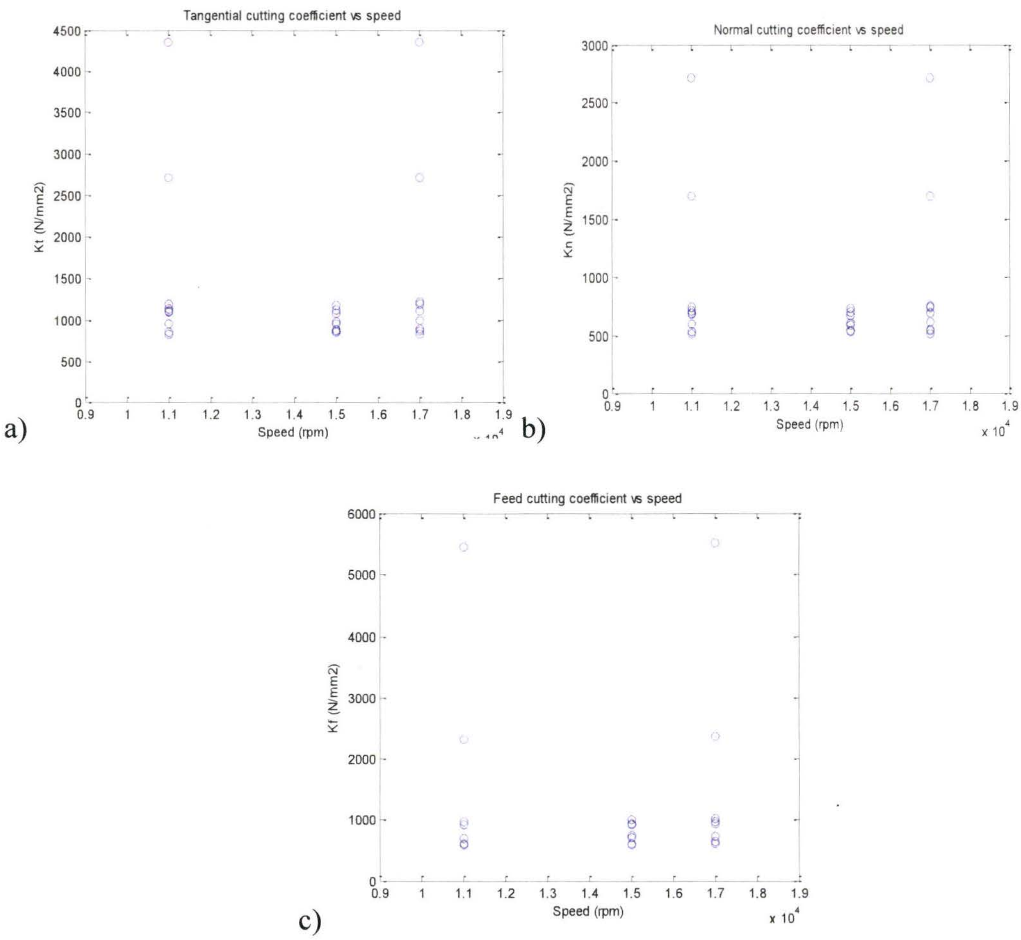

Figure 5-1 Variation of cutting coefficients Vs. speed in a) Tangential, b) Normal and c) feed direction

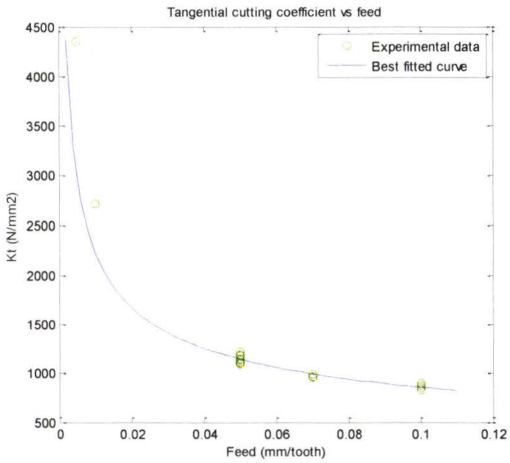

a)

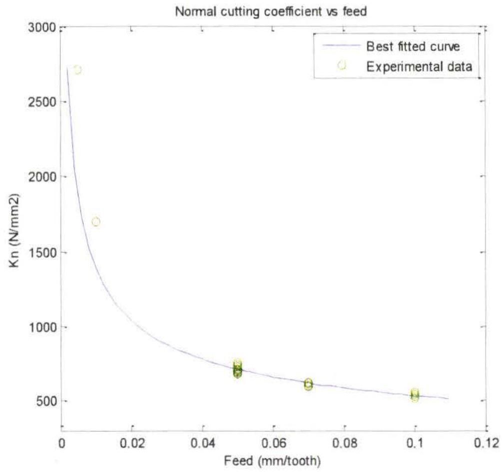

b)

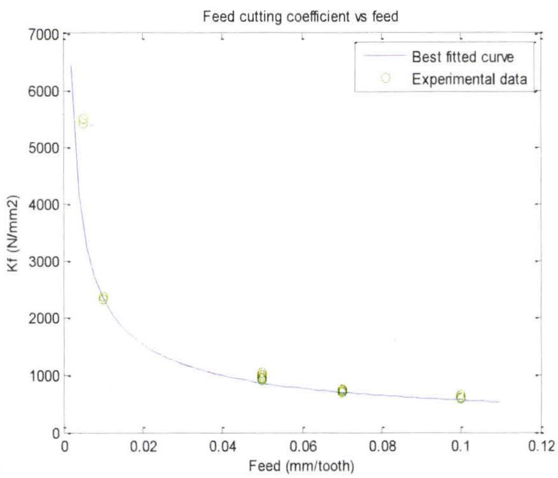

c)

Figure 5-2 Cutting coefficient Vs. feed in a)Tangential, b)Normal and c)feed direction

Table 5-4 shows the calibrated values of the equation constants from experimental data for the cutting coefficients in tangential, normal and axial direction. As a result of cutting coefficients variation as a function of chip thickness, the cutting coefficients are computed instanteneously for each insert in the simulation model based on the actual dynamic chip thickness cut by each insert which vary as a result of system vibrations and tool setting errors.

Table 5-4 Calibrated constants for cutting coefficient model

	P *(N/mm²)*	*Q*
Kt (N/mm²)	325.17	0.418
Kn (N/mm²)	202.85	0.418
Kf (N/mm²)	130.33	0.628

5.3 Experimental validation of cutting coefficient model (Plunge milling with single insert)

5.3.1 Experimental work

Experimental validation of the simulation model was done for the case of plunge milling using one insert. The first set was carried out with a cutter with one insert used in the cutting coefficient determination. This was done to validate the correctness of the cutting coefficient model as well as to validate the ability of the model to deal with the process dynamics with only one insert cutting and for the case of a rigid workpiece. Furthermore, this can determine the ability of the proposed model to simulate intermittent plunge milling in which only one insert is cutting. In this phase, an Aluminum workpiece was directly mounted on the dynamometer. Pilot holes of the same diameters (20 mm) were produced using one insert. Cutting tests were performed at cutting speeds and feeds which are different from the conditions used in the determination of the cutting coefficients but within the studied range of speeds and feeds. This aims to check the accuracy of extracting the cutting coefficients as well as to validate the model for the case of one insert. Additionally, the use of single insert aims to check the ability of the model to correctly compute the cutting area without the influence of other factors present with the use of double inserts that can affect the evaluation of the cutting area (i.e. radial and axial runout).

5.3.2 Results

Chatter-free plunge milling tests with a single insert were performed on a rigid workpiece to validate the identified cutting coefficients for a feed rate range from 0.005 to 0.1 mm/tooth. The predicted and experimental cutting forces for the case of a single insert plunge milling operation carried out at different cutting conditions are shown in Figure 5-3, Figure 5-4 and Figure 5-5. The validity of the mechanistic model using the determined cutting force coefficients was checked at various cutting conditions within the range of the test matrix but not used in the determination of the cutting coefficients. A good agreement in the magnitude and trend can be noticed between the simulated and the measured cutting forces. This validates the cutting coefficient power model as well as the ability of the simulation model to deal with the dynamics of a single insert. The maximum deviation between the measured and predicted cutting forces for cases used for validation was shown to be less than 5% for all the cases. Cutting forces Fx and Fy showed an oscillating trend in both the predicted and measured results for both cases. This is explained by the fact that cutting is carried out by one insert and no cancellation of force by the other insert occurs. In experimental results, an oscillation in the measured axial Fz was observed. This can be attributed to a misalignment between the centre line of the pilot hole and the centre of the plunge milling cutter used to enlarge it, which was not considered in the model. This can lead to an uneven width of cut during cutting which vary periodically at each cutter revolution.

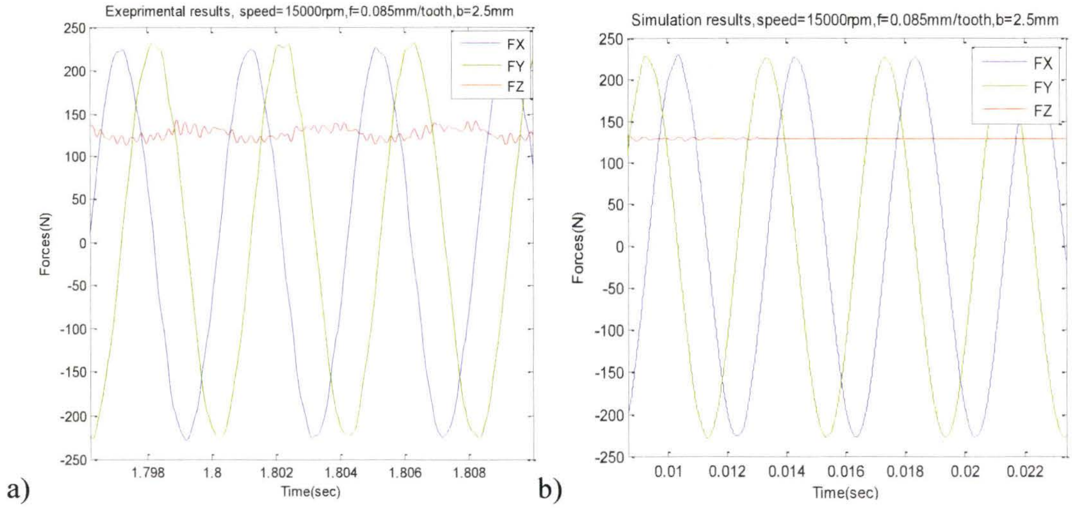

Figure 5-3 a) Measured and b) predicted cutting forces at 15000 rpm, 0,085 mm/tooth and 2.5 mm.

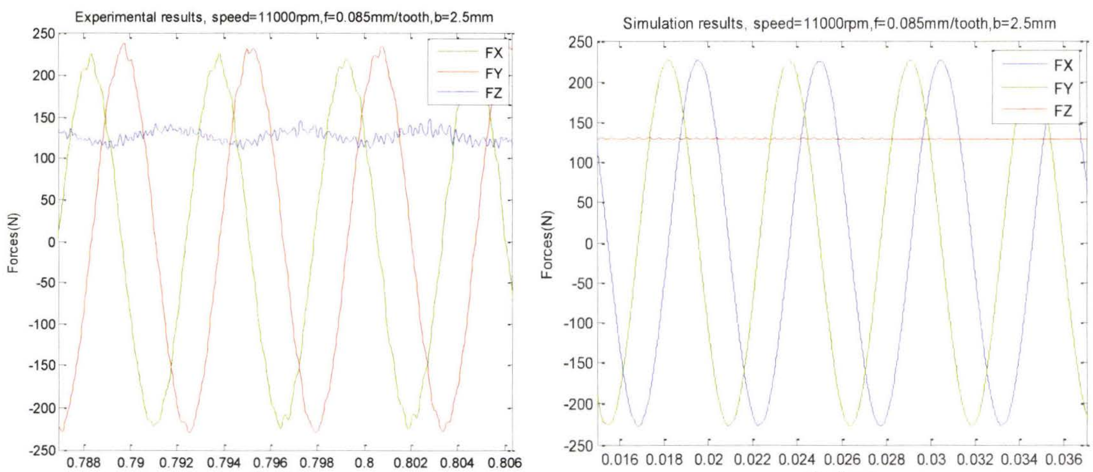

Figure 5-4 a) Measured and b) Predicted cutting forces at 11000 rpm, 0.085 mm/tooth, 2.5mm

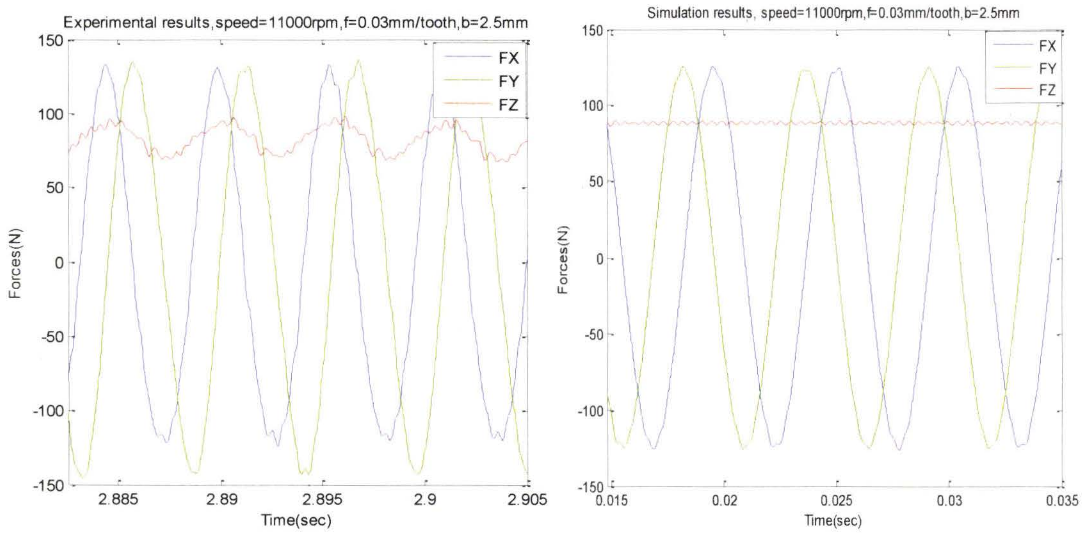

Figure 5-5 a) Measured and b) Predicted cutting forces at 11000 rpm, 0.03 mm/tooth, 2.5 mm

Figure 5-6, Figure 5-7 and Figure 5-8 show the comparison between the measured and predicted cutting forces in the axial, x and y directions respectively for different values of feed per tooth. It can be noticed that there is a good agreement between the experimental and simulation results of the cutting forces over the whole range of the studied feed rate with a deviation ranging from 1.5 % to 8%. It can be concluded that the simulation model was able to correctly simulate the dynamics of plunge milling with a single insert cutting. Additionally, the good agreement between the measured and predicted cutting forces validates the proposed simulation model for a single insert as well as it validated the correctness of the cutting coefficient model over the tested range of speed and feed rate.

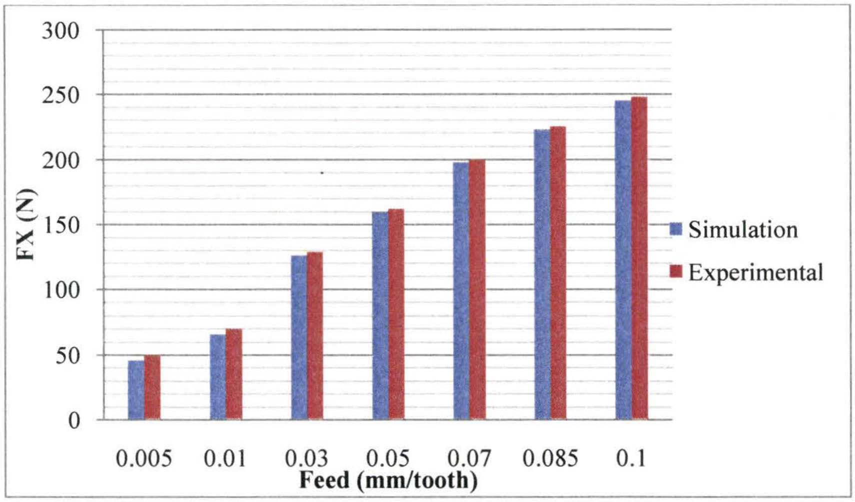

Figure 5-6 Magnitude of measured and predicted FX at different feeds.

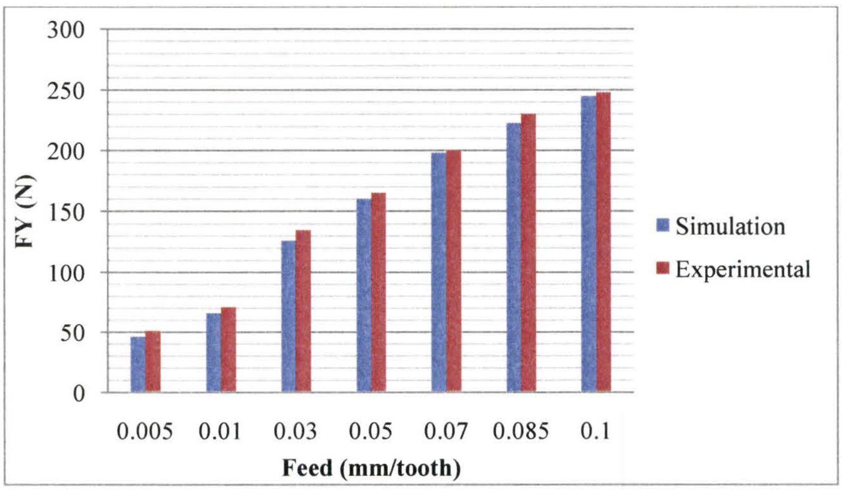

Figure 5-7 Magnitude of measured and predicted FY at different feeds.

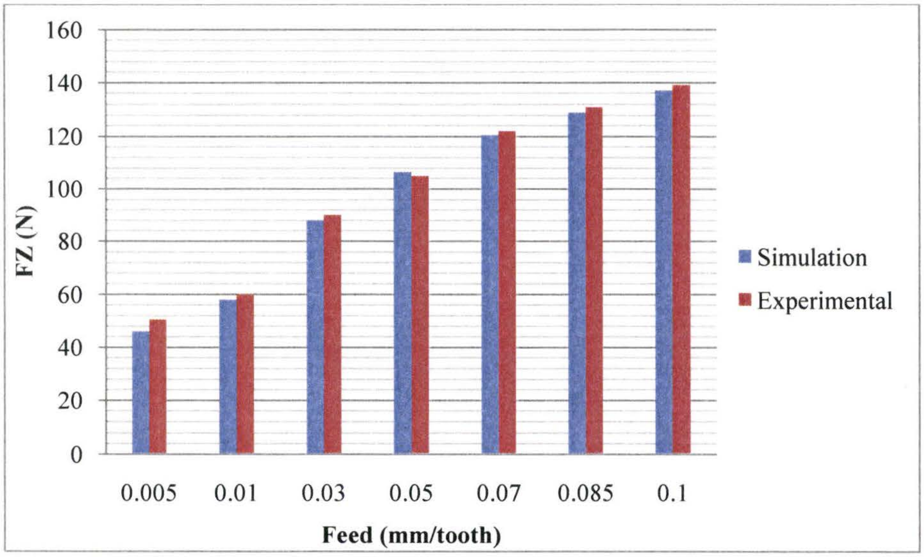

Figure 5-8 Magnitude of measured and predicted FZ at different feeds.

Chapter 6: Plunge Milling of A Rigid Workpiece

6.1 Introduction

In this chapter, plunge milling for a system with a rigid workpiece is studied experimentally and numerically. Experimental cutting tests were carried out to validate the proposed model as well as the predicted stability lobe for a rigid workpiece. This aims to check the ability to deal with the dynamics of double inserts cutting at the same time as well as to check the correctness of the dynamic model and the cutting coefficient model.

6.2 Experimental work

Experimental cutting tests were carried out to validate the simulation model as well as the predicted stability lobe for plunge milling of systems with a rigid workpiece. For this case, the set up is similar to the one used for cutting coefficient determination where the workpiece was mounted directly to the dynamometer and is considered rigid. Experimental validation was carried out at different speeds, feeds and width of cuts to cover a wide range of cutting conditions representing different cases of stable and unstable cutting to study the process stability and to validate the presented model when considering the dynamics of the tool only. Drills of different diameters were used to generate through pilot holes with different diameters to achieve a variation in the width of cut. This helps to validate the predicted cutting force, dynamic chip area and stability limits of plunge milling from the time domain simulation model. The holes were then enlarged using plunge milling a cutter to a diameter of 25 mm and depth of 15 mm (i.e. half of the plate thickness) using two PVD coated carbide inserts.

6.3 Results and discussion

Plunge milling cutting tests with two inserts were carried out to validate the proposed model at different cutting speeds, feeds and width of cut for the case of a rigid workpiece. This aims to check the ability of the model to deal with the dynamics of two inserts plunge milling, which includes the effect of radial and axial runout and their effect on the dynamic chip area. The workpiece for this case is considered rigid based on setup and only the cutter dynamics is considered in the simulation. On the other hand, cutting coefficients used in the mechanistic model are computed based on the actual chip thickness removed by each insert at each time step. This aims to consider the variation of chip thickness between inserts based on radial and axial runout and system vibrations, which can affect the prediction of cutting forces. Stability lobe diagram of the plunge milling process was predicted using the presented time domain simulation model for a system with a rigid workpiece as shown in Figure 6-1. The dynamics of the cutter used in the simulation are extracted from the experimental modal analysis of the cutter and workpiece. In the simulation, the boundary between stable and unstable cutting conditions is identified through the force and vibration signals, force and/or vibration spectra and phase plots of the cutter. The ratio of dynamic cutting force, predicted using the dynamic cutting force model where the regenerative effects on the chip thickness is considered to the static force, where the cutting system is assumed to be rigid, is used as a chatter stability criterion. Chatter occurrence is indicated by a ratio higher than 1.3 as given in [61]. This criterion is valid for full and half immersion cutting, which is the case in this work, but it has difficulties detecting chatter at small radial immersions. The stability lobe diagram is constructed by running the simulation model at a specific spindle speed while increasing the depth of cut with equal increment until a case of chatter is predicted. Once chatter is predicted, a smaller increment is selected either to increase or decrease the depth of cut to accurately determine the coordinate of the point on the stability lobe that corresponds to the stability limit at the studied rotational speed. The same procedure is performed at different rotational speeds to determine the corresponding stability limit as a function of the depth of cut at which chatter occurs. Cutting tests were planned based on the predicted stability lobe diagram to cover different cutting conditions for stable and unstable cutting. This aims to check the ability of the proposed model to realistically predict the cutting forces and dynamics of the plunge milling process in order to validate the predicted stability lobe diagram and hence, to validate the model.

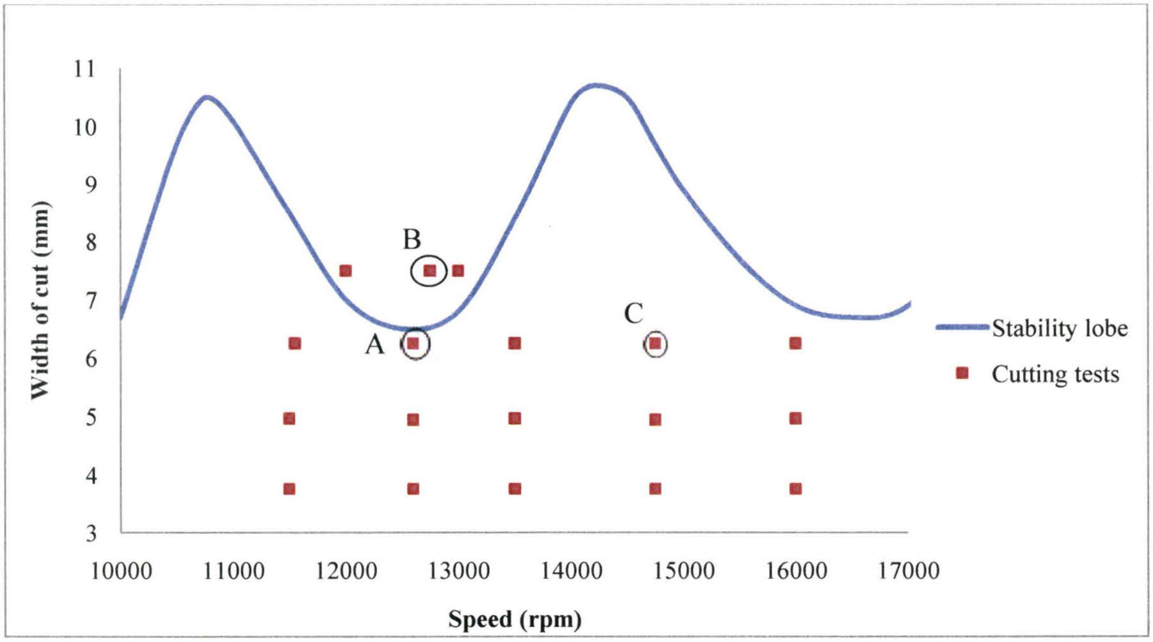

Figure 6-1 Predicted stability lobe diagram for system with rigid workpiece

Stable cutting was found for plunge milling of system with rigid workpiece at 12600 rpm with feed rate of 0.0819 mm/tooth and 6.5 mm width of cut, which corresponds to point A in Figure 6-1. This is demonstrated by the chatter-free signal of measured forces and system vibration as shown in Figure 6-2. This result is in accordance with the predicted stability lobe as this cutting condition is within the stable zone of the predicted stability diagram. Stable cutting is characterized by a dominant FFT peak in Fx and Fy at a frequency corresponding to the rotational speed (i.e. 1 x RPM) as a result of tool setting errors. This is mainly due to the fact that one insert will cut deeper in the workpiece leading to uneven area cut by each insert. This is illustrated by the high peak of force and vibration power spectra at 210 Hz which corresponds to the rotational speed. This is attributed to the radial runout of the tool that appears as a peak at the rotational speed in the lateral directions, X and Y. Additionally, peaks at multiple of the rotation speed were noticed at 480 Hz which corresponds to the tooth passing frequency caused by the forced vibration due to the tool cutting action. The same observation was noticed by Altintas [96, 104, 105] for stable cutting which showed a dominant peak at a frequency corresponding to the rotational speed as a result of radial and axial runout.

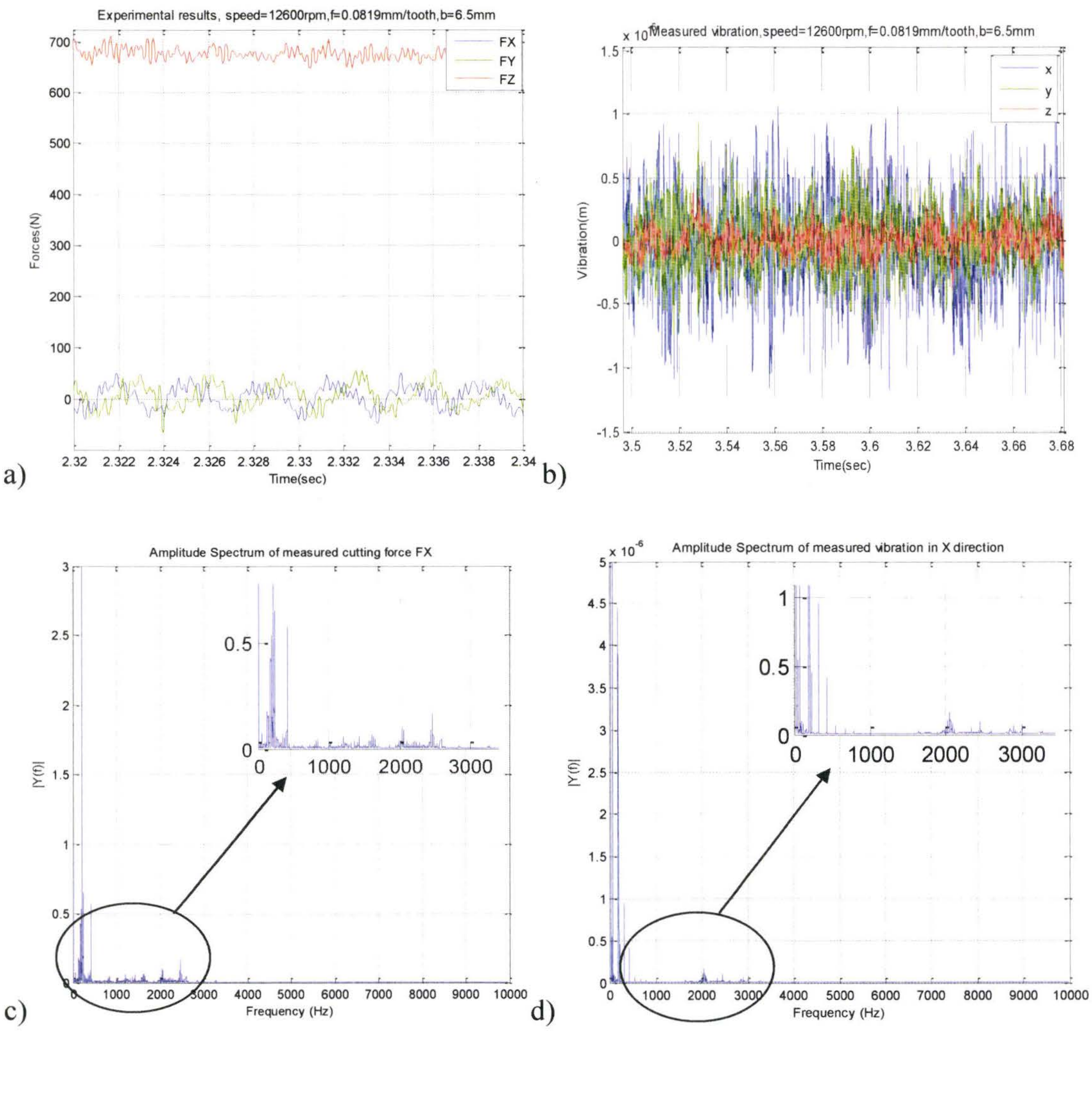

a) b) c) d)

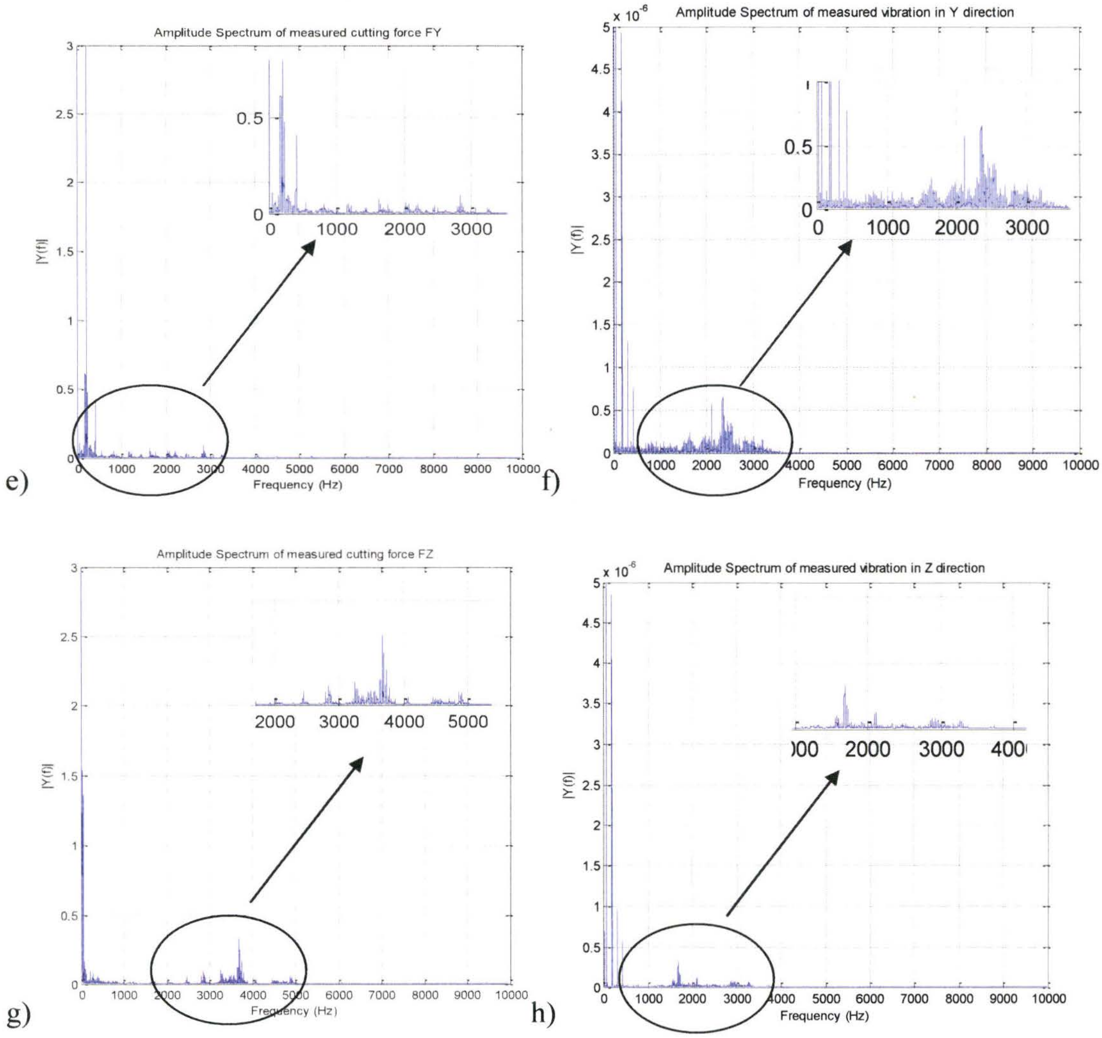

Figure 6-2 Experimental results for stable plunge milling at 12600 rpm, f=0.0819 mm/tooth, b=6.5mm a) cutting forces, b)System vibrations, c) FFT of FX, d) FFT of x vibration, e) FFT of FY, f) FFT of y vibration, g) FFT of FZ, h)FFT of z vibration.

Simulations results of the same cutting condition are shown in Figure 6-3. Similar to experimental results, stable cutting is indicated by the simulation results as shown by the chatter-free predicted cutting forces and system vibrations. Good agreement can be noticed between the measured and simulated cutting forces and system vibrations. This indicates the ability of the model to simulate the dynamics of the plunge milling process for a rigid workpiece and to provide a reliable tool to be used for process planning prior to machining.

This is shown by the agreement in trend and magnitude of forces and vibration in the signal level as well as the frequency components of the signals that is demonstrated in the FFT of both force and vibration signals in x, y, and z directions. In fact, the model was able to predict the cutting force with a maximum deviation of 4 % as compared to 18 % for an available model in the literature [104]. This is mainly attributed to the horizontal approach used in this research to accurately evaluate the cutting area by considering the contribution of both main and side edges into cutting as compared to previous work where only the main edge is considered in the model to evaluate the cutting area [96, 104, 105]. A chatter-free cutting is also observed in the simulated surface generated during cutting. The simulation model was able to predict the waviness of the surface cut by each insert during cutting in order to predict the chip thickness by considering the regenerative behaviour of chatter during cutting. This can enhance the ability of the model to determine the borderline between stable and unstable cutting for the stability analysis of the process. For this cutting condition, it can be shown that the surfaces generated by both inserts are in phase leading to a steady dynamic chip thickness and hence, to stable cutting. The same observation can be noticed from the tool motion plot which shows a synchronized closed orbital motion indicating chatter-free cutting. Similarly, the predicted dynamic chip thickness cut by each insert shows a stable trend indicating chatter-free cutting. The dynamic nature of the chip thickness results from the tool lateral vibration as well as the tool runout which lead to uneven chip load for each insert as shown in Figure 6-3.

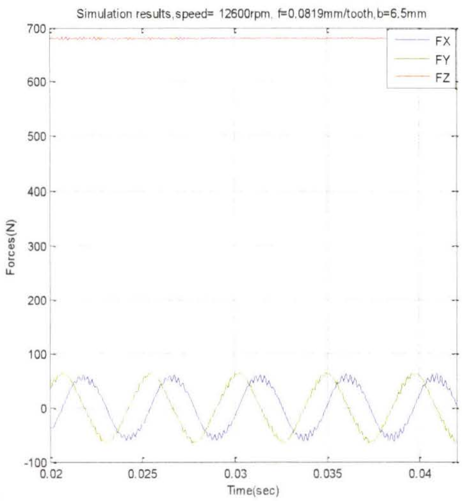

Simulation results, speed= 12600rpm, f=0.0819mm/tooth, b=6.5mm
Forces(N)
Time(sec)
FX
FY
FZ

a)

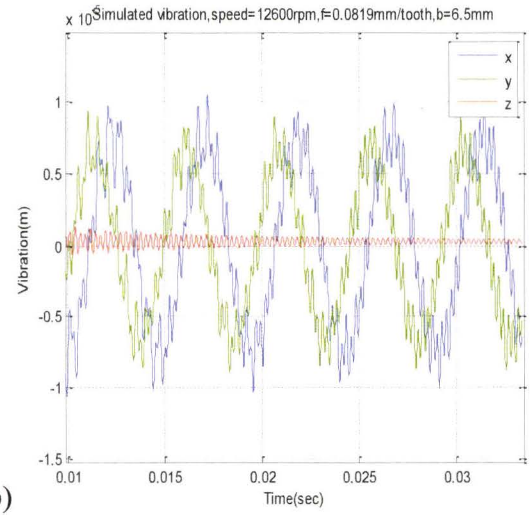

Simulated vibration, speed=12600rpm, f=0.0819mm/tooth, b=6.5mm
Vibration(m)
Time(sec)
x
y
z

b)

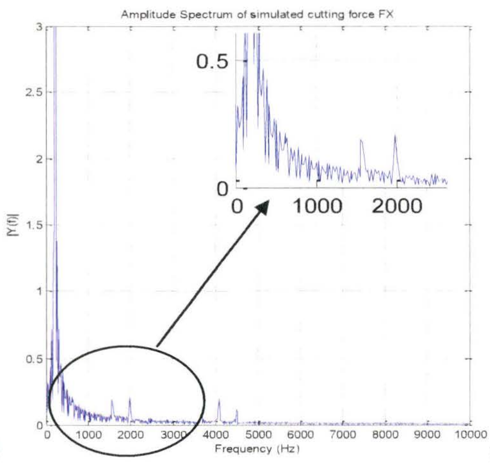

Amplitude Spectrum of simulated cutting force FX
|Y(f)|
Frequency (Hz)

c)

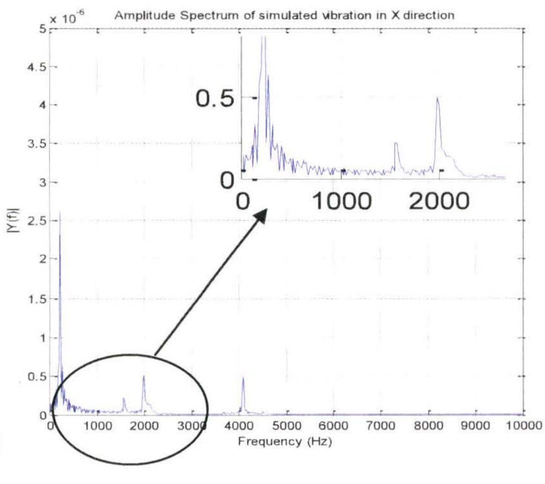

Amplitude Spectrum of simulated vibration in X direction
|Y(f)|
Frequency (Hz)

d)

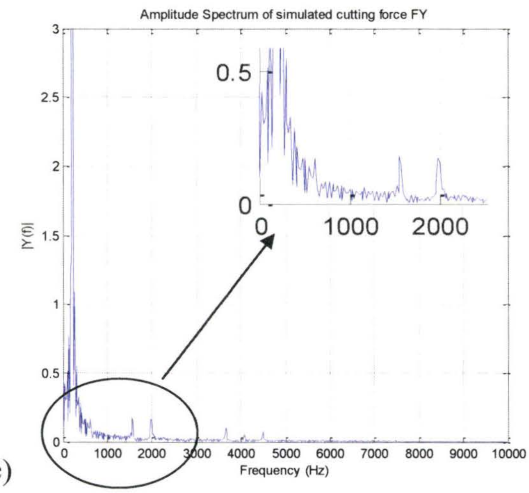
Amplitude Spectrum of simulated cutting force FY
|Y(f)|
Frequency (Hz)

e)

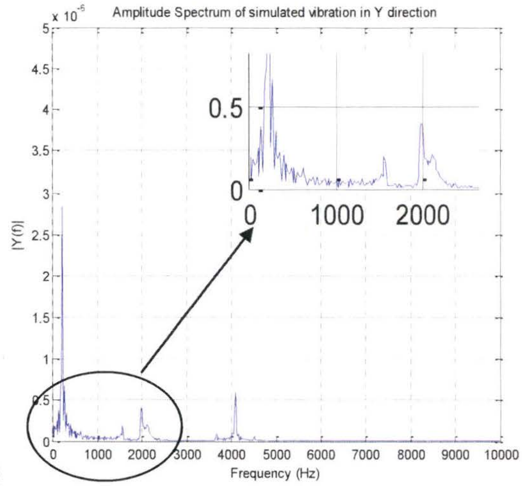
Amplitude Spectrum of simulated vibration in Y direction
x 10^-5
|Y(f)|
Frequency (Hz)

f)

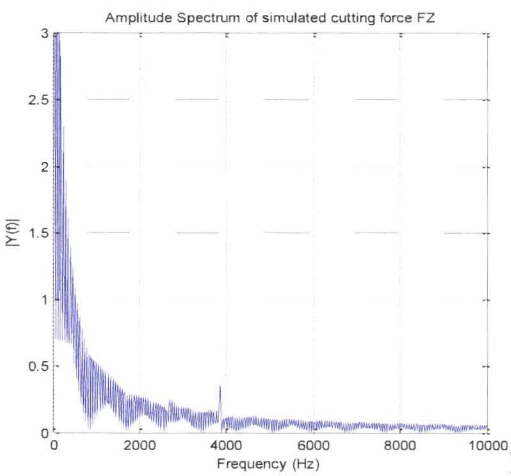
Amplitude Spectrum of simulated cutting force FZ
|Y(f)|
Frequency (Hz)

g)

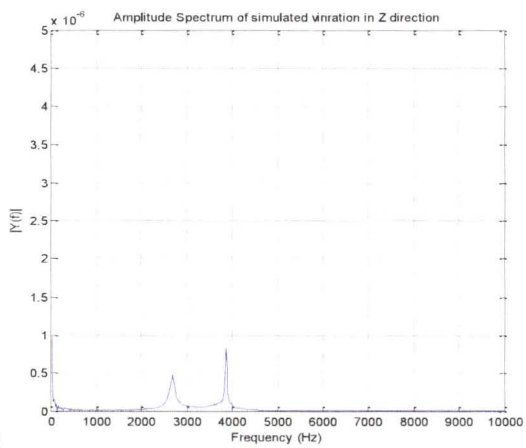
Amplitude Spectrum of simulated vinration in Z direction
x 10^-6
|Y(f)|
Frequency (Hz)

h)

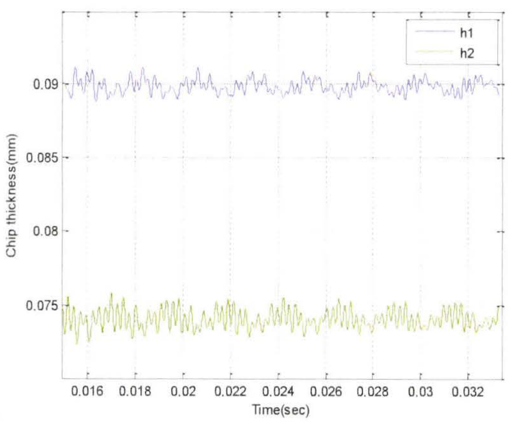
h1
h2
Chip thickness(mm)
Time(sec)

i)

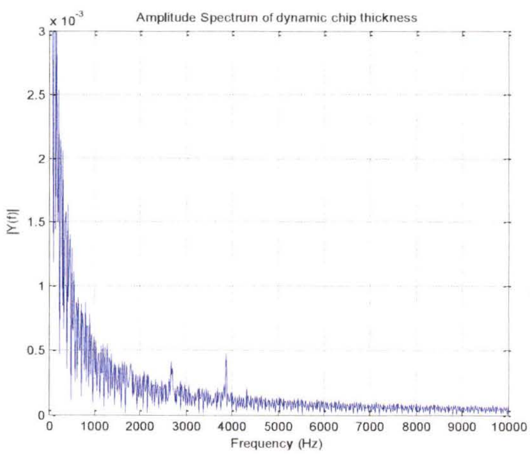
Amplitude Spectrum of dynamic chip thickness
x 10^-3
|Y(f)|
Frequency (Hz)

j)

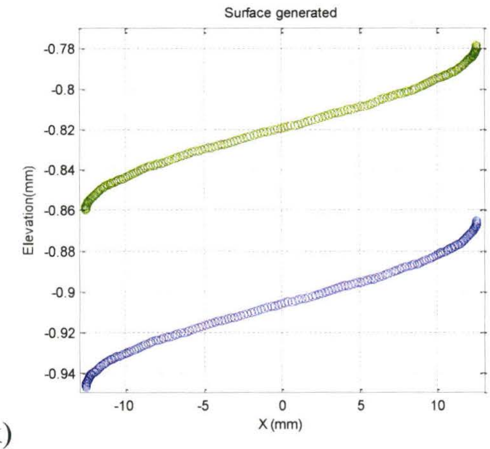

k)

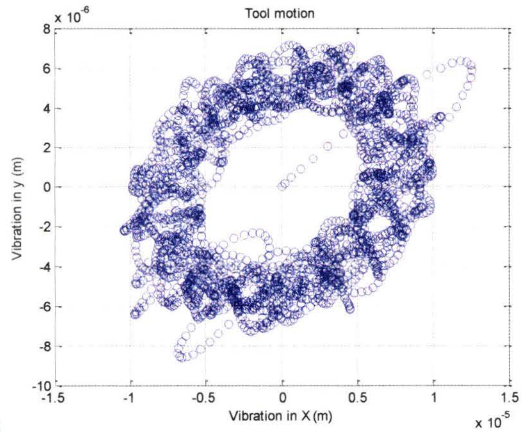

l)

Figure 6-3 Simulation results for stable plunge milling at 12600rpm, f=0.0819 mm/tooth, b=6.5mm a) cutting forces, b)System vibrations, c) FFT of FX, d) FFT of x vibration, e) FFT of FY, f) FFT of y vibration, g) FFT of FZ, h)FFT of z vibration, i) Dynamic chip thickness, k) surface generated, l) tool motion.

Figure 6-4 and Figure 6-5 show the measured and predicted cutting forces and vibrations respectively for plunge milling at 12750 rpm with 0.0809 mm/tooth feed rate and 7.5 mm width of cut which corresponds to point B on stability diagram. A case of unstable cutting can be observed in the measured cutting force and system vibrations of this cutting condition in Figure 6-4. This result validates the predicted stability lobe as this cutting condition belongs to a chatter zone based on the predicted diagram. Chatter behaviour is demonstrated by the characteristic continuously growing trend of measured force and vibration signals, which indicate the occurrence of chatter during plunge milling. It can be noticed for a rigid workpiece, that chatter vibrations are mainly dominated by the tool vibration in the lateral direction (i.e. X and Y). This is mainly attributed to the higher flexibility of the tool in the lateral direction as compared to the other modes specially, to the axial direction where the tool benefits from the axial rigidity of the spindle. This is illustrated by the dominant peaks of power spectrum of measured cutting forces and system vibrations at frequencies corresponding to the tool lateral modes at 1550 Hz and 2080 Hz for Fx and Fy. On the other hand, tool vibration due to torsional vibration appears at a frequency corresponding to the torsional mode at 3400 Hz in the axial force and vibration signal. The dominance of the torsional mode in chatter vibration for the plunge milling of a rigid workpiece was observed by Ko [105] at which chatter vibration was attributed to the coupled torsional-axial mode of the tool as a result of the design of the tool for chip evacuation. However, the tool lateral modes were not found to affect the stability of plunge milling. On the other hand, a high peak appears in the power spectrum of the measured axial vibration of the system around a frequency of 4800 Hz with side bands spaced by a frequency corresponding to the rotational speed can be mainly due to forced vibration from bearing defects that excited the torsional mode of the tool in resonance.

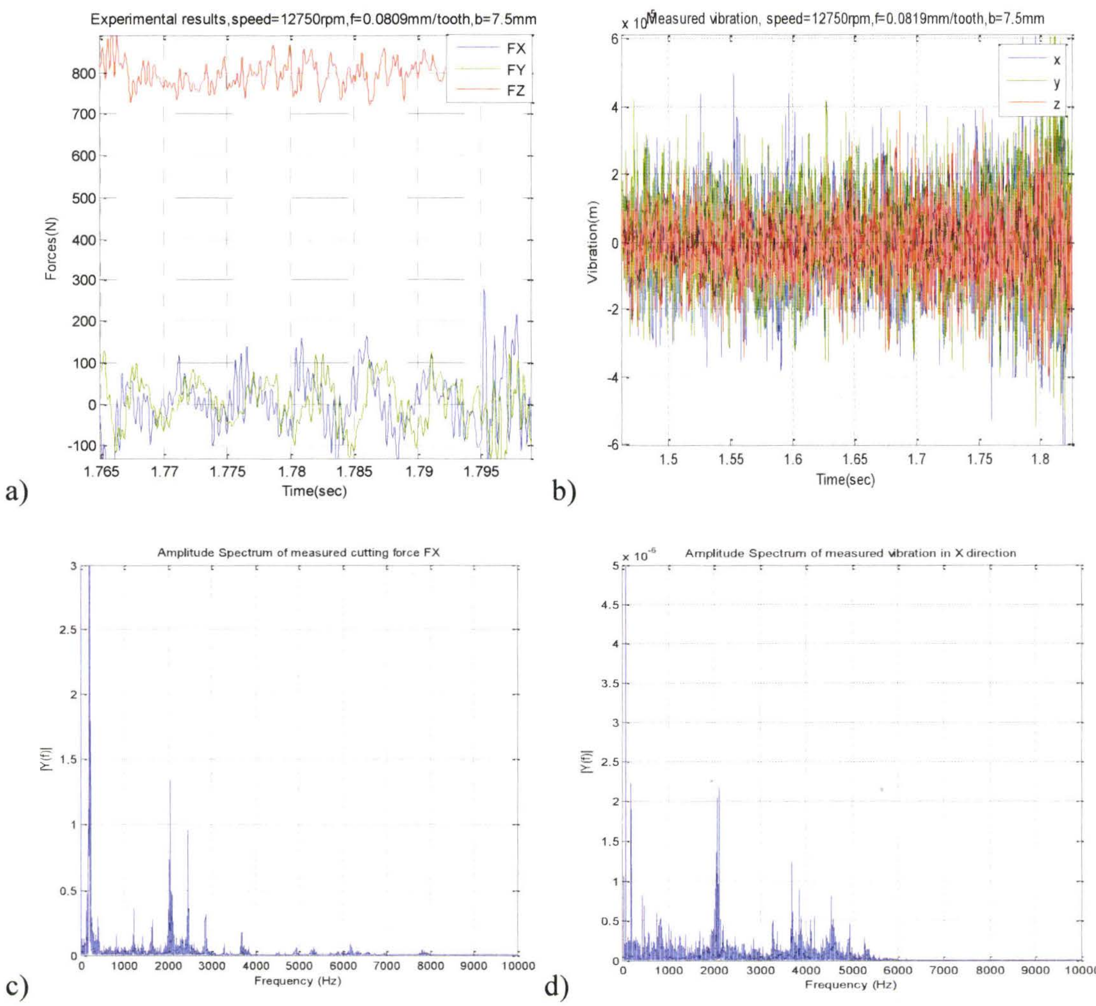

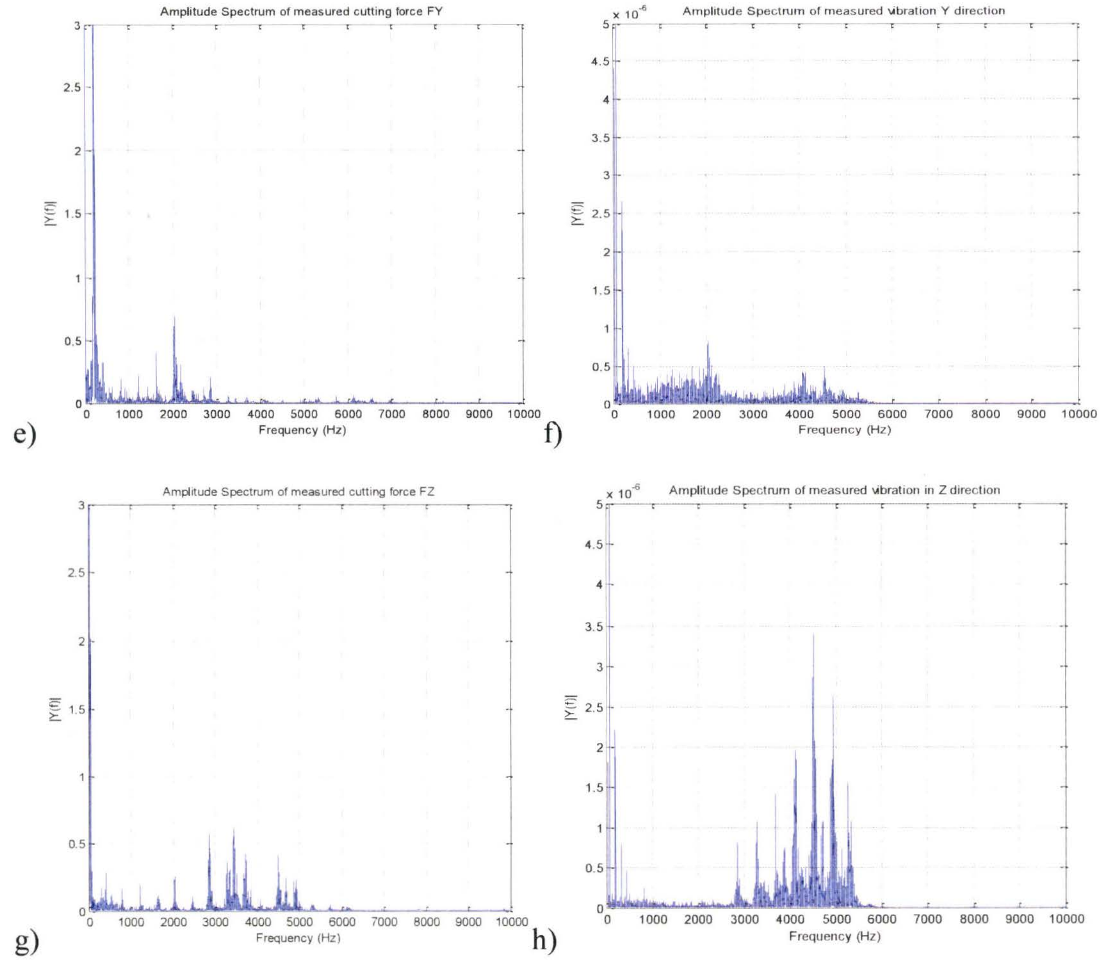

Figure 6-4 Experimental results for unstable plunge milling at 12750rpm, f=0.0809 mm/tooth, b=7.5mm a) cutting forces, b) System vibrations, c) FFT of FX, d) FFT of x vibration, e) FFT of FY, f) FFT of y vibration, g) FFT of FZ, h)FFT of z vibration.

Simulation results for the same cutting conditions indicate chatter behaviour in predicted signals and power spectra of cutting forces and vibrations as shown in Figure 6-5. A good agreement between experimental and simulation results can be noticed with respect to force and vibration signals. This is illustrated by the good agreement in the magnitude and the frequency component of both measured and simulated force and system vibration as shown in the time signal and the power spectra of cutting forces and system vibrations in x, y, and z directions. Similar to experimental results, unstable cutting was predicted to be the result of cutter lateral dynamics as appears by the dominance of lateral modes as compared to system axial vibrations. The simulation model was able to predict the surface waviness generated by each insert during cutting to predict the chip thickness by considering the regenerative behaviour of chatter during cutting. This can enhance the ability of the model to determine the borderline between stable and unstable cutting for the stability analysis of the process. For this cutting condition, it can be shown that the surfaces generated by each insert are out of phase with a phase shift (ε), leading to a growing dynamic chip thickness and hence, to unstable cutting due to regenerative effect. Accordingly, the predicted dynamic chip thickness shows an unstable trend with a frequency corresponding to the tool lateral modes as indicated by the high peak at 2100 Hz in the chip thickness spectrum as compared to the case of chatter-free cutting. Additionally, the presence of chatter is indicated by the predicted tool motion characterized by diverged quasi-periodic orbits with an elliptical shape moving away from the origin [40-43]

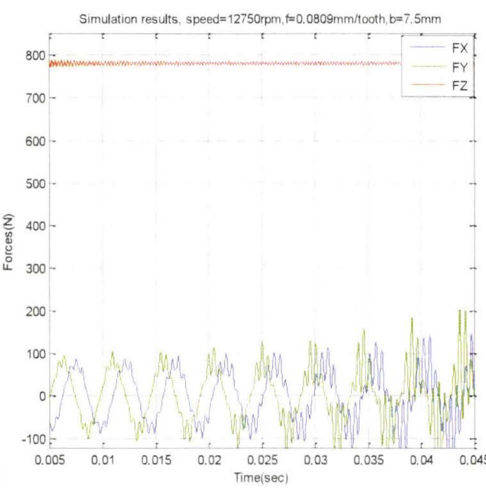

a)

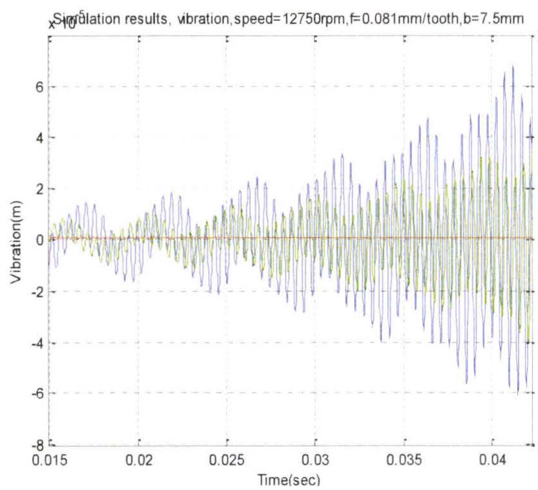

b)

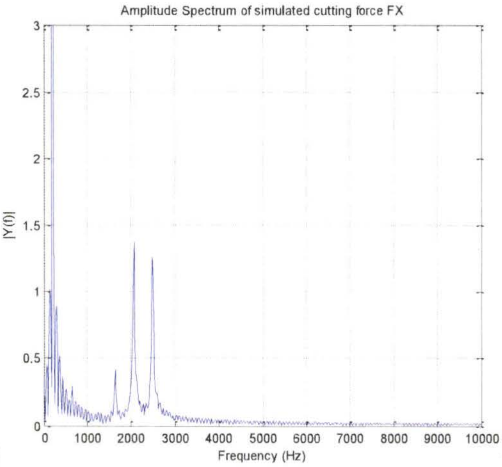
Amplitude Spectrum of simulated cutting force FX
|Y(f)|
Frequency (Hz)

c)

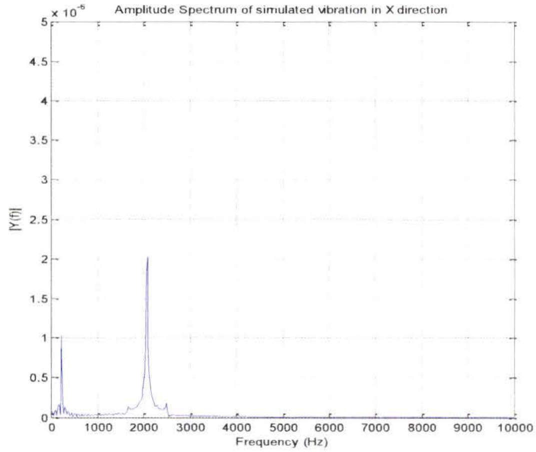
x 10^-6
Amplitude Spectrum of simulated vibration in X direction
|Y(f)|
Frequency (Hz)

d)

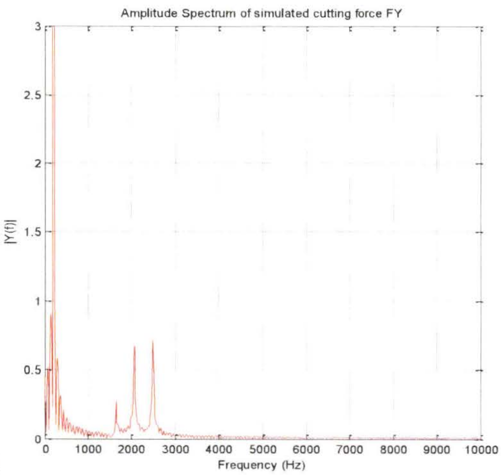
Amplitude Spectrum of simulated cutting force FY
|Y(f)|
Frequency (Hz)

e)

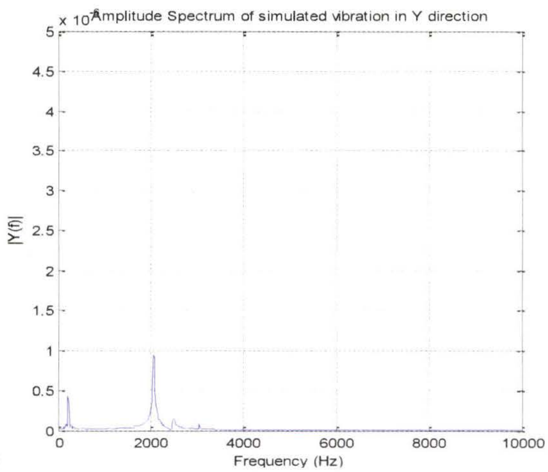
x 10
Amplitude Spectrum of simulated vibration in Y direction
|Y(f)|
Frequency (Hz)

f)

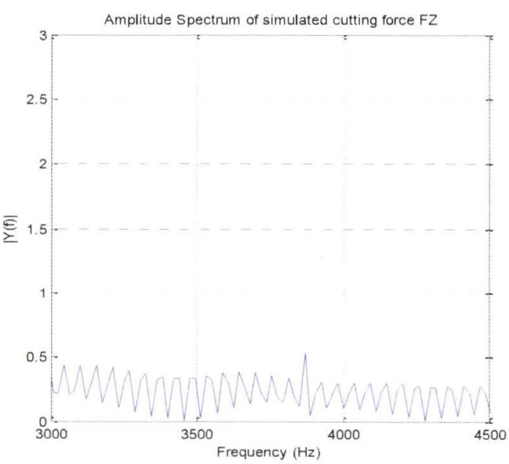
Amplitude Spectrum of simulated cutting force FZ
|Y(f)|
Frequency (Hz)

g)

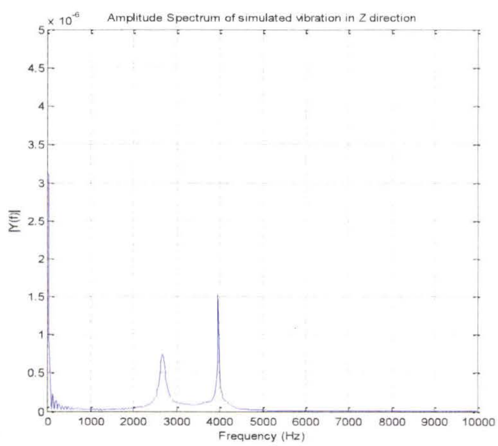
x 10^-6
Amplitude Spectrum of simulated vibration in Z direction
|Y(f)|
Frequency (Hz)

h)

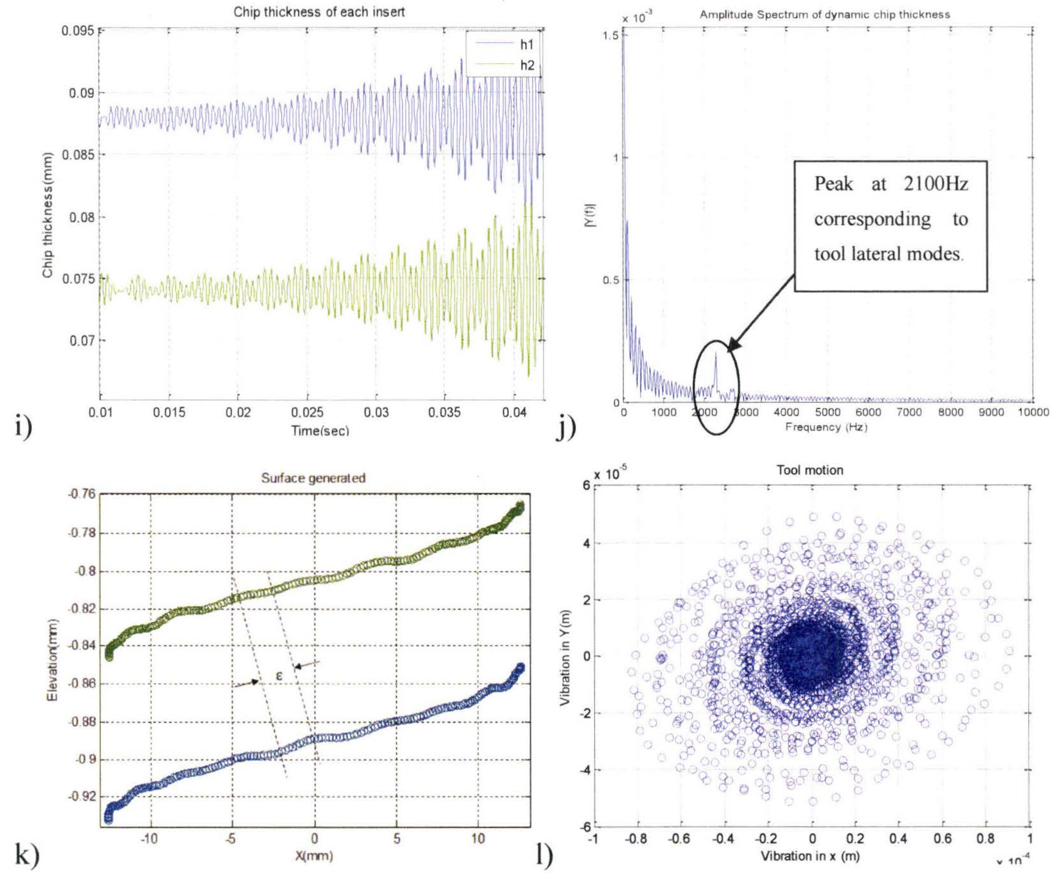

Figure 6-5 - Simulation results for unstable plunge milling at 12750rpm, f=0.0809mm/tooth, b=7.5mm a) cutting forces, b) System vibrations, c) FFT of FX, d) FFT of x vibration, e) FFT of FY, f) FFT of y vibration, g) FFT of FZ, h)FFT of z vibration, i) Dynamic chip thickness, j)FFT of chip thickness, k) surface generated, l)Tool motion plot.

Chatter-free cutting is observed for this case of plunge milling for a system with a rigid workpiece at 14750 rpm with a feed rate of 0.07 mm/tooth and 6.25 depth of cut. This is demonstrated at the measured force and vibration signals and power spectra which indicate a stable trend as shown in Figure 6-6. Simulation results for the same cutting conditions are shown in Figure 6-7. Good agreement between the measured and simulated cutting force and system vibration was found in the x, y, and z directions. This is illustrated by the agreement in the magnitude, trend and frequency components of force and vibration signals. This shows the ability of the model to simulate the dynamics of the plunge milling process and to accurately predict the cutting forces with a smaller margin of error compared to the models available in the literature.

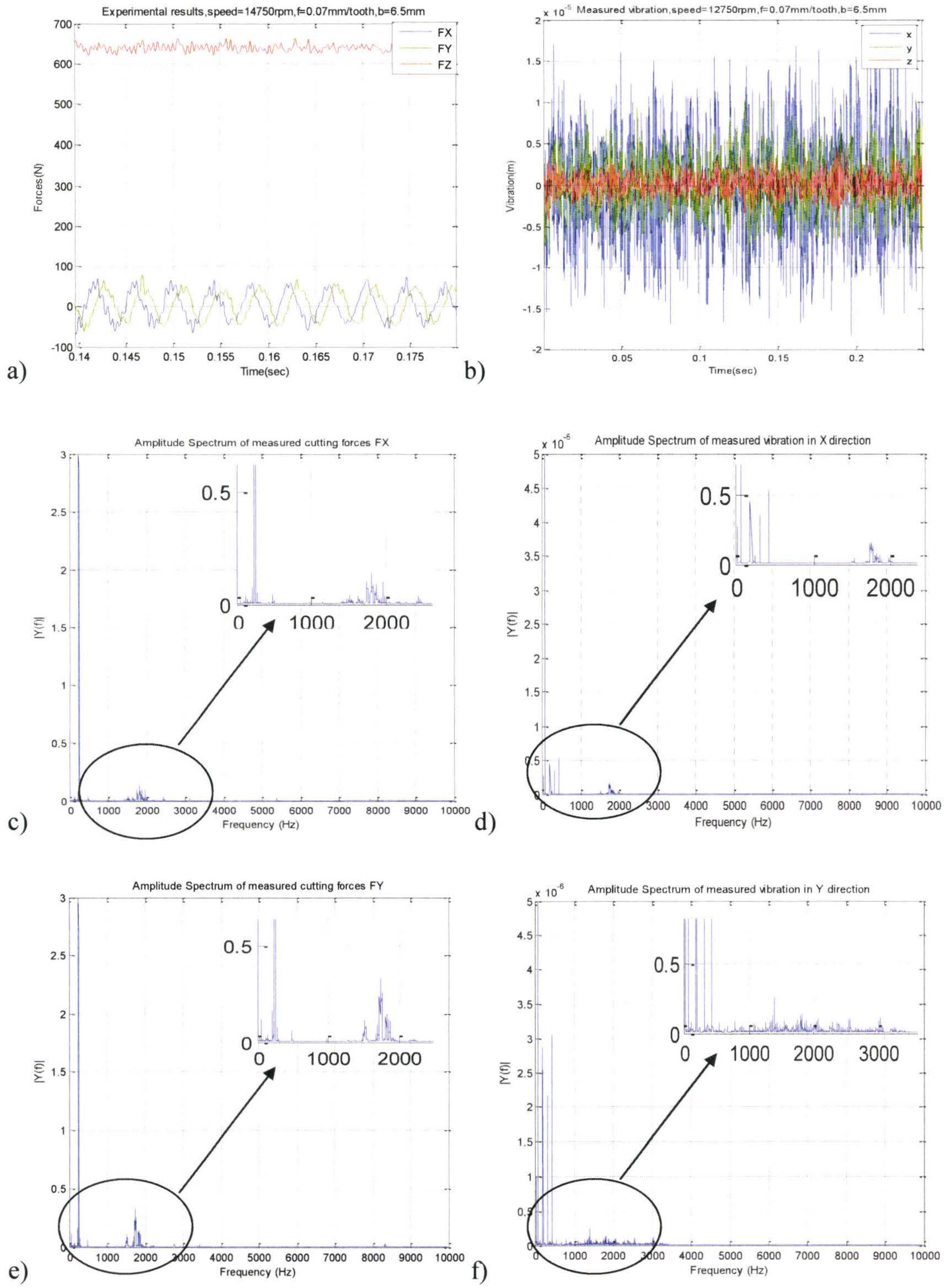
a)
Experimental results,speed=14750rpm,f=0.07mm/tooth,b=6.5mm
Forces(N)
Time(sec)
FX
FY
FZ
b)
x 10^-5 Measured vibration,speed=12750rpm,f=0.07mm/tooth,b=6.5mm
Vibration(m)
Time(sec)
x
y
z
c)
Amplitude Spectrum of measured cutting forces FX
|Y(f)|
Frequency (Hz)
d)
x 10^-6 Amplitude Spectrum of measured vibration in X direction
|Y(f)|
Frequency (Hz)
e)
Amplitude Spectrum of measured cutting forces FY
|Y(f)|
Frequency (Hz)
f)
x 10^-6 Amplitude Spectrum of measured vibration in Y direction
|Y(f)|
Frequency (Hz)

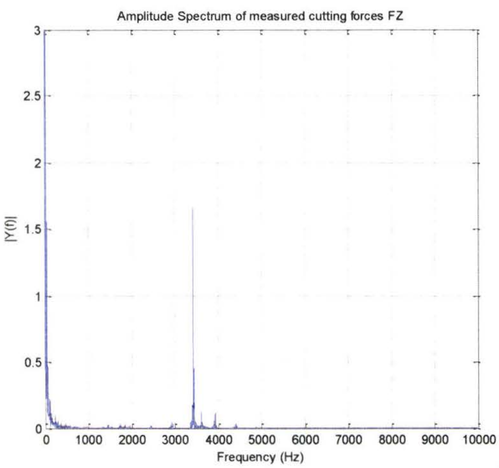

g)

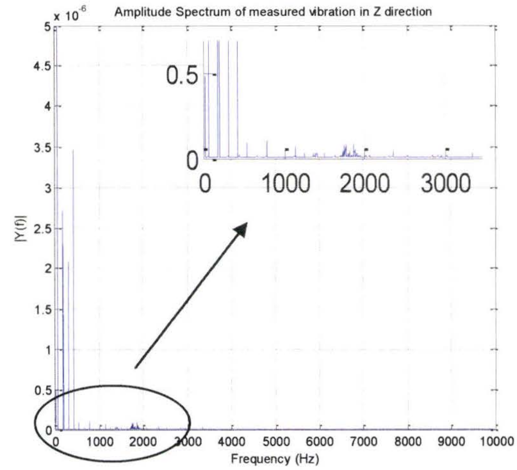

h)

Figure 6-6 Experimental results for unstable plunge milling at 14750 rpm, f=0.07 mm/tooth, b=6.25mm a) cutting forces, b) System vibrations, c) FFT of FX, d) FFT of x vibration, e) FFT of FY, f) FFT of y vibration, g) FFT of FZ, h)FFT of z vibration.

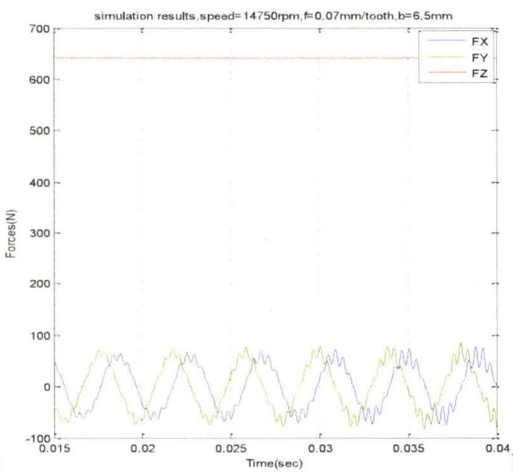

a)

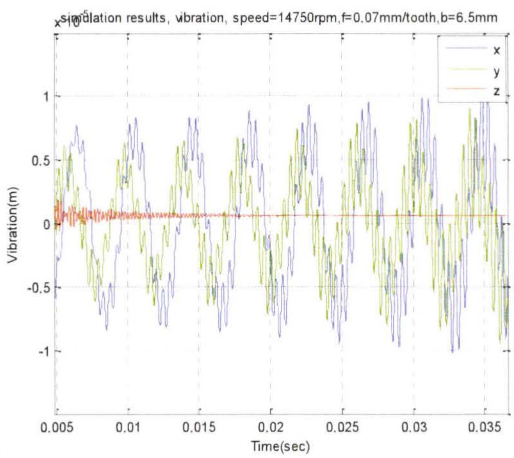

b)

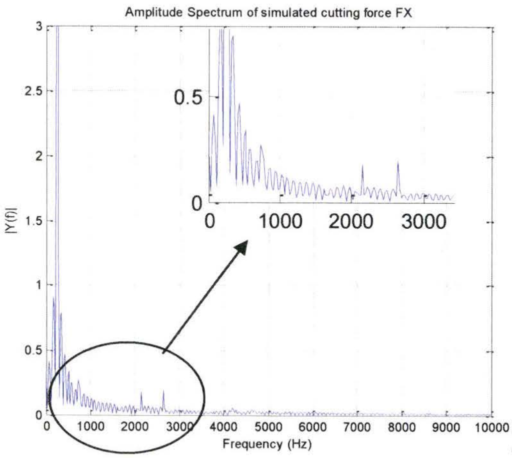
Amplitude Spectrum of simulated cutting force FX
|Y(f)|
Frequency (Hz)

c)

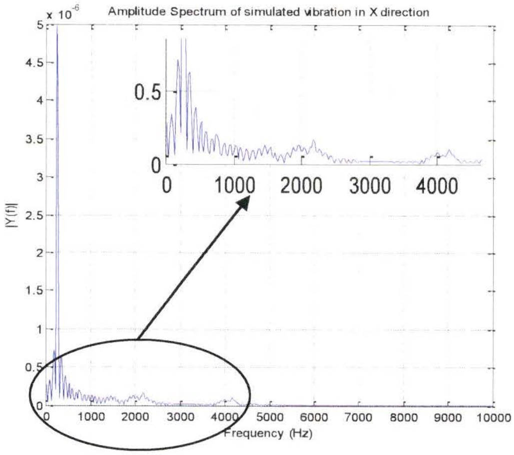
Amplitude Spectrum of simulated vibration in X direction
x 10^-6
|Y(f)|
Frequency (Hz)

d)

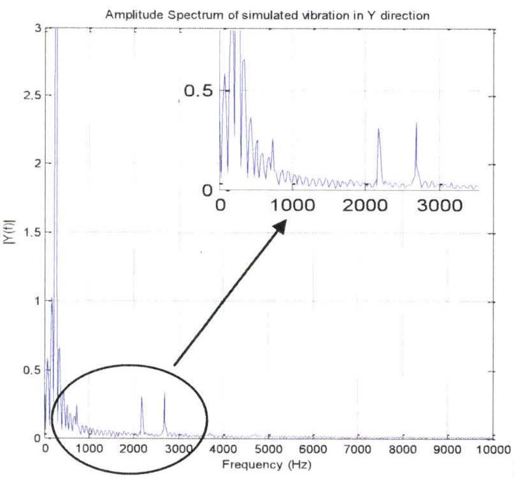
Amplitude Spectrum of simulated vibration in Y direction
|Y(f)|
Frequency (Hz)

e)

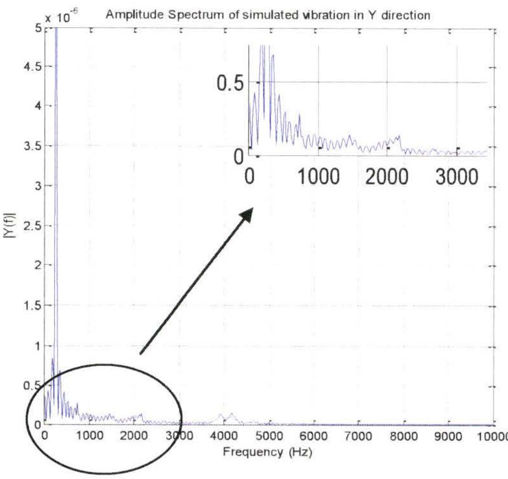
Amplitude Spectrum of simulated vibration in Y direction
x 10^-6
|Y(f)|
Frequency (Hz)

f)

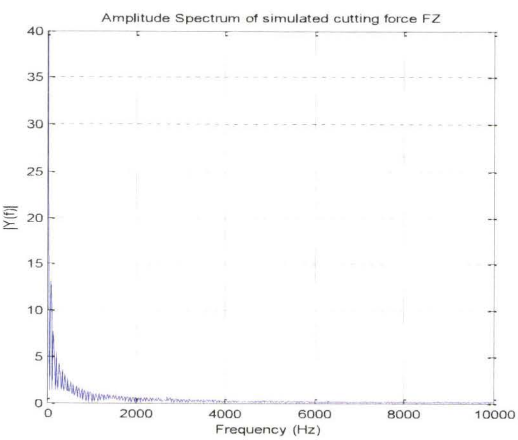
Amplitude Spectrum of simulated cutting force FZ
|Y(f)|
Frequency (Hz)

g)

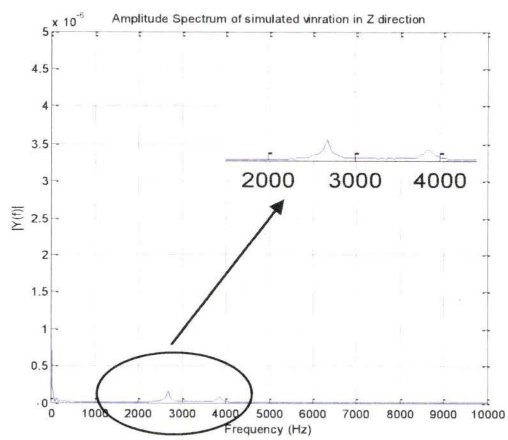
Amplitude Spectrum of simulated vinration in Z direction
x 10^-6
|Y(f)|
Frequency (Hz)

h)

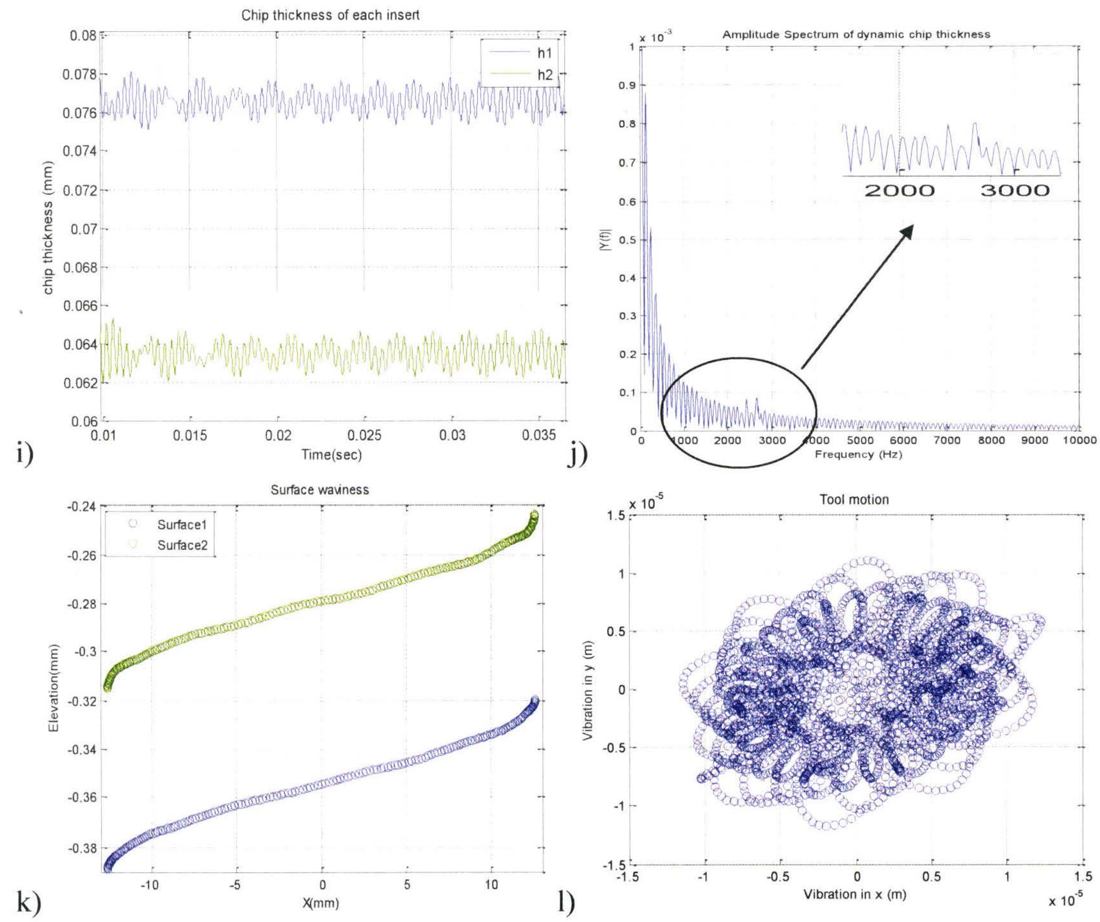

Figure 6-7 Simulation results for unstable plunge milling at 14750rpm, f=0.07mm/tooth, b=6.25mm a) cutting forces, b) System vibrations, c) FFT of FX, d) FFT of x vibration, e) FFT of FY, f) FFT of y vibration, g) FFT of FZ, h)FFT of z vibration, i) Dynamic chip thickness, j)FFT of chip thickness, k) surface generated, l)Tool motion plot.

6.4 Conclusion

In this chapter, plunge milling with double inserts of systems with rigid workpiece was studied both experimentally and numerically. In this system, only the tool dynamics is considered in the simulation to model the dynamics and stability of plunge milling for systems with the workpiece considered to be rigid.

Experimental validation of the proposed model as well as the predicted stability lobe was carried out at different cutting conditions that represent several cases of stable and unstable cutting for a rigid workpiece.

A very good agreement was found between the measured and predicted cutting forces and system vibrations for stable and unstable cutting. This is demonstrated in the agreement in trend and magnitude of measured and predicted cutting force and vibration signals as well as their power spectra. This validated the predicted stability lobe and the simulation model with respect to the prediction of the cutting forces, system vibrations and the process stability for better process planning and control. The experimental validation demonstrated the ability of the model to deal with the dynamics of two inserts, which includes the tool setting errors, as well as to the correctness of the cutting coefficient model. It was noticed that for a system with a rigid workpiece, chatter vibration occurred mainly due to the tool lateral dynamics as it is illustrated by the high FFT peaks at frequencies corresponding to tool modes (1500 Hz, 2050 Hz) in X and Y directions for case of chatter. On the other hand, it was noticed for the case of a rigid workpiece that the plunge milling process is very rigid in the axial direction as it benefits from the spindle axial rigidity, which is the main idea of plunge milling to have most of the cutting action in the axial direction. Additionally, it can be noticed that the cutting forces and, correspondingly, the system vibration increase with the increase of feed per tooth and width of cut, which represent the chip load. The same trend was observed for plunge milling by Ko [96,104,105].

Chapter 7: Plunge Milling of A Flexible Workpiece

7.1 Introduction

The effect of workpiece dynamics on the plunge milling dynamics and stability is studied in this chapter. Both measured and predicted results of plunge milling of systems with a flexible workpiece are presented in this chapter for different cutting conditions to analyze how the dynamics of the workpiece can affect the process stability and dynamics.

The dynamics of both the milling cutter and the workpiece were considered in the simulation results as well as the variation of the workpiece dynamics with respect to hole location to simulate the actual condition of cutting. Experimental validation of the simulation model and the predicted stability lobe is performed at different cutting conditions (i.e. combination of speed, feed and width of cut) to check the validity of the model for a wide range of cutting conditions and to cover several cases of stable and unstable cutting.

7.2 Modal Testing

Modal testing was performed on the workpiece at different points to study the variation of workpiece dynamics in the axial direction according to the hole location as a result of workpiece fixation when lifted to introduce through holes. A top view of the modeled aluminum plate used in cutting tests detailing the supported edges at which the workpiece is lifted with respect to the dynamometer is shown in Figure 7-1. The variation of the measured workpiece dynamics in accordance to hole location for first and second axial mode are illustrated in Figure 7-2 and Figure 7-3 respectively.

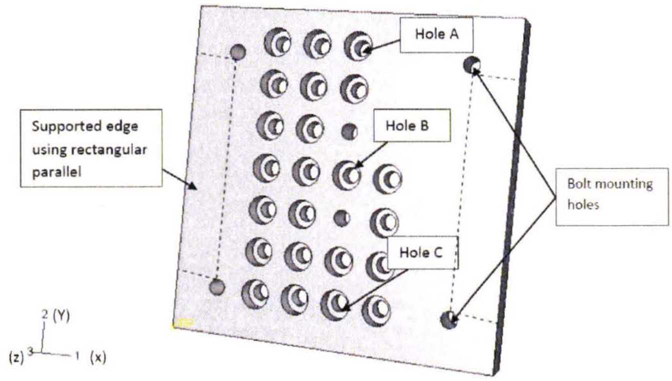

Figure 7-1 - The modeled Aluminum plate

The variation in the measured workpiece dynamics is presented by means of the mode shapes in axial direction, damping ratio as well as the variation of modal stiffness.

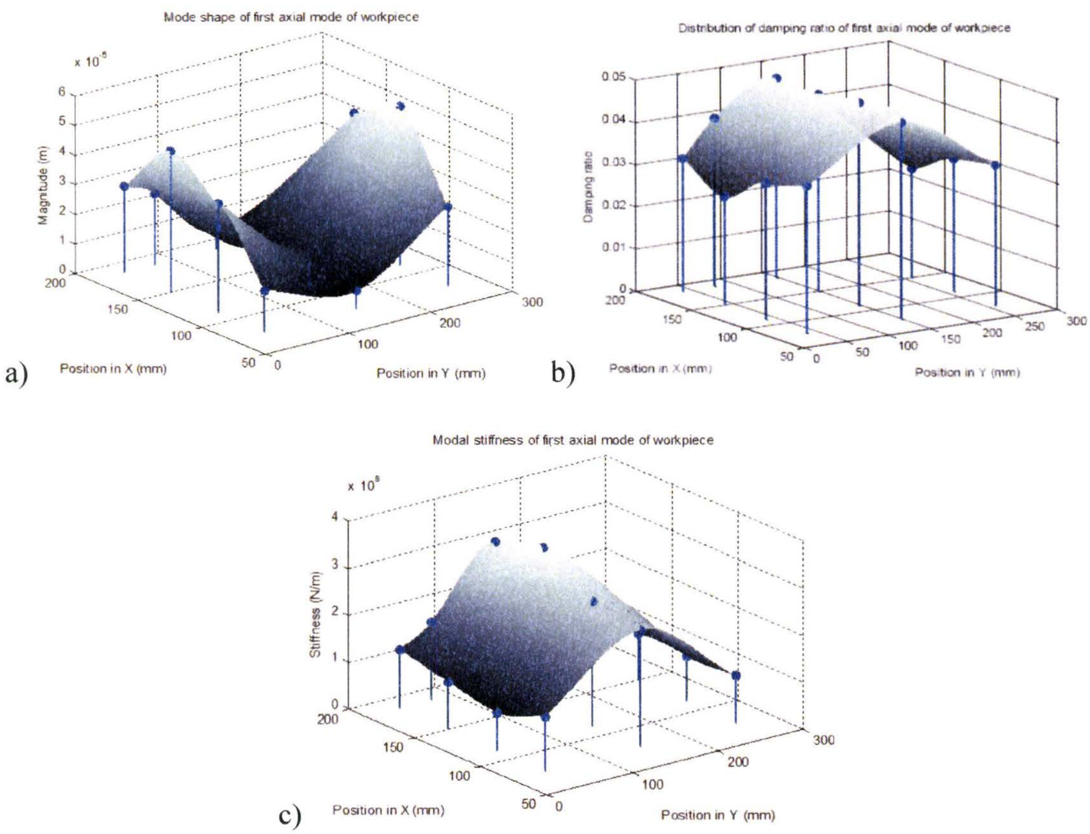

Figure 7-2 - Workpiece dynamics for first axial mode at 1750 Hz a) Mode shape, b) Damping ratio, c) Stiffness

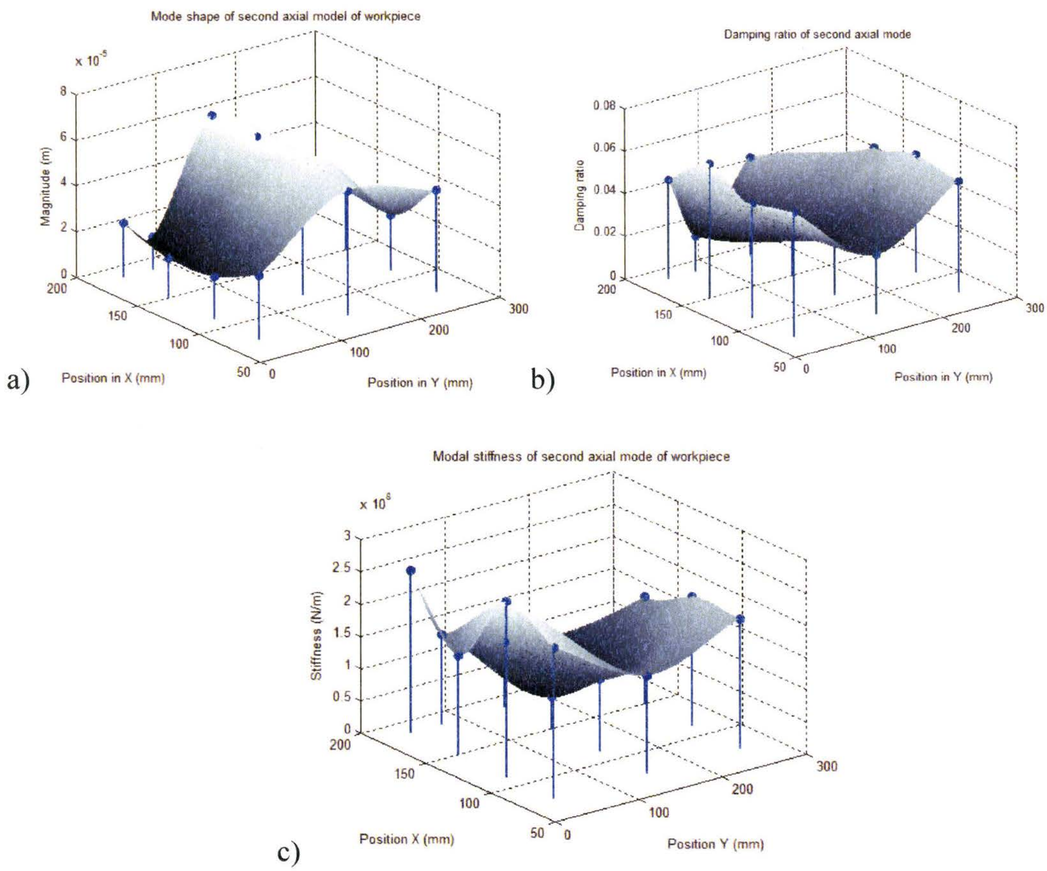

Figure 7-3 - Workpiece dynamics for second axial mode at 2020 Hz a) Mode shape, b) Damping ratio, c) Stiffness

This helps to use the actual dynamics of the workpiece in the simulation for better modeling of plunge milling based on the actual system dynamics at each cutting location. It can be noticed from Figure 7-2 that for the first axial mode at 1750 Hz, high workpiece deflection is found for the holes located away from the supported edges. This appears in the increase of deflection towards the middle path of the workpiece (i.e. hole A, B and C) as well as the corresponding decrease in damping ratio and stiffness that indicates the increase of flexibility for these locations. Additionally, higher deflection occurs at holes close to the unsupported edges compared to the centre of plate. This is illustrated by the increase of workpiece deflection as well as the decrease in damping ratio and stiffness for both holes (A) and (C) close to the unsupported edges compared to hole (B) at the centre of the workpiece. This can be attributed to the fact that the unsupported edges of the plate act as a cantilever with its fixed end corresponding to the vertical plane containing the bolts. On the other hand, it was noticed that the second axial mode of workpiece at 2020 Hz is the dominant mode for holes at the middle of the plate whereas the first axial mode is dominant at holes located near the unsupported edges of the workpiece as shown in Figure 7-3. This conclusion is very important to be considered in the simulation model in order to use the appropriate workpiece dynamics and consider the actual dominant mode in the axial direction in accordance to the hole location

7.3 Experimental work

Plunge milling cutting tests were carried out to validate the simulation model and the predicted stability for the case of a system with a flexible workpiece. For the case of the flexible workpiece, the Aluminum workpiece was mounted on two-side edge supports to lift it off of the dynamometer to be able to produce through pilot holes and to study the effect of workpiece flexibility on process dynamics and stability. This arrangement increases the flexibility of the workpiece in the axial direction and hence, its dynamics has to be considered in the model along with its variation with respect to the hole location. Drills of different diameters were used to generate through pilot holes with different diameters to achieve a variation in the width of cut. This helps to validate the predicted cutting force, dynamic chip area and stability limits of plunge milling from the time domain simulation model. The holes were then enlarged using a plunge milling cutter to a diameter of 25 mm and depth of 15 mm (i.e. half of the plate thickness) using two PVD coated carbide inserts. Experimental validation of the predicted stability lobe and the simulation model was done at different speeds, feeds and width of cut within the studied range of cutting conditions to cover several cases of stable and unstable cutting conditions. This helps at checking the validity of the simulation model for a wide range of cutting conditions as well as determining the correctness of the predicted stability lobe in evaluating the boundaries between stable and unstable cutting conditions when considering the dynamics of the workpiece, specially in the axial direction, with double inserts plunge milling.

7.4 Results and Discussions

Similar to the case of the system with a rigid workpiece, plunge milling cutting tests with two inserts were carried out to validate the proposed model at different cutting speeds, feeds and width of cut for the case of a flexible workpiece. The variation of workpiece dynamics as a function of the hole location is considered in the simulation to consider the actual workpiece dynamics for each validation case for better prediction and modeling results. On the other hand, cutting coefficients used in the mechanistic model are computed based on the actual chip thickness removed by each insert at each time step to consider the variation of chip thickness between inserts based on the radial and axial runout and system vibration, which can affect the prediction of cutting forces. A stability lobe diagram of the plunge milling process was predicted using the time domain simulation model presented for a system with a flexible workpiece as shown in Figure 7-4. Both the dynamics of the plunge milling cutter dynamics and the workpiece are considered in the simulation. The stability lobe corresponds to the case where the dynamics of the workpiece of a location of high flexibility in the axial direction is considered in the simulation. The dynamics of the workpiece and cutter used in the simulation are extracted from the experimental modal analysis of the cutter and workpiece. In the simulation, the boundary between stable and unstable cutting conditions is identified through the force and vibration signals, force and/or vibration spectra and phase plots of the cutter and workpiece. The same chatter criterion used for the system with a rigid workpiece was used in this case. Cutting tests were planned based on the predicted stability lobe diagram to cover different cutting conditions for stable and unstable cutting. This aims to check the ability of the proposed model to realistically predict the cutting forces and dynamics of the plunge milling process in order to validate the predicted stability lobe diagram and hence, to validate the model.

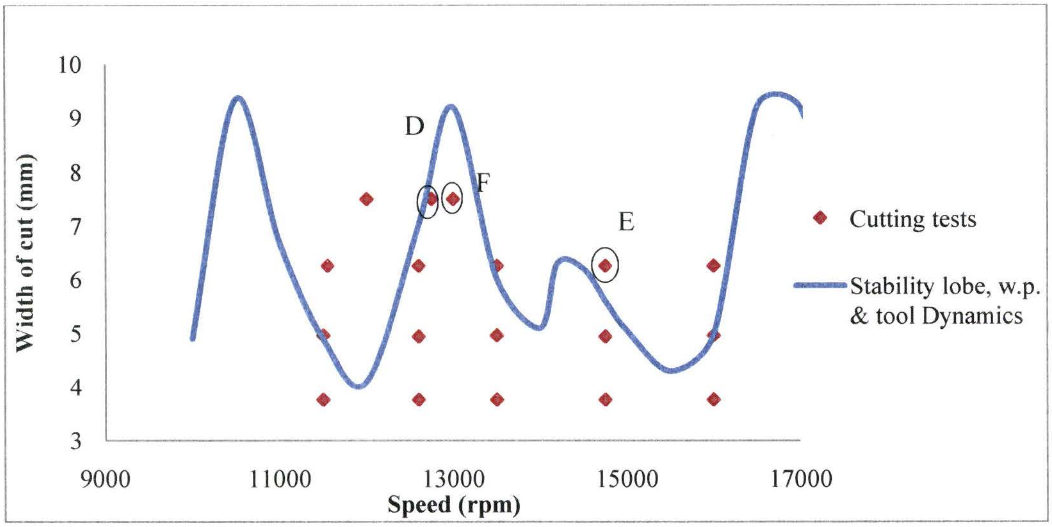

Figure 7-4 - Predicted stability diagram for flexible workpiece

Experimental results of point D in Figure 7-4, which corresponds to plunge milling of a flexible workpiece at 12750 rpm with a feed rate of 0.0809 mm/tooth are shown in Figure 7-5 Stable cutting can be observed by the chatter-free trend of the measured forces and system vibration signals as shown in Figure 7-5. This result is in agreement with the predicted stability lobe as this cutting condition is within the stable zone of the predicted stability diagram. A dominant peak of force and vibration power spectra can be observed at 245 Hz. This frequency corresponds to the rotational speed (1 x RPM) as a result of the tool setting errors which dominate the system vibration in stable cutting. The same result was observed by Ko [104] at chatter-free cutting for plunge milling of a rigid workpiece. On the other hand, a peak corresponding to the workpiece axial mode at 1750 Hz can be noticed in both measured and predicted force and vibration spectra, which was not present for the case of plunge milling for a system with a rigid workpiece. This illustrates the importance of axial mode of the workpiece as compared to the high axial rigidity of the spindle for a system with a flexible workpiece which can affect the stability of the system. This is mainly due to the low rigidity of the workpiece as compared to the high axial rigidity of the tool which can affect the main advantage of plunge milling which takes its main benefit from the high spindle rigidity in the axial direction. This consideration was not taken into account in previous models dealing with plunge milling [96, 104, 105] as the workpiece dynamics and its variation was not modeled.

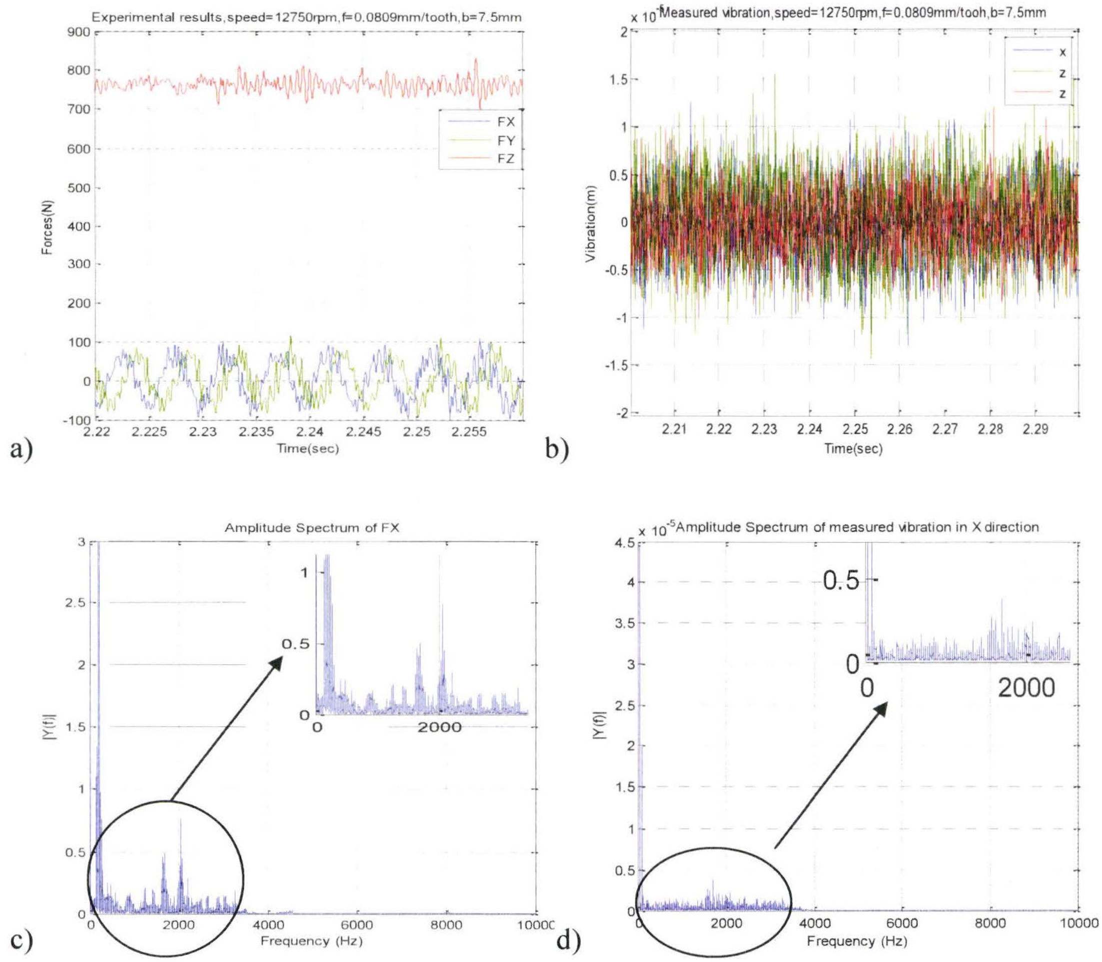

e) f) g) h)

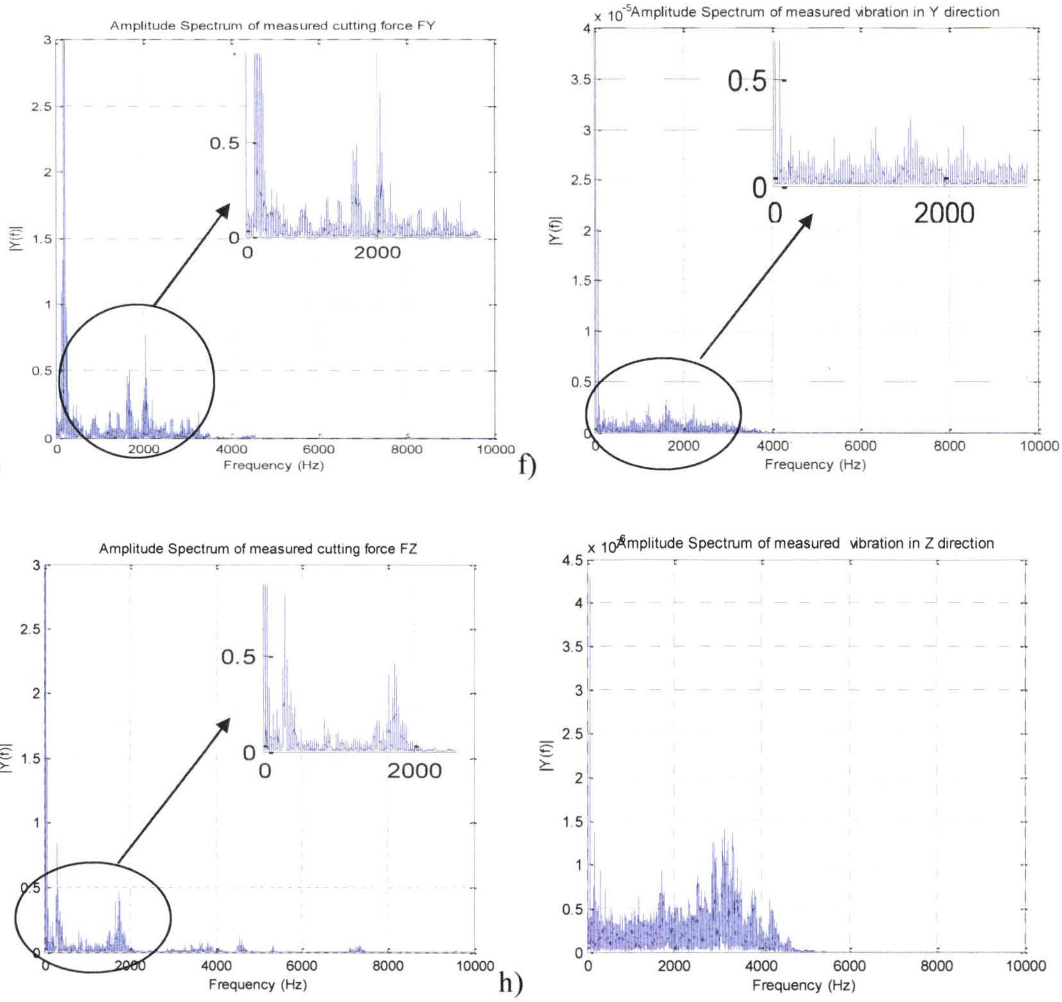

Figure 7-5 - Experimental results for stable plunge milling at 12750rpm, f=0.0809mm/tooth, b=7.5mm a) cutting forces, b)System vibrations, c) FFT of FX, d) FFT of x vibration, e) FFT of FY, f) FFT of y vibration, g) FFT of FZ, h)FFT of z vibration.

Similar to experimental results, stable cutting is indicated in the simulation results by the chatter-free predicted cutting forces and system vibrations as shown in Figure 7-6. A good agreement can be noticed in the trend and magnitude of forces and vibration signals and the frequency components of the signals shown in the FFT of both force and vibration signals in x, y, and z directions. Additionally, it was shown that the proposed model was able to simulate the fluctuation in the axial force due to workpiece axial vibrations similar to measured signals. This is shown by the peak at a frequency corresponding to the workpiece axial mode at 1750 Hz in the FFT of axial force Fz. This indicates the ability of the model to simulate the dynamics of the plunge milling process when the dynamics of the workpiece is considered and to provide a reliable tool to be used for process planning prior to machining.

Chatter-free cutting is also observed in the simulated vibration marks generated during cutting. The simulation model was able to predict the surface generated by each insert during cutting in order to predict the chip thickness by considering the regenerative behaviour of chatter during cutting. This can enhance the ability of the model to determine the borderline between stable and unstable cutting for stability analysis of the process. For this cutting condition, it can be shown that the surfaces generated by both inserts are in phase leading to a steady dynamic chip thickness and hence, to stable cutting. The predicted dynamic chip thickness cut by each insert shows a stable trend indicating chatter-free cutting. The dynamic nature of chip thickness is attributed to the workpiece axial vibration as shown in the FFT of chip thickness with a frequency corresponding to the workpiece axial mode (1750 Hz). Tool setting errors affects the balance of chip area removed by each insert as they lead to uneven chip load for each insert as shown in the predicted chip thickness.

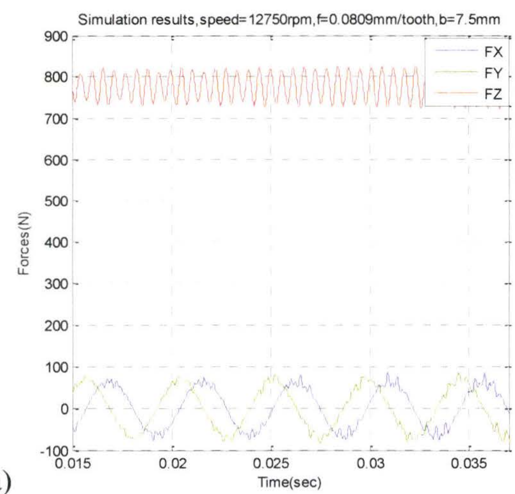

a)

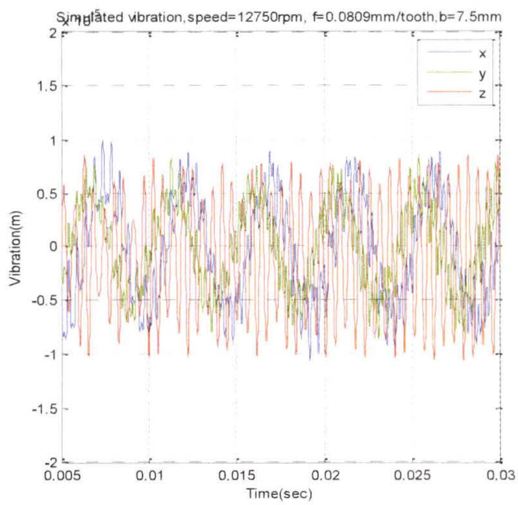

b)

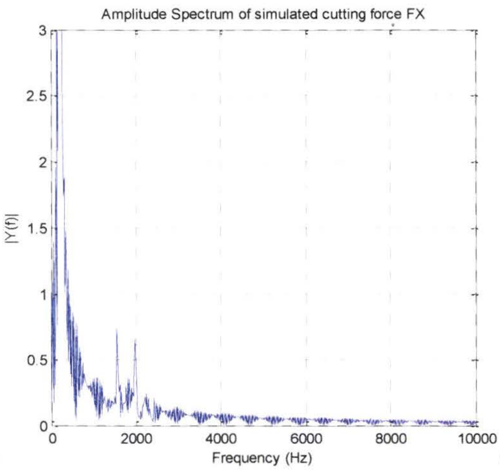
Amplitude Spectrum of simulated cutting force FX
|Y(f)|
Frequency (Hz)
c)

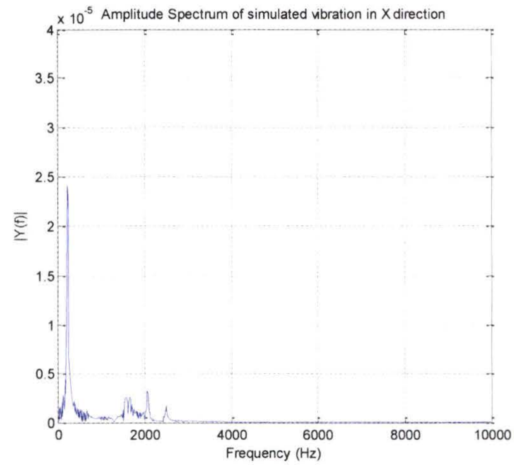
x 10^-5 Amplitude Spectrum of simulated vibration in X direction
|Y(f)|
Frequency (Hz)
d)

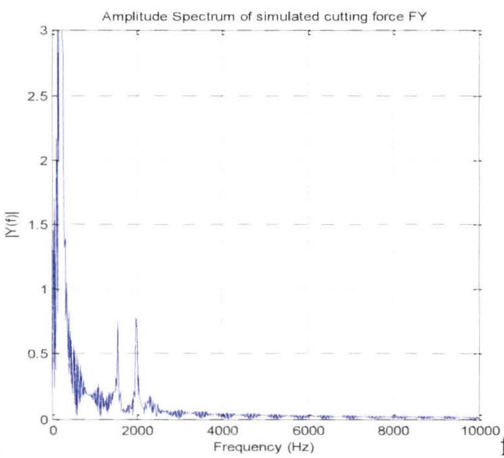
Amplitude Spectrum of simulated cutting force FY
|Y(f)|
Frequency (Hz)
e)

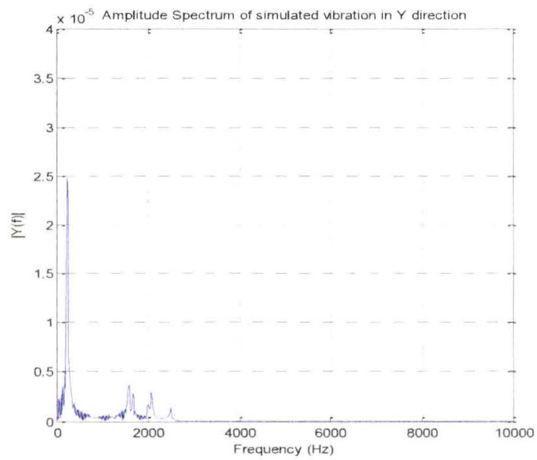
x 10^-5 Amplitude Spectrum of simulated vibration in Y direction
|Y(f)|
Frequency (Hz)
f)

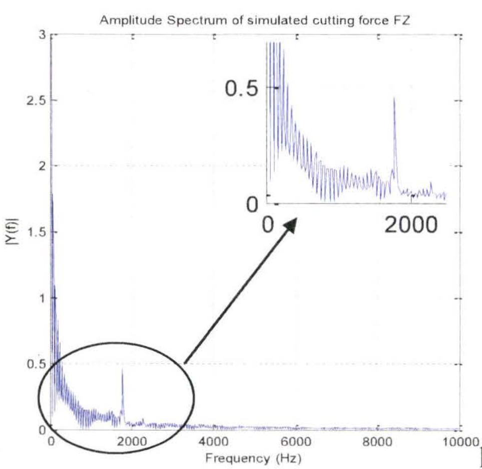
Amplitude Spectrum of simulated cutting force FZ
|Y(f)|
Frequency (Hz)
g)

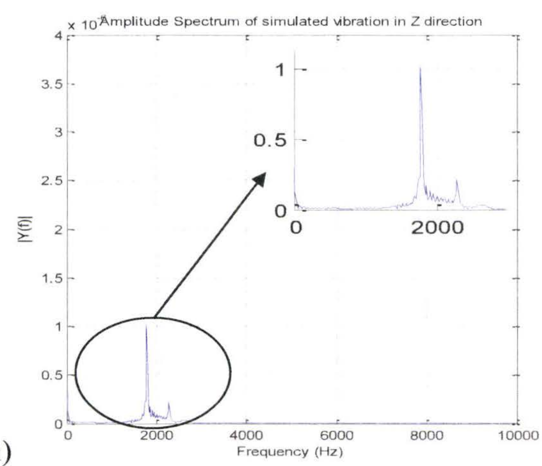
Amplitude Spectrum of simulated vibration in Z direction
|Y(f)|
Frequency (Hz)
h)

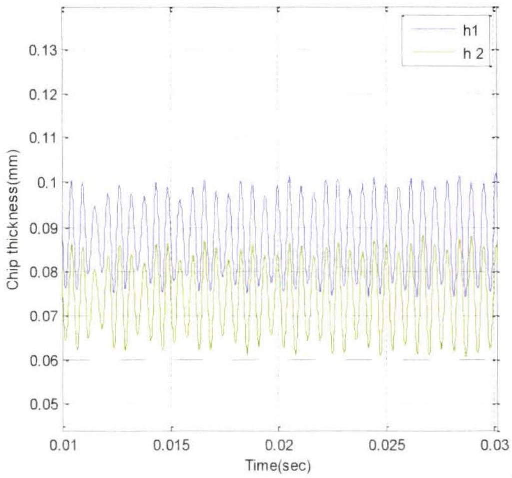

i)

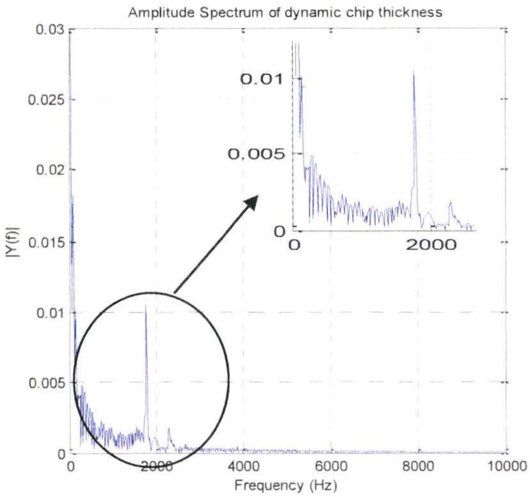

j)

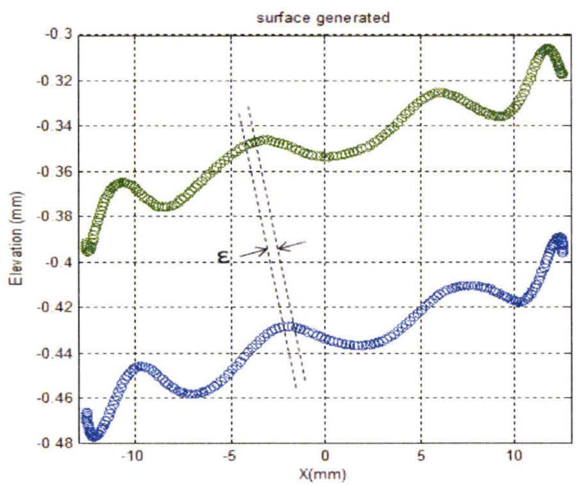

k)

<u>Figure 7-6 - Simulation results for stable plunge milling at 12750rpm, f=0.0809mm/tooth, b=7.5mm a) cutting forces, b)System vibrations, c) FFT of FX, d) FFT of x vibration, e) FFT of FY, f) FFT of y vibration, g) FFT of FZ, h)FFT of z vibration, i) Dynamic chip thickness, j) FFT of dynamic chip thickness, k) Surface generated.</u>

The measured and predicted cutting forces and vibrations for plunge milling at 14750 rpm with 0.07 mm/tooth feed rate and 6.25 mm width of cut are shown in Figure 7-7 and Figure 7-9 respectively. This corresponds to point E on the predicted stability diagram. A chatter behavior can be observed in the measured cutting force and system vibrations as indicated by the characteristic continuously growing trend of measured force and vibration signals, which indicate the occurrence of chatter in cutting [3-50] as shown in Figure 7-7. This result validates the predicted stability lobe as this cutting condition belongs to the chatter zone in the predicted diagram. For systems with a flexible workpiece, it can be noticed that chatter vibrations are mainly originated by the workpiece dynamics in the axial direction. This is illustrated by the dominance of a peak at a frequency equal to 1750 Hz in the power spectra of measured cutting forces and system vibration in the axial direction. This chatter frequency corresponds to the first mode of the workpiece in the axial direction which highlights the importance of workpiece dynamics for systems with flexible workpiece. It can be concluded that for a system with a flexible workpiece, chatter mainly occurs due to the flexibility of the system in the axial direction due to the low rigidity of the workpiece axially compared to the high spindle axial rigidity as demonstrated by the dominance of the 1750 Hz peak in the force and vibration spectra in the axial direction.

a)
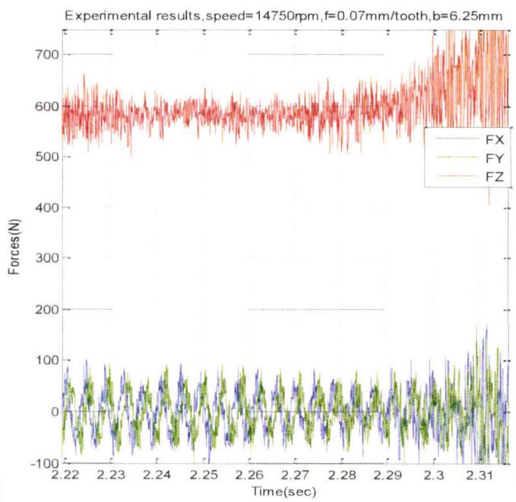

b)
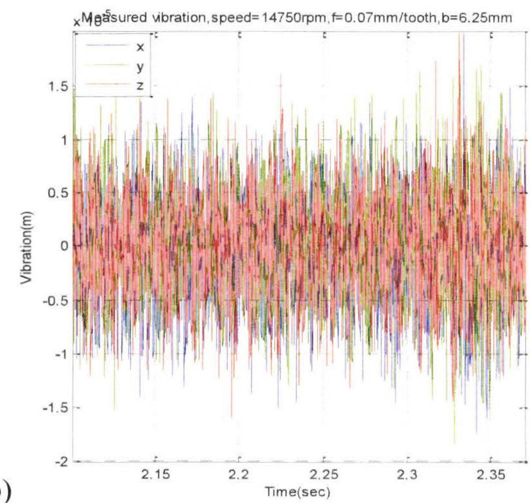

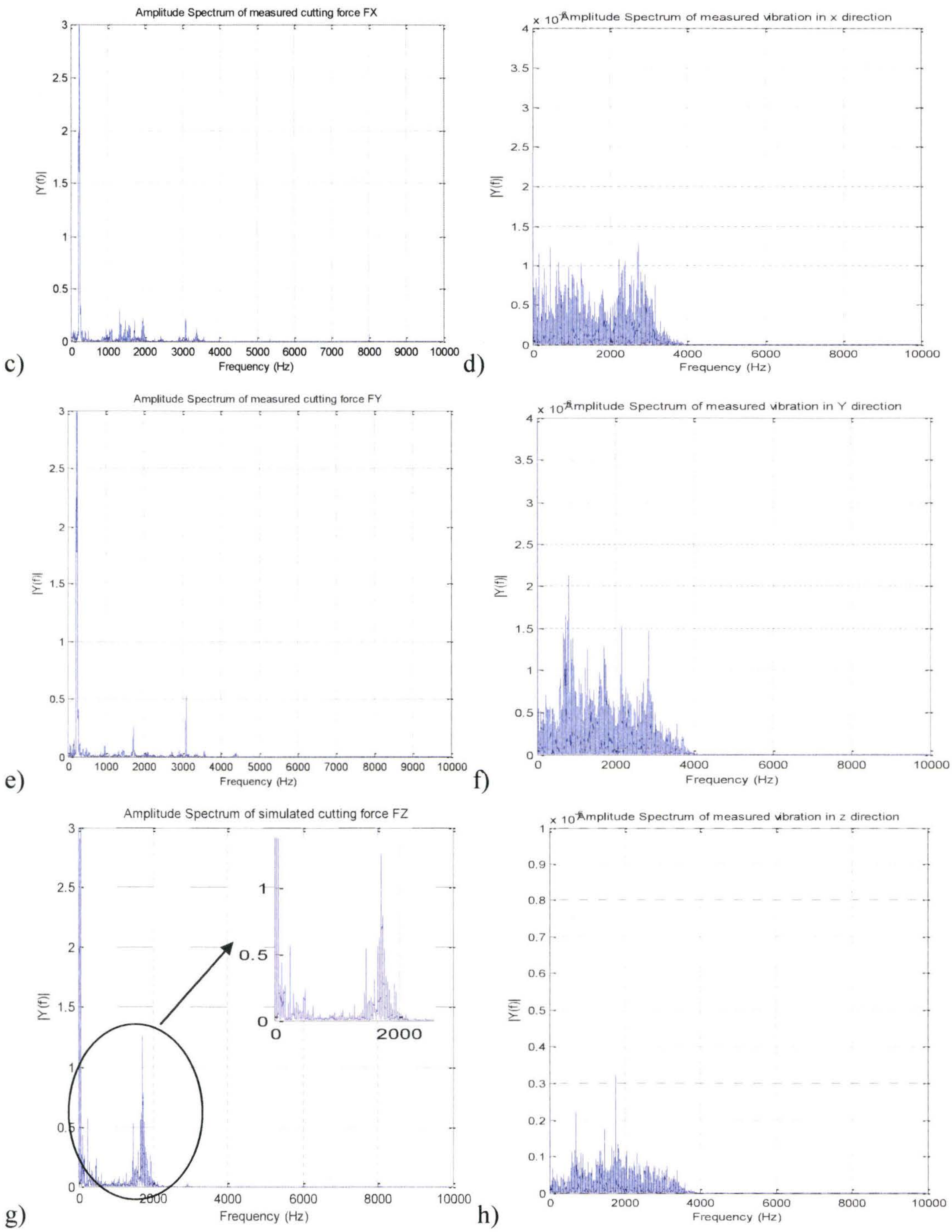

Figure 7-7 - Experimental results for unstable plunge milling at 14750rpm, f=0.07mm/tooth, b=6.25mm a) cutting forces, b) System vibrations, c) FFT of FX, d) FFT of x vibration, e) FFT of FY, f) FFT of y vibration, g) FFT of FZ, h)FFT of z vibration.

Unstable cutting can be noticed in the predicted signals and power spectra of cutting forces and vibrations for the same cutting conditions as shown in Figure 7-9. Good agreement between experimental and simulation results can be noticed with respect to force and vibration signals in the magnitude and the frequency component of both measured and simulated in the x, y, and z directions. Similar to the experimental results, unstable cutting was predicted to be the result of workpiece axial dynamics as appears by the dominance of the workpiece first axial mode at 1750 Hz as compared to system (i.e. tool and workpiece) lateral vibrations.. Additionally, for this cutting condition, it can be shown that the vibration marks left by each insert during cutting are out of phase with a phase shift (ε), leading to a growing dynamic chip thickness and the generation of a periodic self-excitation force and hence, to unstable cutting due to the regenerative effect. This phenomenon is considered as the main chatter mechanism during cutting processes as described by Tobias and Tlusty [2-7]. It was described that no chatter occurs with a phase shift close to zero, where the two surfaces are in phase and no periodic self excitation force would be generated. On the other hand, a maximum self-excitation occurred when the phasing is close to 90° as shown in Figure 7-8. It can be shown that for this cutting condition that the phase shift is close to 90° leading to chatter generation. Accordingly, the predicted dynamic chip thickness shows an unstable trend with a frequency corresponding to the workpiece axial mode. A higher peak corresponding to the workpiece axial mode (i.e. 1750 Hz) is noticed in the chip thickness spectrum as compared to the case of chatter-free cutting.

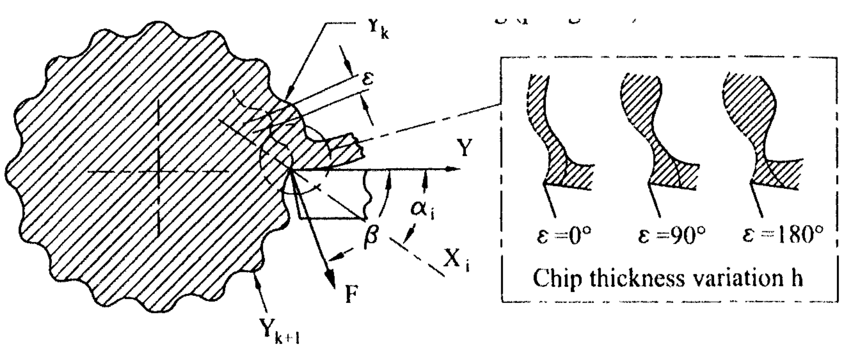

Figure 7-8 Effect of phase shift on regeneration of surface waviness [7]

a)

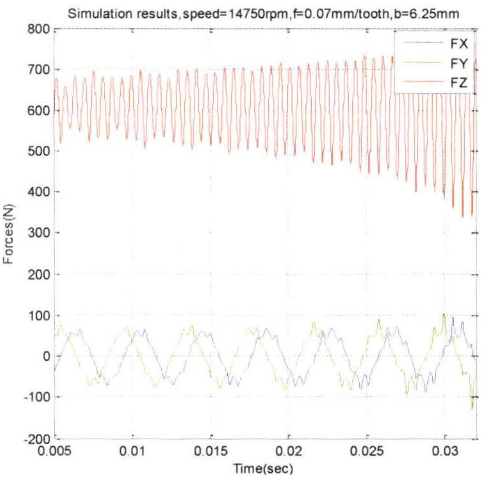
Simulation results,speed=14750rpm,f=0.07mm/tooth,b=6.25mm
FX
FY
FZ
Forces(N)
Time(sec)

b)

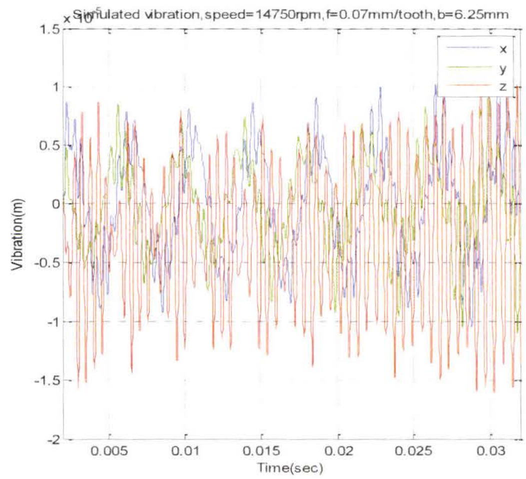
Simulated vibration,speed=14750rpm,f=0.07mm/tooth,b=6.25mm
x
y
z
Vibration(m)
Time(sec)

c)

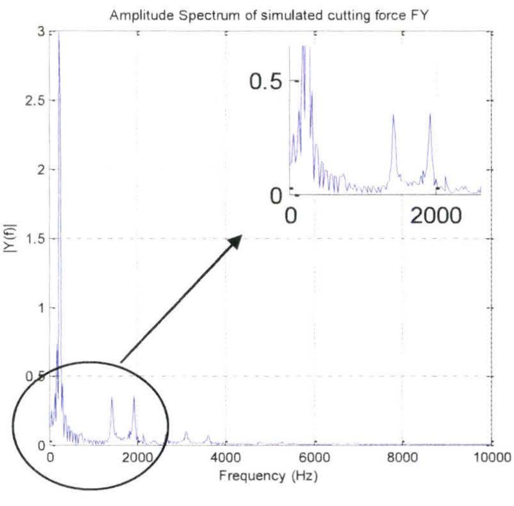
Amplitude Spectrum of simulated cutting force FY
|Y(f)|
Frequency (Hz)

d)

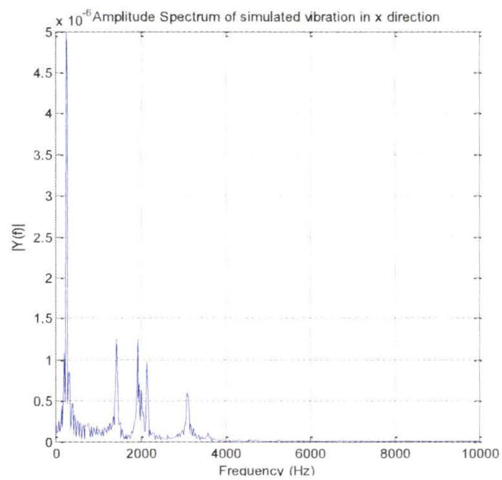
Amplitude Spectrum of simulated vibration in x direction
|Y(f)|
Frequency (Hz)

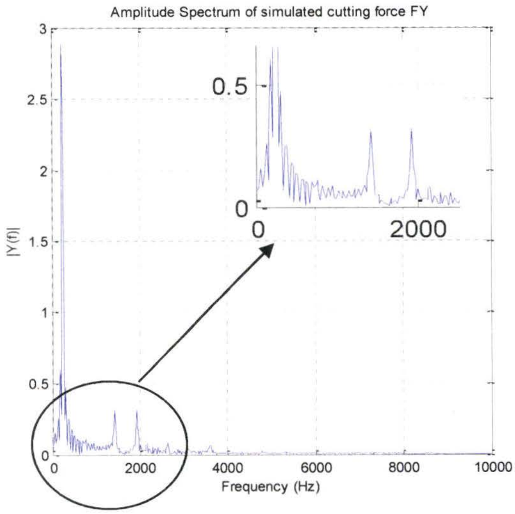
Amplitude Spectrum of simulated cutting force FY
|Y(f)|
Frequency (Hz)
e)

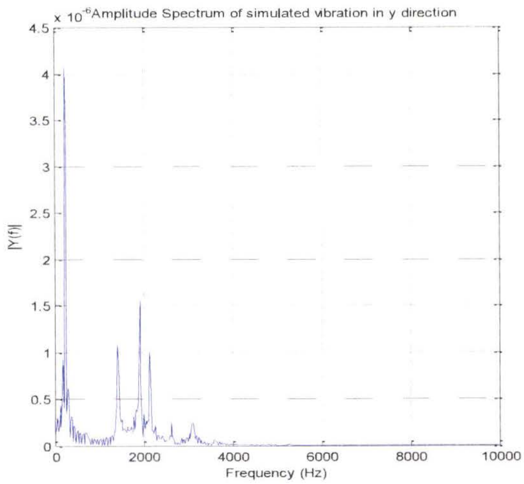
x 10^-6 Amplitude Spectrum of simulated vibration in y direction
|Y(f)|
Frequency (Hz)
f)

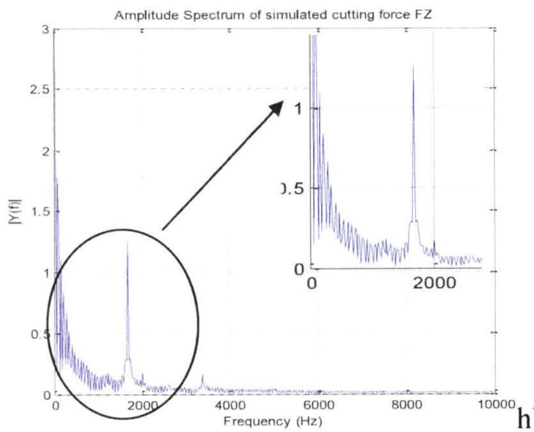
Amplitude Spectrum of simulated cutting force FZ
|Y(f)|
Frequency (Hz)
g)

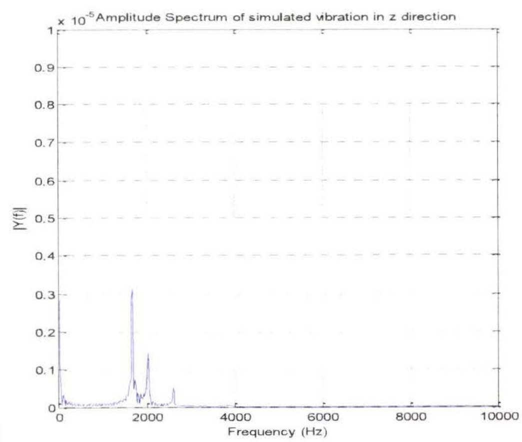
x 10^-5 Amplitude Spectrum of simulated vibration in z direction
|Y(f)|
Frequency (Hz)
h)

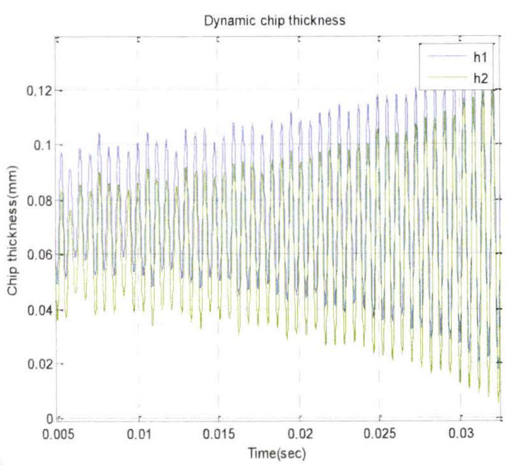
Dynamic chip thickness
h1
h2
Chip thickness(mm)
Time(sec)
i)

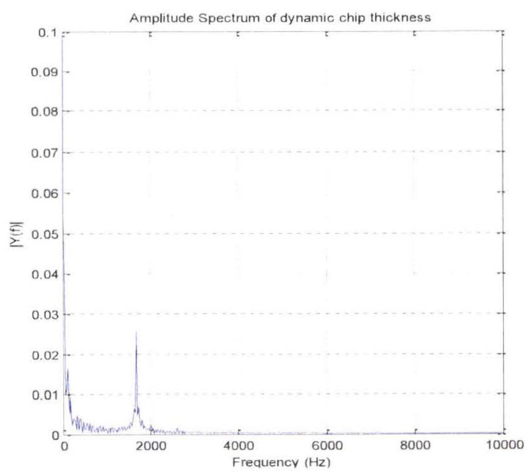
Amplitude Spectrum of dynamic chip thickness
|Y(f)|
Frequency (Hz)
j)

k) 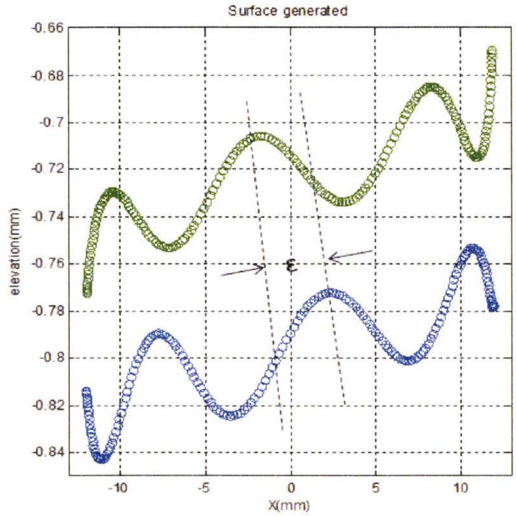

Figure 7-9 - Simulation results for unstable plunge milling at 14750rpm, f=0.07mm/tooth, b=6.25mm a) cutting forces, b) System vibrations, c) FFT of FX, d) FFT of x vibration, e) FFT of FY, f) FFT of y vibration, g) FFT of FZ, h) FFT of z vibration, i) Dynamic chip thickness, j) FFT of chip thickness and k) Surface generated.

Another case of stable cutting can be shown in Figure 7-10 and Figure 7-11 which show respectively, the experimental and simulation results for point F on the stability lobe. It corresponds to plunge milling at 13000 rpm, with feed rate of 0.0795 mm/tooth and 7.5 mm width of cut. Stable cutting is demonstrated by the chatter-free dynamic force and vibration for both measured and predicted signals. This observation is in accordance with the predicted stability lobe as this combination of cutting speed and feed falls within the stable zone indicated by the predicted diagram. A good agreement in the trend and magnitude of measured and predicted cutting force and vibration signals as well as their power spectra can be noticed for the x, y, and z directions. The FFT of measured and predicted results are dominated by the indicated peak at a frequency corresponding to the rotational speed (i.e. 216 Hz) as a result of tool setting errors, indicating stable cutting. On the other hand, the effect of workpiece dynamics is illustrated by the peak at 1750 Hz, which corresponds to the workpiece axial mode for measured and predicted axial force and vibration signals. However, it can be noticed that the peak at 1750 Hz is of smaller magnitude indicating stable cutting as compared to the case of unstable cutting in Figure 7-7.

Additionally, it can be shown that the vibration marks left by each insert are in phase, leading to stable cutting. The same observation is noticed in the predicted dynamic chip thickness, which shows a stable dynamic chip thickness. The dynamic behaviour of chip thickness is attributed mainly to workpiece axial vibration as indicated by the power spectrum of chip thickness showing a peak at 1750 Hz.

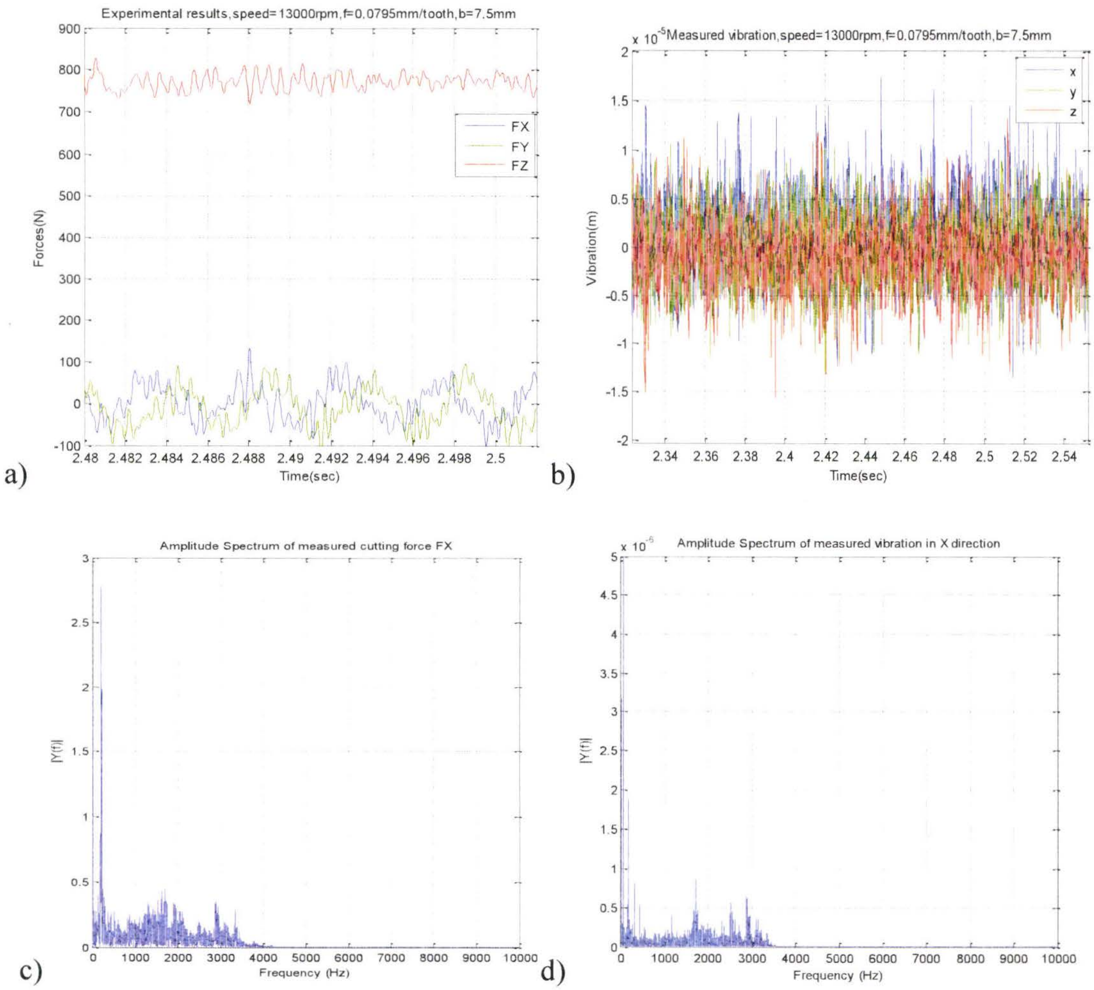

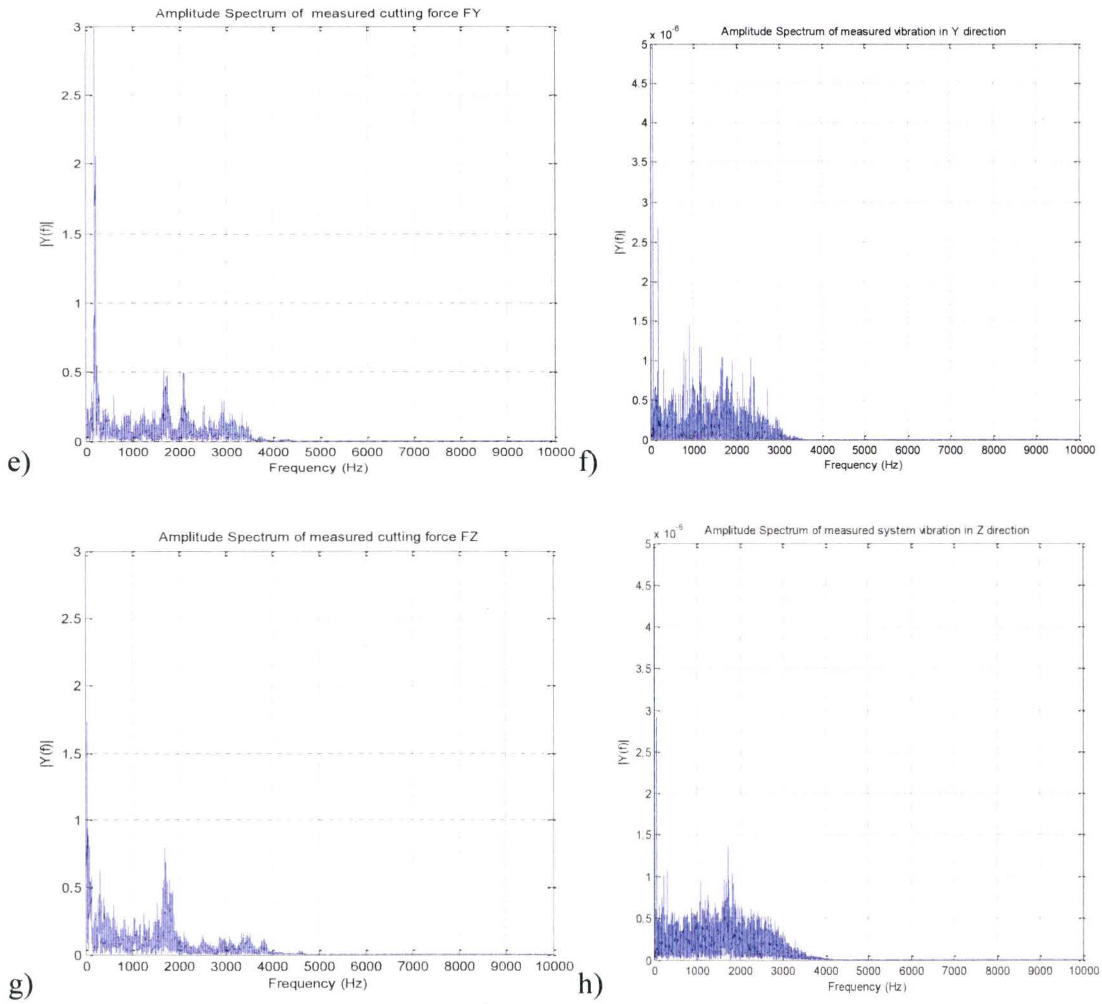

Figure 7-10 Experimental results for stable plunge milling at 13000rpm, f=0.0795 mm/tooth, b=7.5mm a) cutting forces, b) System vibrations, c) FFT of FX, d) FFT of x vibration, e) FFT of FY, f) FFT of y vibration, g) FFT of FZ, h)FFT of z vibration.

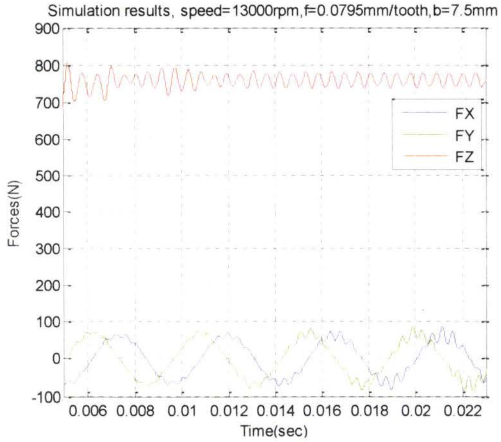
Simulation results, speed=13000rpm,f=0.0795mm/tooth,b=7.5mm
Forces(N)
Time(sec)
FX
FY
FZ

a)

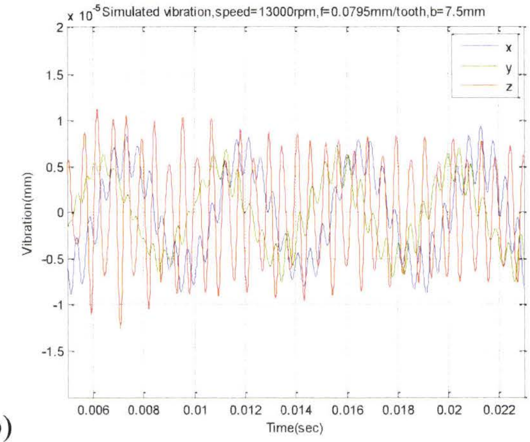
x 10^-5 Simulated vibration,speed=13000rpm,f=0.0795mm/tooth,b=7.5mm
Vibration(mm)
Time(sec)
x
y
z

b)

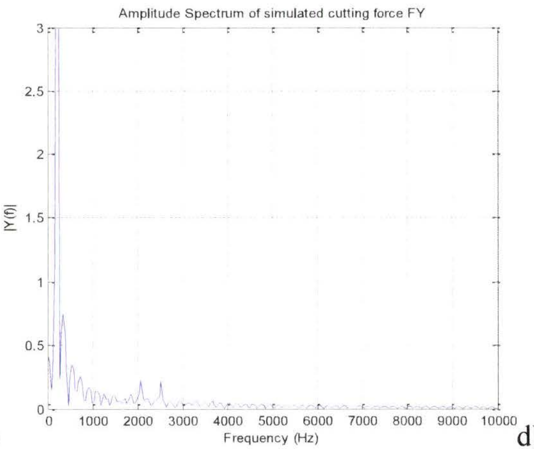
Amplitude Spectrum of simulated cutting force FY
|Y(f)|
Frequency (Hz)

c)

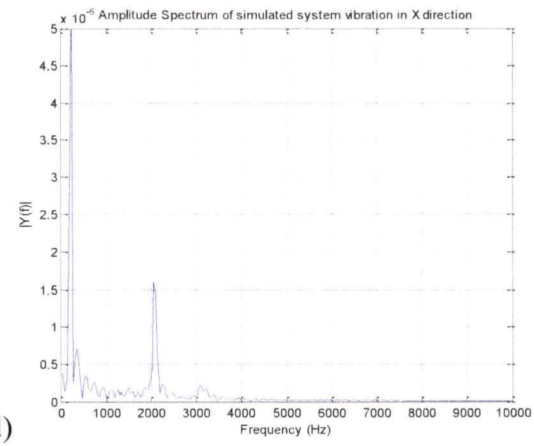
x 10^-5 Amplitude Spectrum of simulated system vibration in X direction
|Y(f)|
Frequency (Hz)

d)

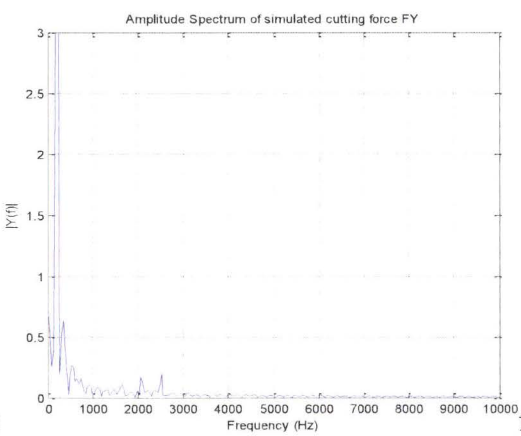
Amplitude Spectrum of simulated cutting force FY
|Y(f)|
Frequency (Hz)

e)

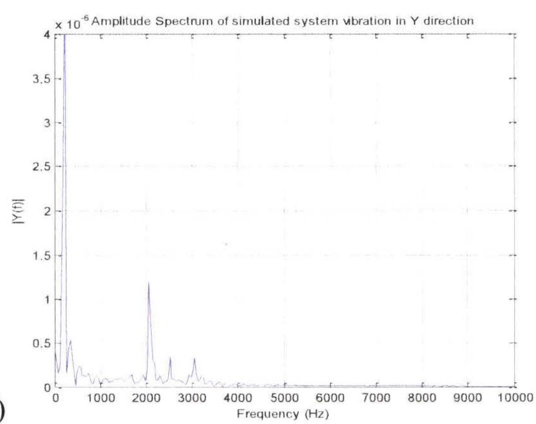
x 10^-6 Amplitude Spectrum of simulated system vibration in Y direction
|Y(f)|
Frequency (Hz)

f)

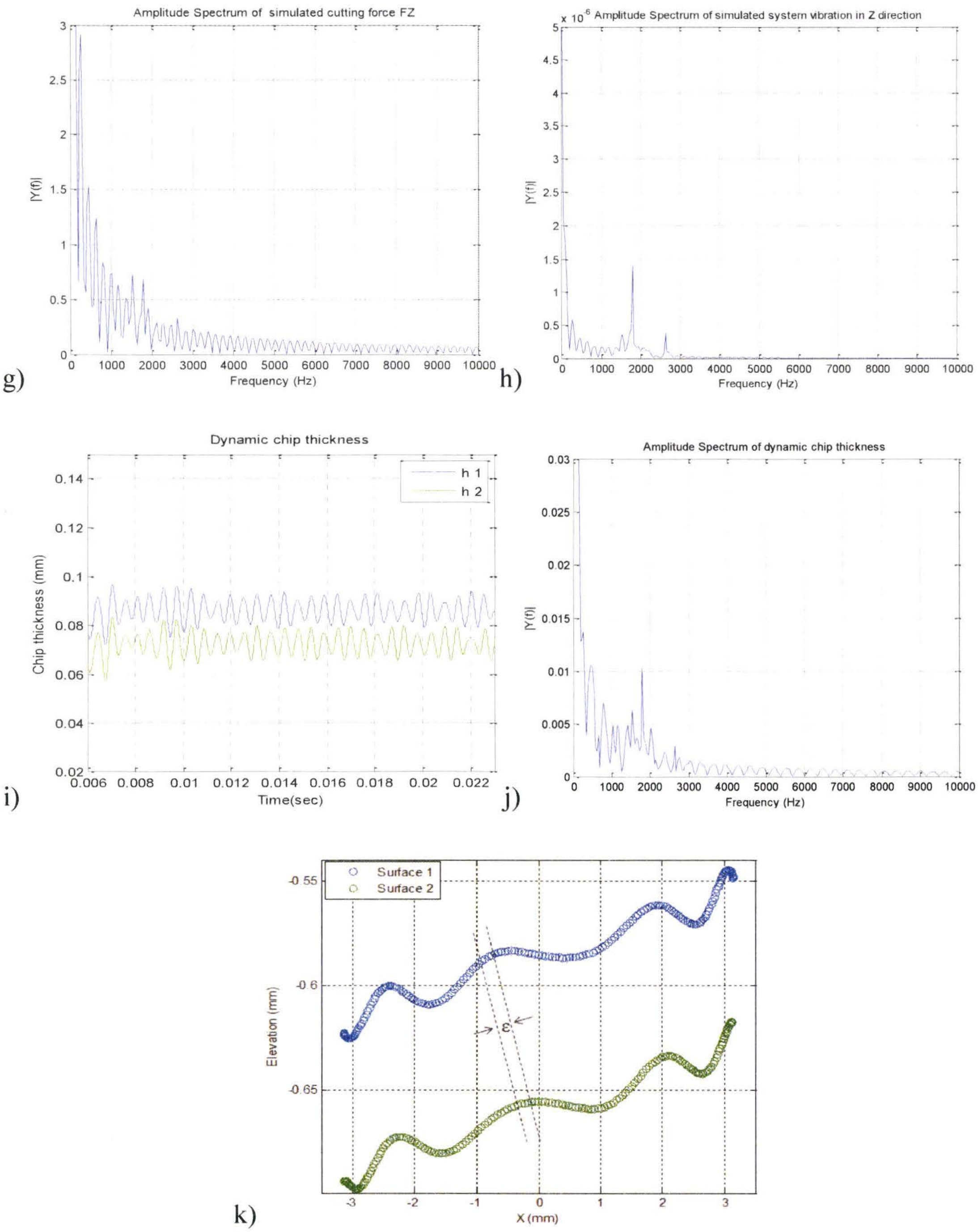

Figure 7-11 Simulation results for stable plunge milling at 13000rpm, f=0.0795 mm/tooth, b=7.5mm a) cutting forces, b) System vibrations, c) FFT of FX, d) FFT of x vibration, e) FFT of FY, f) FFT of y vibration, g) FFT of FZ, h) FFT of z vibration, i) Dynamic chip thickness, j) FFT of chip thickness and k) Surface generated.

Further validation in the model can be shown in Figure 7-12 to Figure 7-14 which show the experimental and simulation results for different cutting test at different cutting conditions to cover a wide range of speeds, feeds and width of cut.

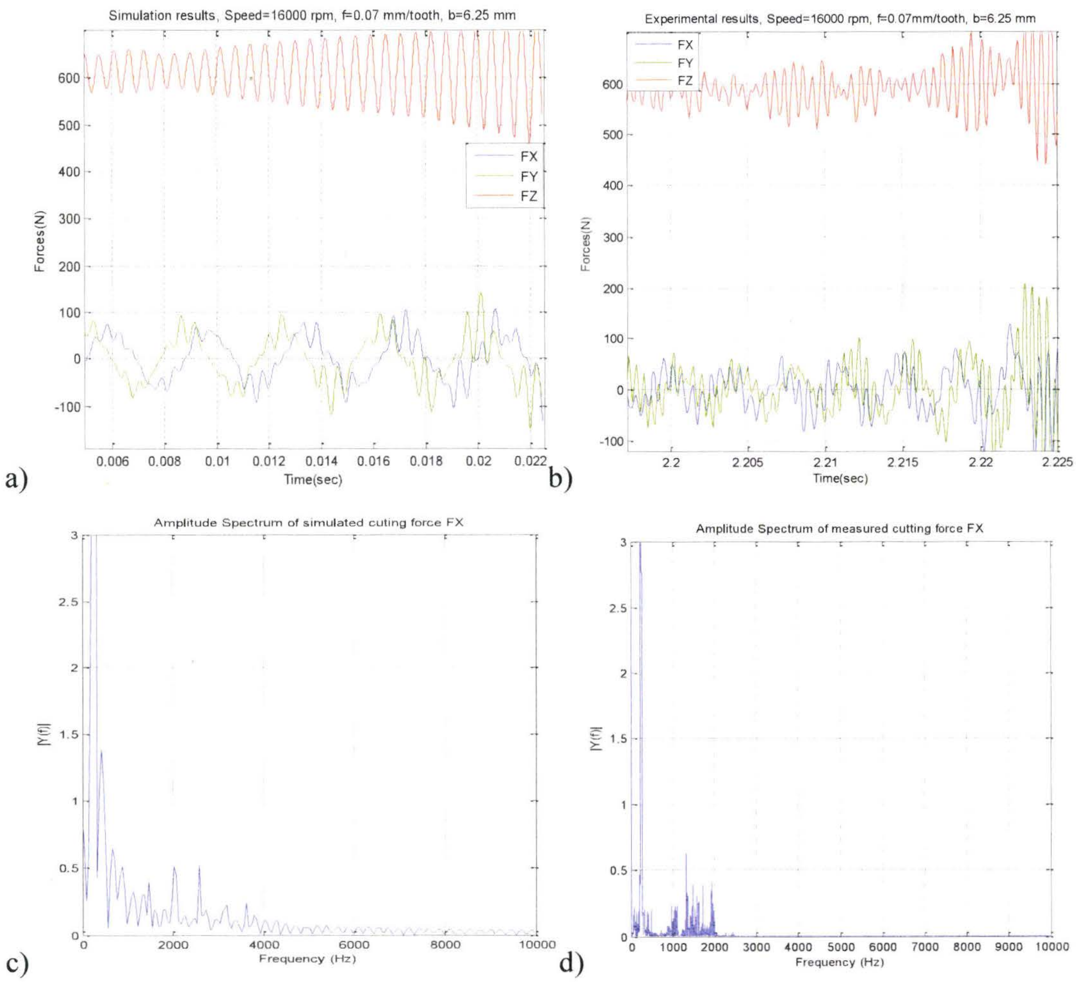

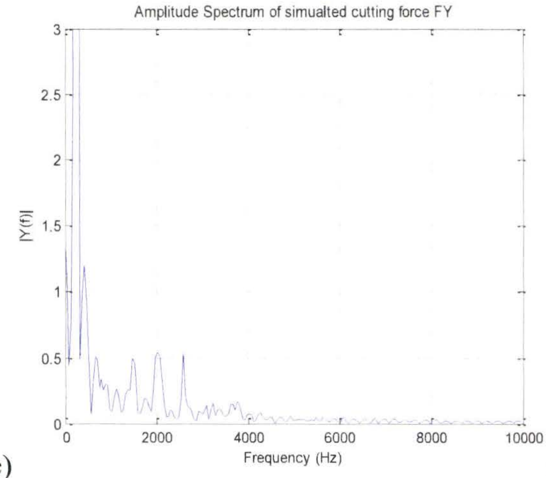
Amplitude Spectrum of simualted cutting force FY
|Y(f)|
Frequency (Hz)

e)

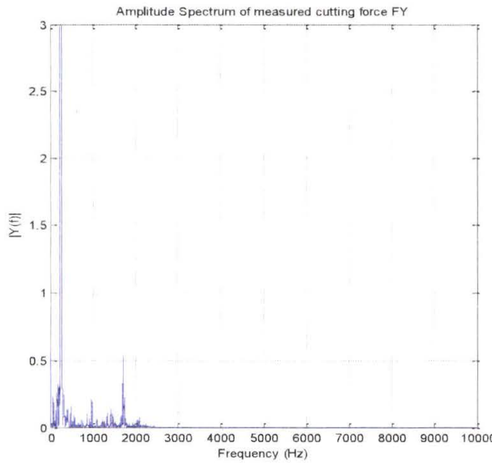
Amplitude Spectrum of measured cutting force FY
|Y(f)|
Frequency (Hz)

f)

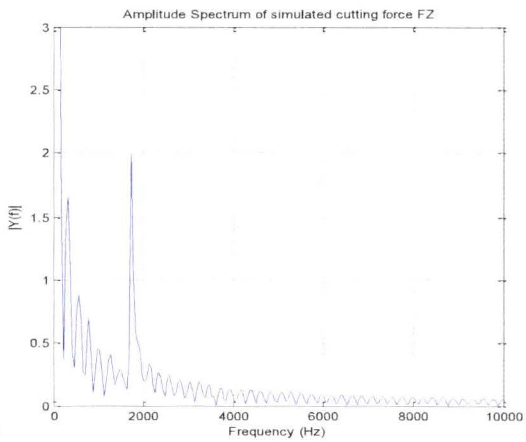
Amplitude Spectrum of simulated cutting force FZ
|Y(f)|
Frequency (Hz)

g)

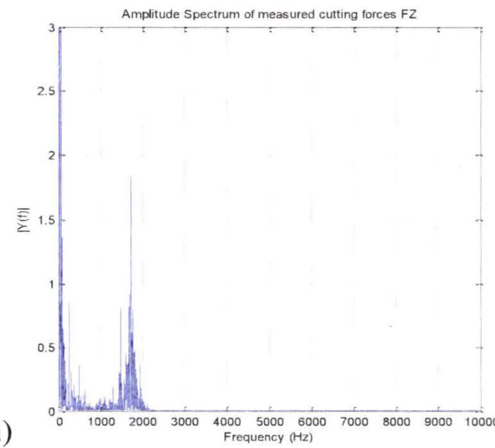
Amplitude Spectrum of measured cutting forces FZ
|Y(f)|
Frequency (Hz)

h)

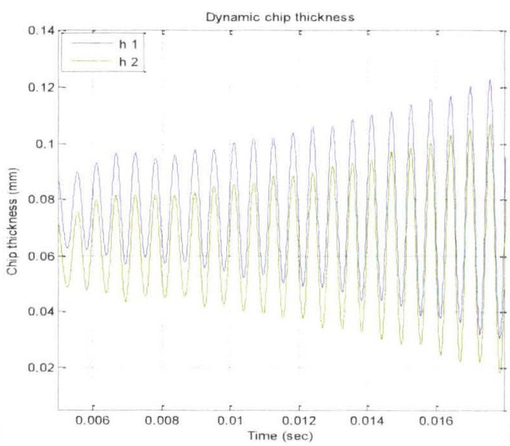
Dynamic chip thickness
h 1
h 2
Chip thickness (mm)
Time (sec)

i)

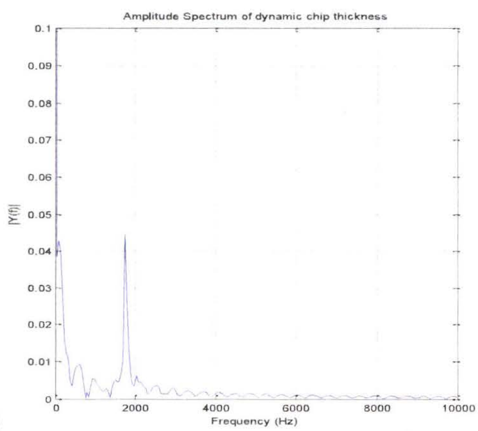
Amplitude Spectrum of dynamic chip thickness
|Y(f)|
Frequency (Hz)

j)

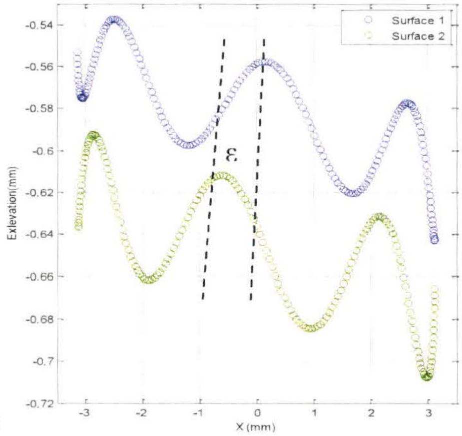

k)

Figure 7-12 Results for case of unstable cutting at 16000 rpm, f=0.07mm/tooth, b=6.25mm a) predicted, b) measured cutting forces, c) predicted, d) measured FFT of FX, e) predicted, f) measured FFT of FY, g) predicted, h) measured FFT of FZ, i) dynamic chip thickness, j) FFT of chip thickness k) Surface generated

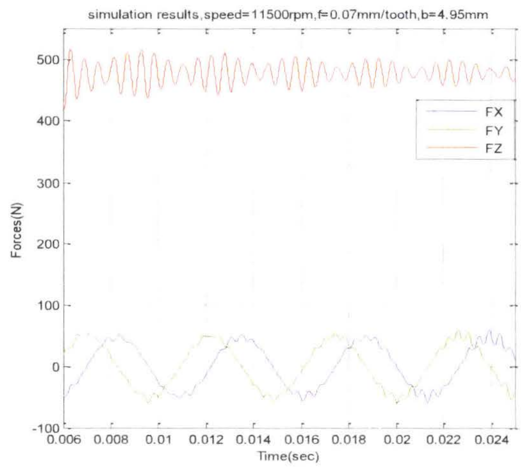

a)

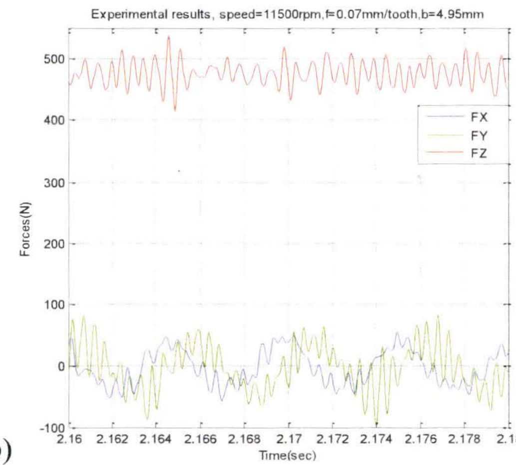

b)

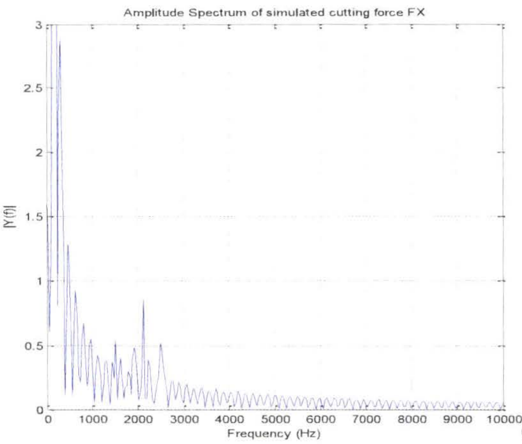
Amplitude Spectrum of simulated cutting force FX
|Y(f)|
Frequency (Hz)
c)

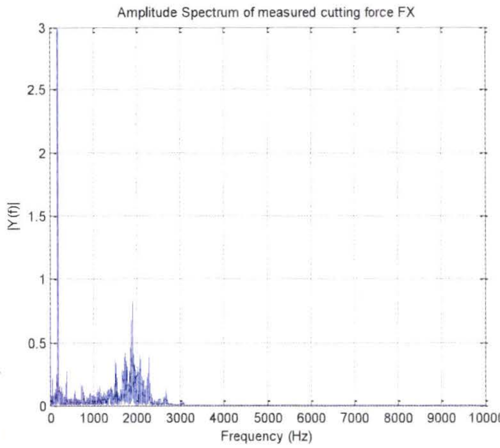
Amplitude Spectrum of measured cutting force FX
|Y(f)|
Frequency (Hz)
d)

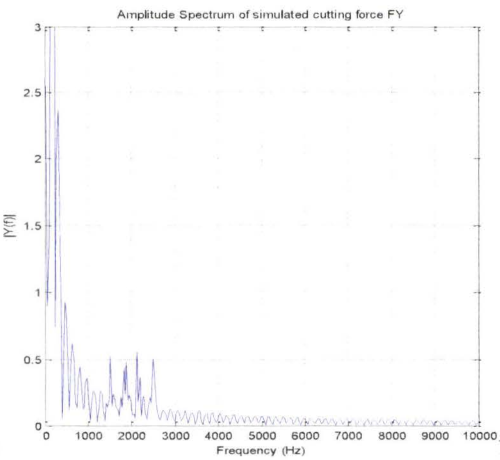
Amplitude Spectrum of simulated cutting force FY
|Y(f)|
Frequency (Hz)
e)

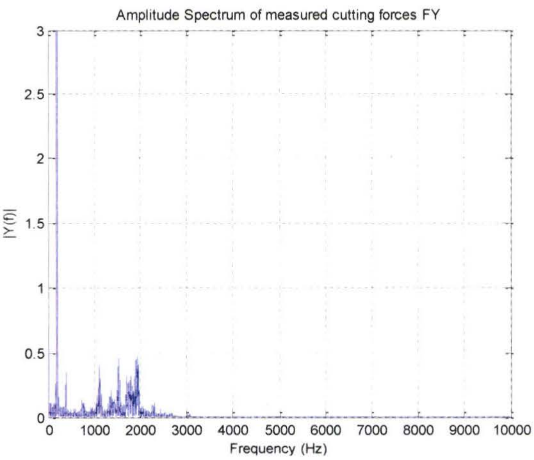
Amplitude Spectrum of measured cutting forces FY
|Y(f)|
Frequency (Hz)
f)

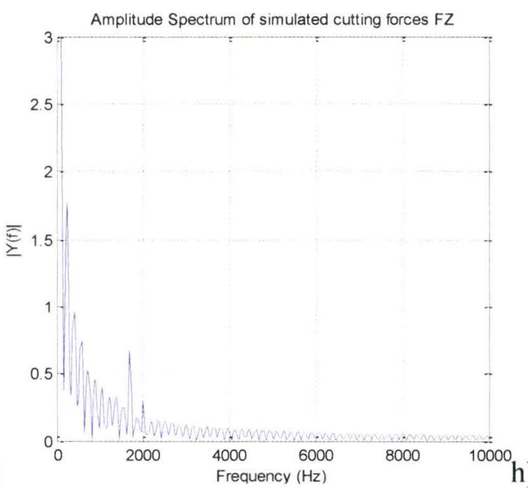
Amplitude Spectrum of simulated cutting forces FZ
|Y(f)|
Frequency (Hz)
g)

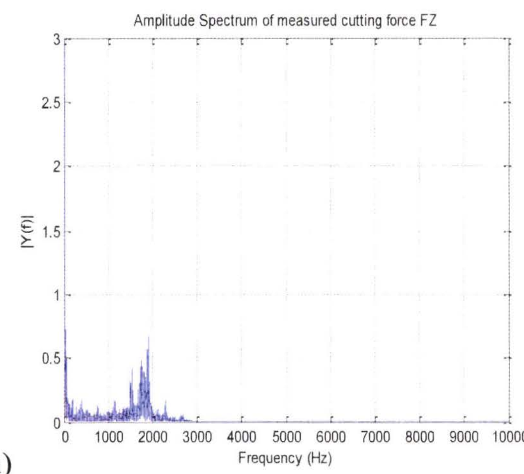
Amplitude Spectrum of measured cutting force FZ
|Y(f)|
Frequency (Hz)
h)

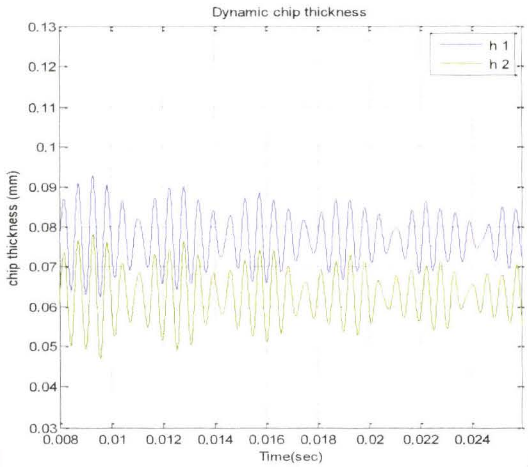

i)

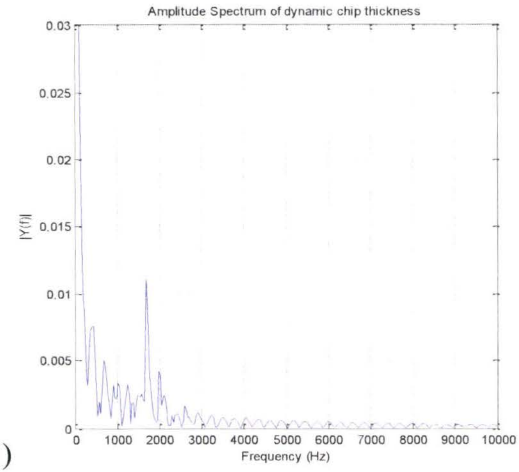

j)

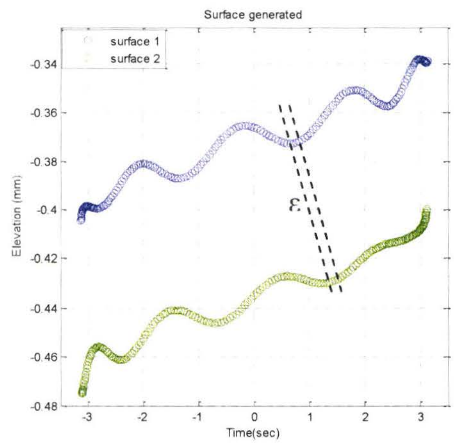

Figure 7-13 Results for case of stable cutting at 11500 rpm, f=0.07mm/tooth, b=4.95 mm a) predicted, b) measured cutting forces, c) predicted, d) measured FFT of FX, e) predicted, f) measured FFT of FY, g) predicted, h) measured FFT of FZ, i) dynamic chip thickness, j) FFT of chip thickness k) Surface generated

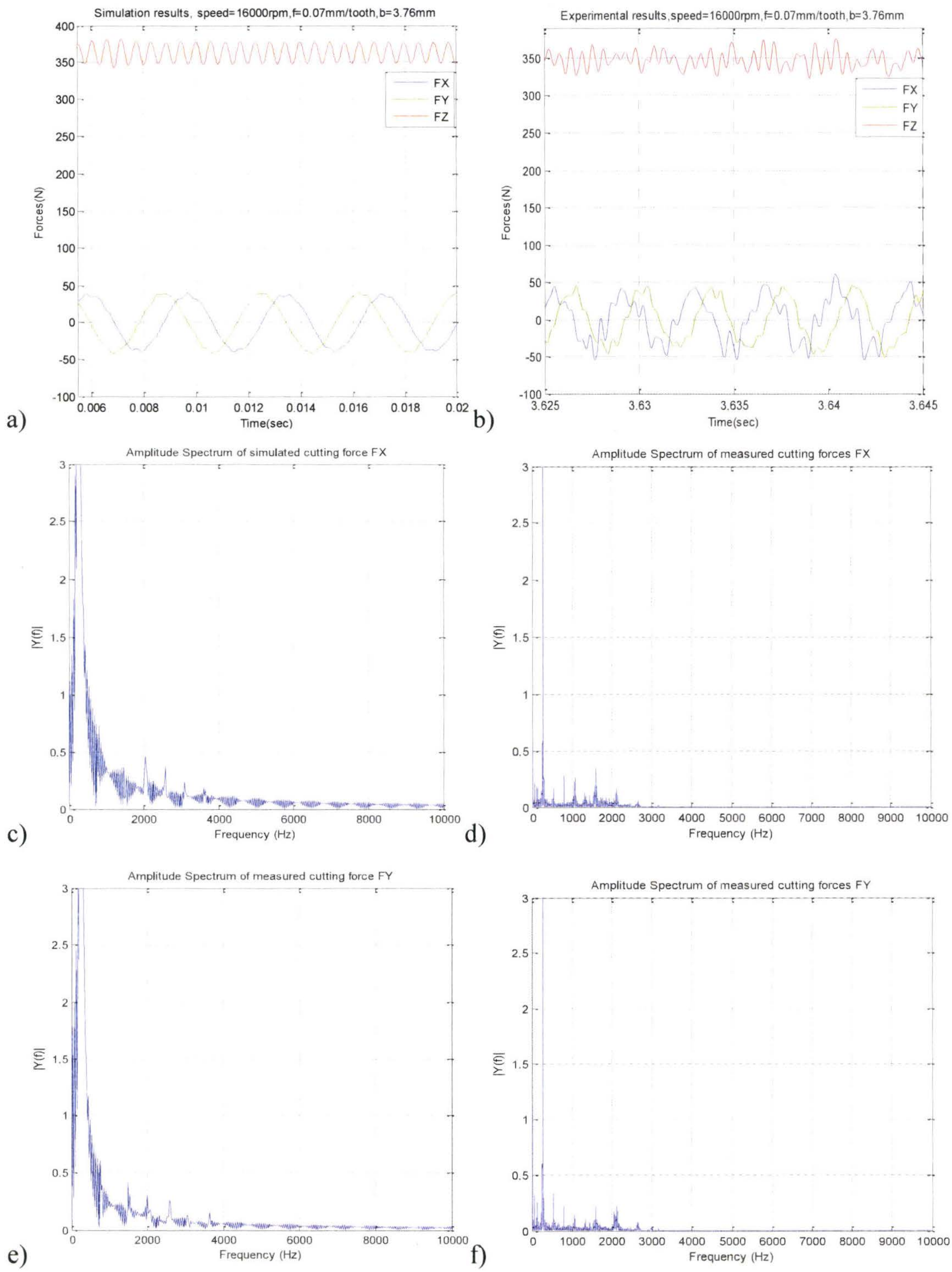
a)
Simulation results, speed=16000rpm,f=0.07mm/tooth,b=3.76mm
Forces(N)
Time(sec)
FX
FY
FZ
b)
Experimental results,speed=16000rpm,f=0.07mm/tooth,b=3.76mm
Forces(N)
Time(sec)
FX
FY
FZ
c)
Amplitude Spectrum of simulated cutting force FX
|Y(f)|
Frequency (Hz)
d)
Amplitude Spectrum of measured cutting forces FX
|Y(f)|
Frequency (Hz)
e)
Amplitude Spectrum of measured cutting force FY
|Y(f)|
Frequency (Hz)
f)
Amplitude Spectrum of measured cutting forces FY
|Y(f)|
Frequency (Hz)

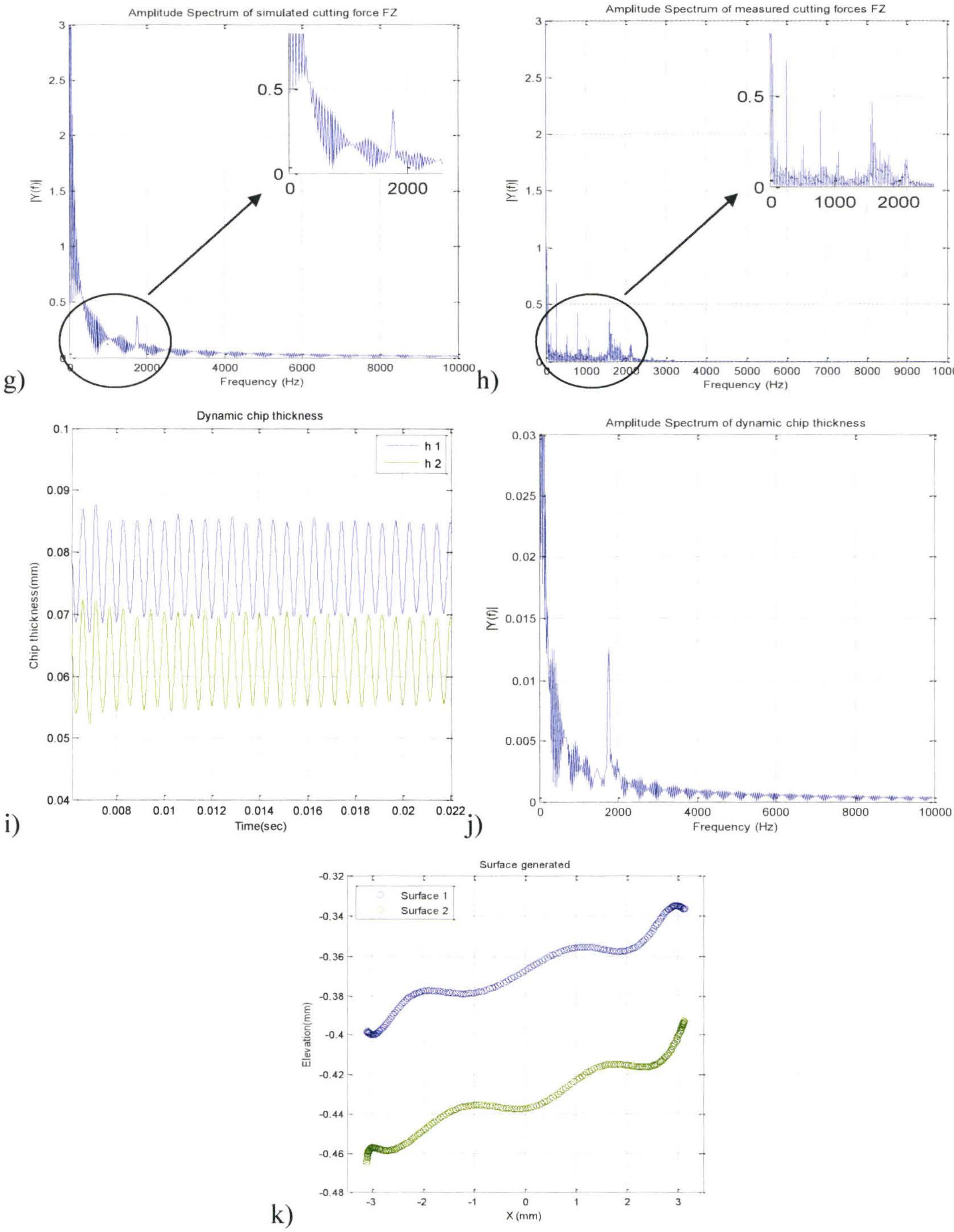

Figure 7-14 Results for case of stable cutting at 16000 rpm, f=0.07mm/tooth, b=3.74 mm a) predicted, b) measured cutting forces, c) predicted, d) measured FFT of FX, e) predicted, f) measured FFT of FY, g) predicted, h) measured FFT of FZ, i) dynamic chip thickness, j) FFT of chip thickness k) Surface generated

Good agreement can be noticed between the measured and predicted results. This is illustrated by the agreement in trend and magnitude of both measured and predicted cutting force signals and power spectra. Additionally, the experimental results are in accordance with the predicted stability lobe indicating its ability to be used as a reliable and cost effective predictive tool for process planning and control prior and during machining. It can be noticed that the cutting forces decrease with the decrease in width of cut and feed rate. This is attributed to the decrease of the chip load which affects directly the value of the cutting force. Additionally, the process tends to be more stable at small widths of cut for the same cutting speed. The same observation was noticed by Tlusty [7] as he described the depth of cut as the "gain" in the self-excitation process; while increasing the depth of cut leads from stable to chatter. Figure 7-15 shows the variation between measured and predicted magnitude of lateral and axial cutting forces at different widths of cut. It shows a good agreement between the measured and predicted axial force values at different radial depths of cut. This validates the proposed model and confirms its ability to correctly predict the cutting forces and hence, the dynamics and stability of the process. The deviation between the measured and predicted axial force was found to range from 4% to 1% which is considered very acceptable for simulation error, especially as compared to the work done in the literature which had a deviation of 12% - 18% in the axial force [96, 104, 105]. This reduction in the difference between experimental and simulation results demonstrates the accuracy of the presented simulation model that depends on the correctness of the approach used for modeling the cutting area as well as the correctness of the cutting coefficient model, which are very critical for force prediction and hence, process modeling.

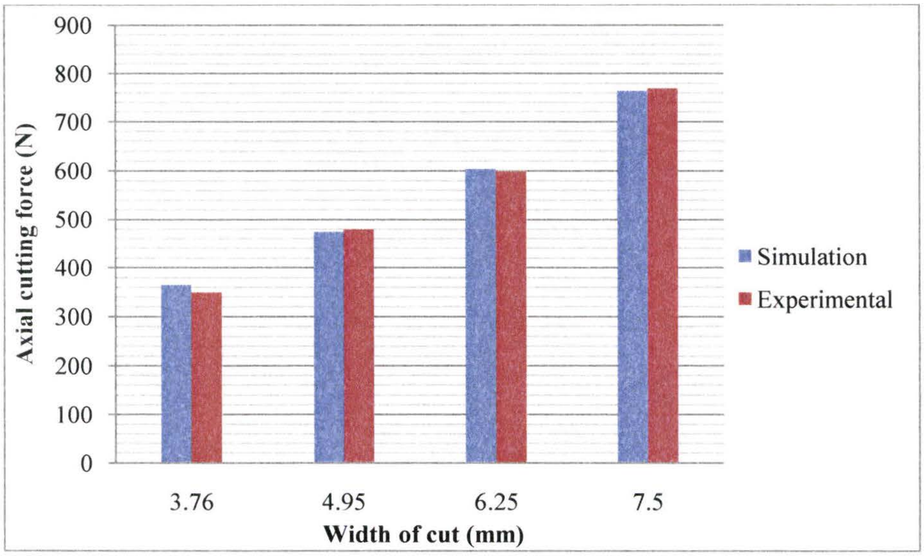

Figure 7-15 Magnitudes and of predicted and measured axial force for plunge milling with double inserts for system with flexible workpiece at different width of cut

7.5 Conclusion

In this chapter, plunge milling with double inserts of systems with flexible workpiece was studied both experimentally and numerically. The dynamics of the workpiece, as well as the tool dynamics, are considered in the simulation to model the dynamics and stability of plunge milling for systems with a flexible workpiece. Additionally, the variation of the workpiece dynamics with respect to the hole location, detected experimentally, was considered in the simulation in order to simulate the cutting process based on the actual parameters. Experimental validation of the proposed model as well as the predicted stability lobe was carried out at different cutting conditions that represent several cases of stable and unstable cutting. A very good agreement was found between the measured and predicted cutting forces and system vibrations for stable and unstable cutting. This is demonstrated in the agreement in trend and magnitude of measured and predicted cutting force and vibration signals as well as their power spectra. This validated the predicted stability lobe and the simulation model when the dynamics of the workpiece is considered for better process planning and control. The experimental validation demonstrated the ability of the model to deal with the dynamics of two inserts for flexible workpiece as well as the correctness of the cutting coefficient model. It was found that for a system with a flexible workpiece, the workpiece dynamics is dominant in the axial direction due to its flexibility as compared to the spindle rigidity. Additionally, chatter behaviour occurred mainly due to the workpiece axial dynamics as compared to the tool lateral dynamics for a system with a rigid workpiece.

The flexibility of the workpiece can play an important role in the stability and dynamics of the machining process. This appeared in the dominance of the workpiece dynamics in the axial direction due to its high flexibility as compared to the tool high axial rigidity. This fact may alter the main advantage of plunge milling which benefits from spindle axial rigidity in the main cutting direction, and hence affects the process stability.

Conclusion and Future work

8.1 Conclusion

This research is focused on the modeling the dynamics and stability of plunge milling while taking into account the flexibility of the workpiece and its variation during cutting as well as different parameters that can affect the process stability, such as the contribution of side edge interaction in cutting. This research aims to develop an effective tool to plan the cutting process prior to machining to increase productivity while maintaining stable cutting to improve the process performance, product quality and reduce cost. The following conclusions can be drawn from the performed analysis and obtained results.

1. A time domain simulation model with a new approach to model the cutting area is developed to study the dynamics of the plunge milling process for systems with rigid and flexible workpiece. This model could predict cutting forces, torque and system vibrations as a function of system (tool and workpiece) dynamics, insert geometry, cutting conditions and tool setting errors.
2. The presented model is based on evaluating the dynamic chip area as a function of the interaction of the present insert, pilot hole and surface left by the previous inserts. This approach allows the consideration of the contribution of both main and side edges of the insert in the cutting action and it is capable of dealing with any geometrical shape of the insert.
3. The effect of side cutting edge on cutting action is more noticeable for higher radial runout as well as lateral vibrations of the system. This is attributed to the engagement of the side edge with the workpiece over higher length and depth.
4. Full immersion plunge milling with a single insert was used to determine the cutting force coefficients to eliminate the effect of radial and axial runout on

cutting coefficients evaluation while realistically simulating the actual cutting action used in the experiments (i.e. full immersion plunge milling).

5. Instantaneous cutting force coefficients are computed as a function of the actual chip thickness removed by each insert to consider its variability due to system vibrations and tool setting errors. This allows better prediction of cutting forces of each insert in order to accurately simulate plunge milling process.
6. Both workpiece and tool dynamics were considered in the time domain simulation model to better simulate the plunge milling process especially for the cases where workpiece flexibility is noticeable. It was noticed that the workpiece dynamics is dominant in the axial direction where it is less rigid as compared to the axial spindle rigidity.
7. Experimental modal analysis is carried out to study the variation of workpiece dynamics as a function of the hole location with respect to its fixation. The results showed that the workpiece dynamics vary at different locations as well as the dominant mode in the axial direction. The variability of workpiece dynamics was considered in the simulation model in order to simulate the plunge milling process based on the actual dynamics of the workpiece for the case of a system with a flexible workpiece.
8. The stability lobe diagram of the plunge milling process was predicted for a system with a rigid and a flexible workpiece by considering the tool and workpiece dynamics. The experimental validation of the predicted lobes shows good accordance with the predicted stability lobe for stable and unstable cutting conditions for a system with a rigid workpiece where only the tool dynamics are considered and for a system with a flexible workpiece where the workpiece dynamics are also taken into account.
9. Experimental cutting tests were carried out for plunge milling with a single and double inserts for rigid and flexible workpieces to validate the proposed model. The proposed model was shown to be able to predict the cutting forces for plunge milling with both a single and a double insert. A good agreement between the

measured and predicted cutting forces and system vibration signals and power spectra was found in the trend and magnitude for both cases of single and double insert plunge milling. Additionally, good agreement was observed between the experimental and simulation results for stable and unstable cutting conditions for systems with rigid and flexible workpiece.

10. Experimental and simulation results showed that for systems with a rigid workpiece, chatter behaviour was found to occur as a result of tool lateral vibration, while it occurred due to the workpiece axial flexibility for systems with a flexible workpiece as a result of the experimental setup at which the workpiece is considered as a relatively thin plate supported along two edges, which increases the workpiece axial flexibility as compared to the tool.

8.2 Future work

The current research can be extended in the future in different areas to cover several interesting points that were not considered before. This includes:

1. Modeling the case of plunge milling of multi-phase material and study its effect on the cutting force, system vibration and stability of plunge milling. Consider the variation of cutting coefficient as a function of the phase cut by each element of the modeled inserts based on its position with respect to the position and orientation of the different phases. Apply the same concept in modeling the plunge milling of composite materials and stacked structures by considering the transition between the matrix and reinforcing element in composites and from one material to the other in stacked structures in order to select the optimum cutting conditions and provide a reliable and cost effective predictive tool for better planning of the process.
2. Extend the simulation model to model and predict the surface roughness of the machined product. In addition to force prediction, this can help at optimizing the cutting conditions to achieve higher productivity based on the criteria of surface quality and power consumption.

3. Consider the effect of nose radius on the area calculation and prediction of the cutting force for better modeling of the plunge milling process.
4. Apply the presented model for case of partial immersion plunge milling in slotting application by considering the variation of system dynamics (i.e. tool and workpiece) during cutting to select the optimum cutting conditions and tool path.
5. Study the case of small radial immersions and its effect on the variation of process dynamics and stability for plunge milling of rigid and flexible workpiece.

References

[1] A. K. M. Amin, M. Abdelgadir, "The Effect of Preheating of Work Material on Chatter During End Milling of Medium Carbon Steel Performed on a Vertical Machining Center (VMC)", Transactions of the ASME (2003), Vol. 125, 674-680.

[2] S. Tobias, W. Fiswick, "Theory of Regenerative Machine Tool Chatter" in "An expert troubleshooting system for the milling process", International Journal of Machine Tools & Manufacture (2007), Vol.47, 1417-1425

[3] S. Tobias, "Machine Tool Vibration", Blackie, 1965.

[4] N. Hanna, S. Tobias, "Theory of Nonlinear Regenerative Chatter", ASME Journal o f Engineering for industry (1974), 247-255.

[5] H. Merrit, "Theory of Self-Excited Machine Tool Chatter, Contribution to Machine Tool Chatter" Journal of Engineering for Industry (1965), 447-454.

[6] F. Koenigsberger, J.Tlusty, "Machine Tool Structures, Vol I", Pergamon press (1970).

[7] J. Tlusty, "Manufacturing Processes and Equipment", Prentice Hall (2000).

[8] J. Tlusty, "Dynamics of High Speed Milling", Transactions of the ASME (1986), Vol. 108, 59-67.

[9] Y. Altintas, "Manufacturing Automation: Metal Cutting Mechanics, Machine Tool vibrations, and CNC Design", Cambridge University Press, 2000.

[10] J. Tlusty, "High Speed Machining", Annals of the CIRP (1993), Vol. 42, 733-738.

[11] F. Ismail, E. Soliman, "A New Method for the Identification of Stability Lobes in Machining", International Journal of Machine tools Manufacturing (1997), Vol. 37, 763-774.

[12] G. Quintana, J. Ciurana, D. Teixidor, "A new experimental methodology for identification of stability lobes diagram in milling operations", International Journal of Machine Tools and Manufacture (2008), Vol. 48, 1637-1645.

[13] E. Solis, C. Peres, J. Jimenez, J. Alique, J. Monje, "A new analytical-experimental method for the identification of stability lobes in high-speed milling", International Journal of Machine Tools and Manufacture (2004), Vol. 44, 1591-1597.

[14] E. Abele, U. Fiedler, "Creating Stability Lobe Diagrams during Milling", CIRP Annals (2004), Vol. 53, 309-312.

[15] E. Kuljanic, M. Sortino, G. Totis, "Multisensor approaches for chatter detection in milling", Journal of Sound and Vibration (2008), Vol. 312, 672-693.

[16] Y. Altintas, M. Weck, "Chatter Stability of Metal Cutting and Grinding", Annals of the CIRP (2004), Vol. 53, 619-642.

[17] E. Soliman, "Active chatter control techniques in peripheral milling", Ph.D. thesis, university of Waterloo, Waterloo (1995).

[18] S. Smith, T. Delio, "Sensor Based Control for Chatter-Free Milling by Spindle Speed Selection", Journal of Engineering for Industry, AMSE (1992), Vol. 114, 107- 114.

[19] S. Smith, J. Tlusty, "Stabilizing Chatter by Automatic Spindle Speed Regulation", Annals of the CIRP (1992), Vol. 41, 433-436.

[20] T. Delio, S. Smith, J. Tlusty, "Use of Audio Signals Chatter Detection and Control", Journal of Engineering for Industry, Transactions of the ASME (1992), Vol. 114,146-157

[21] E. Soliman, F. Ismail, "A control system for chatter avoidance by rmoing the spindle speed", ASME Journal of Manufacturing Science and Engineering (1998), Vol. 120, 674-683.

[22] G. Morgan, R. Cheng, Y. Altintas, K. Ridgway, "An expert troubleshooting system for the milling process", International Journal of Machine Tools & Manufacture (2007), Vol.47, 1417-1425

[23] J. Pratt, H. Nayfeh, "Design and Modeling for Chatter Control", Nonlinear Dynamics (1999), Vol. 19, 49-69.

[24] B. Lee, Y. Tarng, S. Ma, "Modeling of the Process Damping Force in Chatter Vibration", International Journal of Machine Tools and Manufacturing (1995), Vol. 35, 951-962

[25] J. Wang, K. Lee, "Suppression of chatter vibration of a CNC machine centre- an example", Mechanical Systems and Signal Processing (1996), Vol. 10, 551-560.

[26] A. Milecki, "Investigation and control of magneto-rheological fluid dampers", International Journal of Machine Tools and Manufacture (2001), Vol. 41, 379-391.

[27] C. Anderson, S. Semercigil, O. Turan, "A passive adaptor to enhance chatter stability for end mills", International Journal of Machine Tools and Manufature (2007), Vol. (47), 1777-1785.

[28] C. Mei, J. Cherng, Y. Wang, "Active Control of Regenerative Chatter During Metal Cutting Process", Journal of Manufacturing Science and Engineering (2006), Vol. 128, 326-349.

[29] N. Sims, "Vibration absorbers for chatter suppression: A new analytical tuning methodology", Journal of Sound and Vibration (2007), Vol. 31, 592-607.

[30] J. Tlusty, F. Ismail, W. Zaton, "Use of Special Milling Cutters Against Chatter", Manufacturing Engineering Transactions (1983), 408-415.

[31] J. Tlusty, S. Smith, C. Zamudio, "Evaluating the cutting performance of machine centers", CIRP annals (1991), Vol. 40, 405-410.

[32] J. Tlusty, "Dynamics of High Speed Milling", Transactions of the ASME (1986), Vol. 108, 59-67.

[33] Y. Altintas, E. Budak, "Analytical Prediction of Stability Lobes in Milling", Annals of the CIRP (1995) Vol. 44, 357-362.

[34] E. Budak, "Analytical models for high performance milling. Part I: Cutting Forces, Structural Deformations and tolerance integrity", International Journal of Machine Tools & Manufacture (2006), Vol. 46, 1478-1488.

[35] E. Budak, "Analytical models for high performance milling. Part II: Process dynamics and stability", International Journal of Machine Tools & Manufacture (2006), Vol. 46, 1489-1499.

[36] Y. Altintas, "Analytical Prediction of Three Dimensional Chatter Stability in Milling", Japan Society of Mechanical Engineering (2001), Vol. 44, No. 3, 717-723.

[37] E. Budak, E. Ozlu, "Analytical Modeling of Chatter Stability in Turning and Boring Operations: A Multi-Dimensional Approach", CIRP Annals (2007), Vol. 56, 401-404.

[38] R. Landers, A. Ulsoy, "Nonlinear Feed Effect in Machining Chatter Analysis", Journal of Manufacturing Science and Engineering (2008), Vol. 130, 011017-1–011017-8

[39] T. Insperger, G. Stephan, P. Bayly, B. Mann, "Multiple chatter frequencies in milling processes", Journal of Sound and Vibration (2003), Vol. 262, 333-345.

[40] T. Insperger, B. Mann, G. Stephan, P. Bayly, "Stability of up-milling and down-milling, part 1: alternative analytical methods", International Journal of Machine Tools and Manufacture (2003), Vol. 43, 25-34.

[41] B. Mann, T. Insperger, P.Bayly, G. Stephan, "Stability of up-milling and down-milling, part 2: experimental verification", International Journal of Machine Tools and Manufacture (2003), Vol. 43, 35-40.

[42] M. Davies, B. Dutterer, J. Pratt, A. Schaut, "On the Dynamics of High-Speed Milling with Long, Slender Endmills" Annals of the CIRP (1998), Vol. 47, 55-60.

[43] R. Szalai, G. Stephan, "Global dynamics of low immersion high-speed milling", Chaos (2004), Vol. 14, 1069-1077.

[44] B. Mann, B. Edes, S. Easley, K. Young, K. Ma, "Chatter vibration and surface location error prediction for helical end mills", International Journal of Machine Tools and Manufacture (2008), Vol. 48, 350-36.1

[45] V. Gagnol, B. Bouzgarrou, P. Ray, C. Barra, "Model-based chatter stability prediction for high-speed spindles" International Journal of Machine Tools and Manufacture (2007), Vol. 47, 1176-1186.

[46] Y. Altintas, M. Eynian, H. Onozuka, "Identification of dynamic cutting force coefficients and chatter stability with process damping", CIRP Annals (2008), Vol. 57, 371-374.

[47] G. Totis, "RCPM-A new method for robust chatter prediction in milling", International Journal of Machine Tools and Manufacture (2009), Vol. 49, 273-284.

[48] S. Park, Y. Qin, "Robust regenerative chatter stability in machine tools", International Journal of Advanced Manufacturing technology (2007), Vol.33, 389-402.

[49] B. Patel, B. Mann, K. Young, "Uncharted islands of chatter instability in milling", International Journal of Machine Tools and Manufacture (2008), Vol. 48, 124-134.

[50] N. Olgac, R. Sipahi, "A Unique Methodology for Chatter Stability Mapping in Simultaneous Machining", Journal of Manufacturing Science and Engineering (2005), Vol. 127, 791-800.

[51] T. Arvajeh, F. Ismail, "Machining stability in high-speed drilling – Part 1: Modeling vibration stability in bending", International Journal of Machine Tools and Manufacture (2006), Vol. 46, 1563-1572.

[52] J. Roukema, Y. Altintas, "Generalized modeling of drilling vibrations. Part II: chatter stability in frequency domain", International Journal of Machine Tools and Manufacture (2007), Vol. 47, 1474-1485.

[53] J. Gradisek et al. "On stability prediction for milling", International Journal of Machine Tools and Manufacture (2005), Vol. 45, 769-781.

[54] S. Medrol, Y. Altintas, "Multi Frequency Solution of Chatter Stability for Low Immersion Milling", Journal of Manufacturing Science and Engineering (2004), Vol. 126, 459-466.

[55] P. Bayly, J. Halley, B. Mann, M. Davies, "Stability of Interrupted Cutting by Temporal Finite Element Analysis", Journal of Manufacturing Science and Engineering (2003), Vol. 125, 220-225.

[56] M. Davies, J. Pratt, B. Dutterer, T. Burns, "Stability Prediction for Low Radial Immersion Milling", Journal of Manufacturing Science and Engineering (2002), Vol. 124, 217-225.

[57] M. Davies, J. Pratt, B. Dutterer, T. Burns, "The Stability of Low Radial Immersion Milling", Annals of the CIRP (2000), Vol. 49, 37-40.

[58] M. Campomanes, Y. Altintas, "An Improved Time Domain Simulation for Dynamic Milling at Small Radial Immersions", Transactions of the ASME, Journal of Manufacturing Science and Engineering (2003), Vol. 125, 416-422.

[59] J. Tlusty, F. Ismail, "Special Aspects of Chatter in Milling", Transactions of the ASME (1983), Vol. 105, 24-32.

[60] J. Tlusty, F. Ismail, "Basic Non-Linearity in Machining Chatter", Annals of the CIRP (1981) Vol. 30, 299-304.

[61] H. Z. Li, X. Li, X. Chen, "A novel chatter stability criterion for the modeling and simulation of the dynamic milling process in the time domain", International Journal of Advanced Manufacturing Technology (2003), Vol. 22, 619-625.

[62] M. X. Zhao, B. Balachandran, "Dynamics and stability of milling process", International Journal of Solids and Structures (2001), Vol. 38, 2233-2248.

[63] S. Smith, J. Tlusty, "Efficient Simulation Programs for Chatter in Milling", Annals of the CIRP (1993), Vol. 42, 463-466.

[64] M. Zatarain, I. Bediaga, J. Munoa, R. Lizarralde, "Stability of milling process with continuous spindle speed variation: Analysis in the frequency and time domains, and experimental correlation", Annals of the CIRP (2008), Vol. 57, 379-384.

[65] S. Khachan, F. Ismail, "Machining chatter simulation in multi-axis milling using graphical method", International Journal of Machine Tools and Manufacture (2009), Vol. 49, 163-170.

[66] L. Zhongqun, L. Qiang, "Solution and Analysis of Chatter Stability for End Milling in the Time-domain", Chinese Journal of Aeronautics (2008), Vol. 21, 169-178.

[67] Y. Altintas, G. Stephan, D. Medrol, Z. Dombovari, "Chatter stability of milling in frequency and discrete time domain", CIRP Journal of Manufacturing Science and Technology (2008), Vol. 1, 35-44.

[68] S. Turner, D. Merdol, Y. Altintas, K. Ridgway, "Modelling of the stability of variable helix end mills", International Journal of Machine Tools and Manufacture (2007), Vol. 47, 1410-1416.

[69] M. Elbestawi, F. Ismail, R. Du, B. Ullagaddi, "Modelling Machining Dynamics Including Damping in the Tool-Workpiece Interface", American Society of Mechanical Engineers, Production Engineering Division (1991) PED, Vol. 54, 253-263.

[70] F. Abrari, M. Elbestawi, D. Spence, "On the dynamics of ball end milling: Modeling of cutting forces and stability analysis", International Journal of Machine Tools and Manufacture (1998), Vol. 38, 215-237.

[71] O. Omar, T. El-Wardany, E. Ng, M. Elbestawi, "An improved cutting force and surface topography prediction model in end milling", International Journal of Machine Tools and Manufacture (2007), Vol. 47, 1263-1275.

[72] T. Schmitz, J. Couey, E. Marsh, N. Mauntler, D. Hughes, "Runout effects in milling: Surface finish, surface location error, and stability" International Journal of Machine Tools and Manufacture (2007), Vol.47,841-85.

[73] T. Insperger, B. Mann, T. Surmann, G. Stephan, "On the chatter frequencies of milling processes with runout", International Journal of Machine Tools and Manufacture (2008), Vol. 48, 1081-1089.

[74] J. Roukema, Y. Altintas, "Generalized modeling of drilling vibrations. Part I: Time domain model of drilling kinematics, dynamics and hole formation", International Journal of Machine Tools and Manufacture (2007), Vol. 47, 1455-1473.

[75] J. Roukema, Y. Altintas, "Time domain simulation of torsional-axial vibrations in drilling", International Journal of Machine Tools and Manufacture (2006), Vol. 46, 2073-2085.

[76] T. Arvajeh, F. Ismail, "Machining stability in high speed drilling – Part 2: Time domain simulation of a bending-torsional model and experimental validations", International Journal of Machine Tools and Manufacture (2006), Vol. 46, 1573-1581.

[77] N. Sims, "The Self-Excitation Damping Ratio: A Chatter Criterion for Time-Domain Milling Simulations", Journal of Manufacture Science and Engineering (2005), Vol. 127, 433-445.

[78] G. Peigne, H. Paris, D. Brissaud, A. Gouskov, "Impact of the cutting dynamics of small radial immersion milling operations on machined surface roughness", International Journal of Machine Tools and Manufacture(2004), Vol.44,1133-1142.

[79] Le Lan, A. Marty, J. Debongnie, "Providing stability maps for milling operations" International Journal of Machine Tools and Manufacture (2007), Vol. 47, 1493-1496.

[80] M. Anjanappa, D. Anand, J. Kirk, "Identification and optimal control of thin rib machining", ASME Dynamic Systems and Control Division DSC (1987), Vol. 6, 15-23.

[81] M. Anjanappa, D. Anand, J. Kirk, "Application of stochastic optimal control to thin rib machining", IEEE Proceedings D Control Theory and Applications (1991), Vol. 138, 228-236.

[82] S. Smith, D. Dvorak, "Tool path strategies for high speed milling aluminum workpieces with thin webs", Mechatronics (1998), Vol. 8, 291-300.

[83] J. Tlusty, S. Smith, W. R. Winfough, "Techniques for the Use of Long Slender End Mills in High-speed Milling", Annals of the CIRP (1996), Vol. 45, 393-396.

[84] W. Zhao, N. He, K. Wu and L. He, "High efficiency milling of thin-walled components of airplane", Key Engineering Materials (2004), Vol. 259-260, 814-818.

[85] C. K. Chen, Y. M. Tsao, "A stability analysis of turning a tailstock supported flexible work-piece", International Journal of Machine Tools & Manufacture (2006), Vol. 46, 18-25.

[86] M. Sekar, J. Srinivas, K. Rama, S. Yang, "Stability analysis of turning process with tailstock-supported workpiece", International Journal of Advanced Manufacturing Technology (2009), Vol. 43, 862-871.

[87] L. Martinez et al. "Analysis of compliance between the cutting tool and the workpiece on the stability of turning process", International Journal of Machine Tools and Manufacture (2008), Vol. 48, 1054-1062.

[88] F. Ismail, R. Ziaei," Chatter suppression in five-axis machining of flexible parts", International Journal of Machine Tools & Manufacture (2002), Vol. 42, 115-122.

[89] Y. Altintas, D. Montgomery, E. Budak, "Dynamic Peripheral Milling of Flexible Structures", Transaction of the ASME, Journal of Engineering for Industry (1992), Vol. 114, 137-145.

[90] M. A. Davies, B. Balachandran, "Impact Dynamics in Milling of Thin-Walled Structures", Nonlinear Dynamics (2000), Vol. 22, 375-392.

[91] S. Seguy, G. Dessein, L. Arnaud," Surface roughness variation of thin wall milling, related to modal interactions", International Journal of Machine Tools and Manufacture (2008), Vol. 48, 261-274.

[92] I. Mane, V. Gagnol, B. Bouzgarrou, P. Ray, "Stability-based, spindle speed control during flexible workpiece high-speed milling", International Journal of Machine Tools and Manufacture (2008), Vol. 48, 184-194.

[93] V. Thevenot, L Arnaud, G. Dessein, G. Cazenave-Larroche, "Influence of material removal on the dynamic behavior of thin-walled structures in peripheral milling", Machining Science and Technology (2006), Vol. 10, 275-287.

[94]] S. Herranz, F. J. Campa, L. N. Lopez de Lacalle, A. Riverio, A. Lamikiz, E. Ukar, J. A. Sanchez, U. Bravo, "The milling of airframe components with low rigidity: a general approach to avoid static and dynamic problems", Proceedings IMechE part B: Journal of Engineering Manufacture (2005), Vol. 219, 789-801.

[95] U. Bravo, O. Altuzarra, L. Lopez de Lacalle, J. Sanchez, F. Campa, "Stability limits of milling considering the flexibility of the workpiece and the machine", International Journal of Machine Tools & Manufacture (2005), Vol. 45, 1669-1680.

[96] Y. Altintas, J. Ko, "Chatter Stability of Plunge Milling", Annals of the CIRP (2006), Vol. 50, 361-364.

[97] C. Venkatesh, W.Xue,"A study of the built-up edge in drilling with Indexable coated carbide inserts", Journal of Material processing Technology (1996), Vol.58, 379-384.

[98] C.Cluadin, G.Poulachon, M.Lambertin,"Correlation between drill geometry and mechanical forces in MQL conditions",Machining science and Technology(2008), Vol 12, 133-144.

[99] T.Maruish et al,"Finite element modeling of drilling processes with solid and Indexable tooling in metals and stack-ups" International Journal of Machine Tools and Manufacture(2008), Vol.48, 261-274.

[100] S.Wang, C.Venkatesh, W.Xue," Study on modification of endrills for finishing holes", Journal of Materials Processing technology (1991), Vol.28.

[101] C. Needess, U.Gunther, "Radial forces in short hole drilling and their effect on drill performance" Trans. of NAMRI/SME, XX(1992).

[102] S. Wakaola, Y. Yamane, K. Sekiya, N. Narutaki, "High speed and high accuracy plunge cutting for vertical walls", Journal of Material Processing Technology (2002), Vol. 127, 246-250.

[103] Y. Li et al., "Force modelling for cylindrical plunge cutting", International Journal of Advanced Manufacturing Technology (2000), Vol. 16, 863-870.

[104] J. Ko, Y. Altintas "Time domain model of plunge milling operation", International Journal of Machine Tools and Manufacture (2007), Vol. 47, 1351-1361

[105] J. Ko, Y. Altintas, "Dynamics and Stability of Plunge Milling Operations", Journal of Manufacture Science and Engineering (2007), Vol. 129, 32-40.

Appendix A: Different approaches for modeling the cutting area.

A.1. Modeling approaches

Different approaches of modeling the cutting area was studied to understand the advantages and limitations of each approach in order to be able to select the better approach suitable for the insert configuration to be used in the simulation model to evaluate the cutting area.

A.1.1. Horizontal Approach (Axial elements)

- Approach is based on dividing the insert into equal axial elements. The axial position of each element is determined based on the element index and the corresponding radial position is evaluated as a function of the insert geometry.
- The model aims to accurately determine the area cut by each insert to be used in the mechanistic model for process modeling and force prediction.
- Chip thickness is evaluated in the normal direction to the main edge as a function of the position of main edge of the present insert with respect to the main edge of previous insert as in Figure A-1
- The area cut by each insert is evaluated by calculating the width of cut at each element within the cutting zone and multiply their sum by the axial step as shown in Figure A-1. The width of cut at each element is computed by comparing the radial position of each element of the current insert with the corresponding radial position of the previous insert at the same axial level.
- Linear interpolation is used to ensure that width of cut for each element is calculated at the same axial level of the previous element regardless on the number of elements used. This explains the sensitivity of this approach to the vibration in lateral and axial directions and its effect on force prediction.

- Very efficient for modeling the insert profile for cases with entering angle where the insert geometry can be described as a function of its elevation which has a constant increasing trend, same as the index of each element. This fact facilitates the modeling of the side edge and hence, considers and studies its contribution in the cutting.

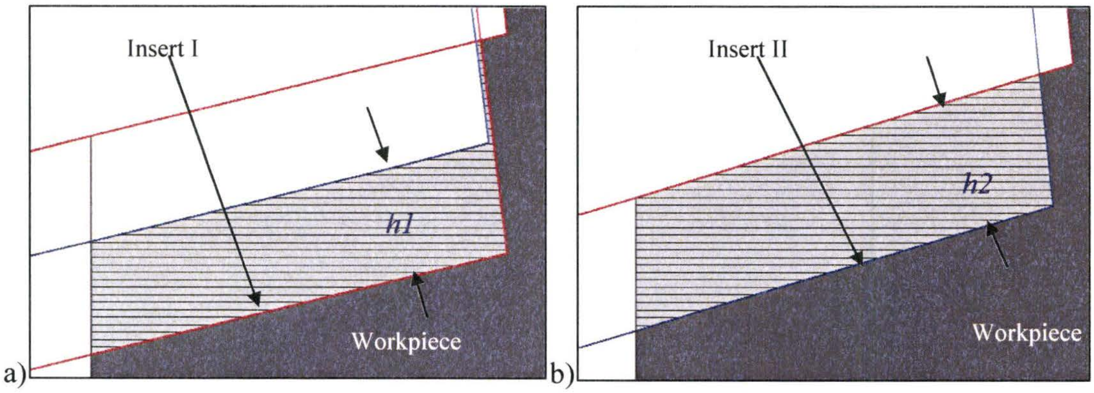

Figure A-1 - Modeled area using Horizontal approach for a) Insert I and b) Insert II

A.1.2. Vertical Approach (Radial elements)

- Approach based on dividing the inserts into equal radial elements. The radial position of each element is determined based on the element index and the corresponding axial position is evaluated as a function of the insert geometry.
- Chip thickness is evaluated in the normal direction to the main edge as a function of the position of main edge of the present insert with respect to the main edge of previous insert.
- The area is predicted by computing the height of each radial element by comparing the axial position of each element of the current insert to the corresponding elevation of the previous insert at the same radial position as shown in Figure A-2. The sum of elements height is then multiplied by the element width to compute the area cut by each insert.
- The contribution of side edge in cutting is not considered in this approach. This is attributed to the fact that the insert profile is modeled as a function of its radial

position which increases for the main edge and decreases for the side edge as opposite to the element index. This is explained by the fact that for case of radial runout, at some point, the area is determined by the main and the side edge of the present insert using the vertical approach. However, this seems to be difficult because the evaluation of chip thickness at a radial element of the main edge requires knowing the axial position of the corresponding element of the side edge of the same insert which is of a higher index. Therefore, the element height is computed with respect to the main edge of the same insert at previous revolutions which was previously determined. This leads to an over prediction of the chip area and hence, higher predicted cutting forces.

- Very efficient for modeling the insert profile for inserts with zero entering angle as the side edge is not involved into cutting in this case.
- For cases of inserts with entering angle, limited ability to accurately model the area removed by each insert due to over prediction of area cut by the main edge and not modeling the actual area cut by the side edge as shown in Figure A-3. This will affect the prediction of chip load and hence the cutting forces used to model the dynamics of the process.
- For cases with entering angle, the area predicted is sensitive to the number of elements as shown in Figure A-3 . Better results are achieved with higher number of elements which leads to a longer running time.

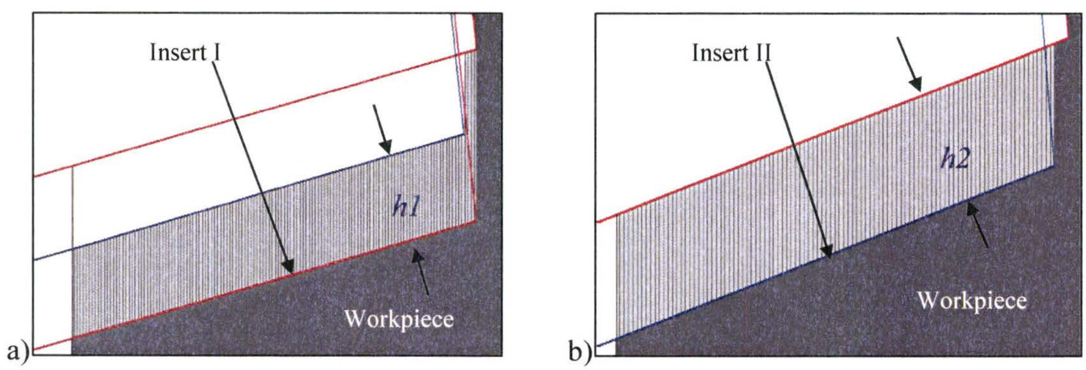

Figure A-2 - Predicted area using Vertical approach for a) Insert I and b) Insert II

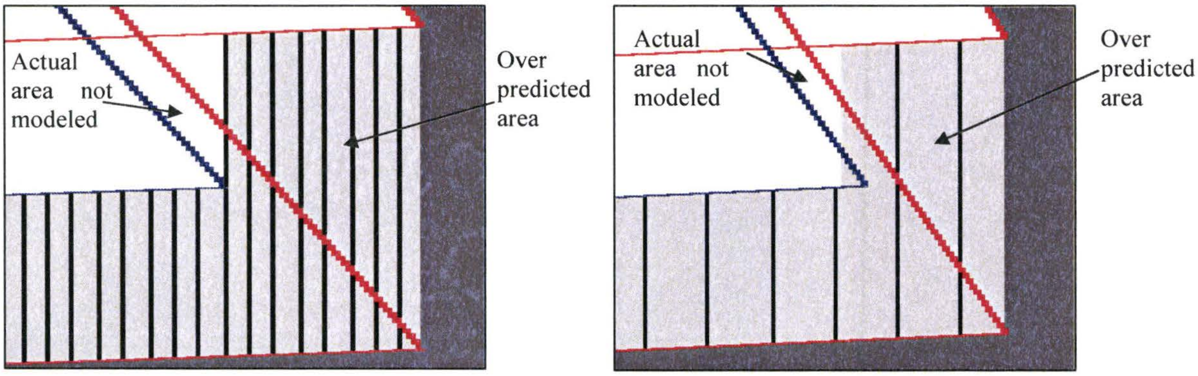

Figure A-3 - Effect of number of elements on the predicted area using vertical approach

A.1.3. Vertical/Horizontal elements

- The approach is based on combining both the vertical and the horizontal approaches to model the insert. The main edge is modeled using the vertical approach by means of radial elements, while the side edge is modeled using the horizontal approach by means of axial element.
- This approach shows better prediction of the area cut by each insert and hence, better predictions of cutting forces compared to the vertical approach.
- Chip thickness is evaluated in the normal direction to the main edge as a function of the position of main edge of the present insert with respect to the main edge of previous insert as in Figure A-4
- The area cut by each insert is divided into area cut by the main edge (area 1 in Figure A-4) and area cut by the side edge (area 2 in Figure A-4)
- Number of elements, both radial and axial, should be selected carefully to avoid any problem related to the transition from radial elements to axial elements at the insert edge (i.e. interface between area 1 and area 2).
- However, longer running time is needed as compared to the vertical and horizontal approaches.

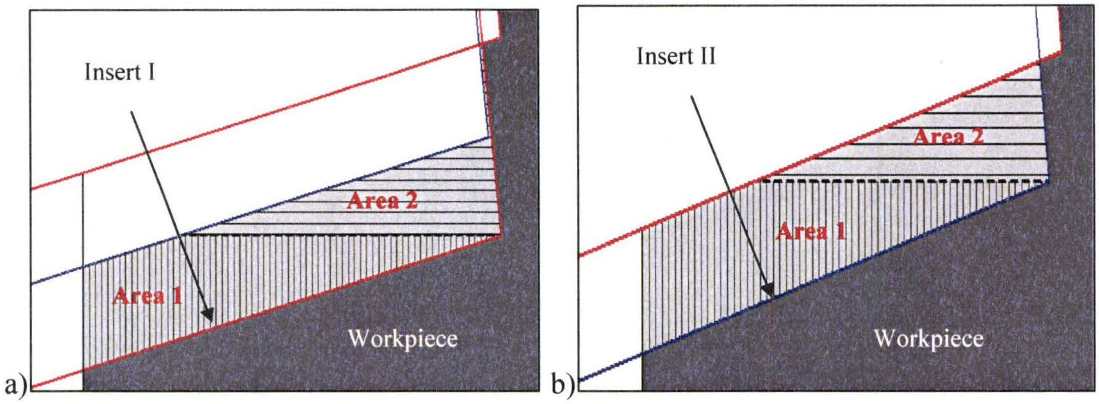

Figure A-4 - Modeled area using Vertical/Horizontal approach for a) Insert I and b) Insert II

A comparison between the studied approaches with respect to the prediction of cutting forces and cutting area can be shown in Figure A-5 and Figure A-6 for two cutting conditions.

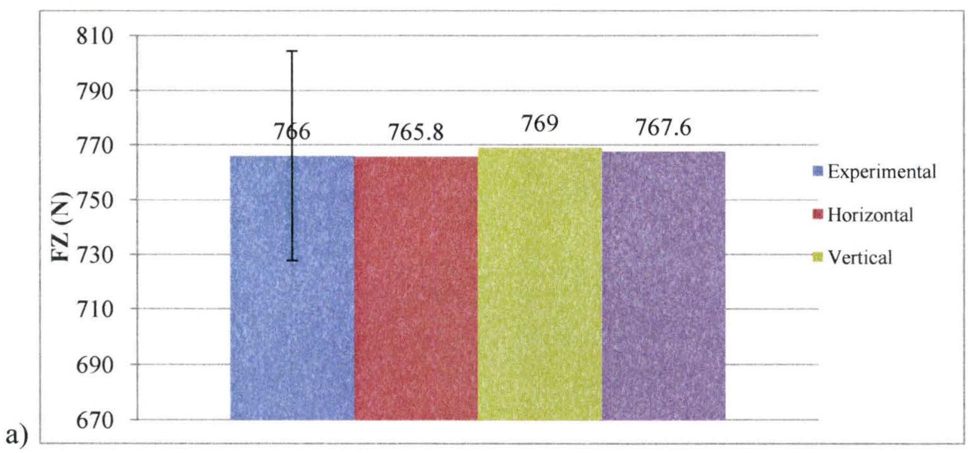

b) 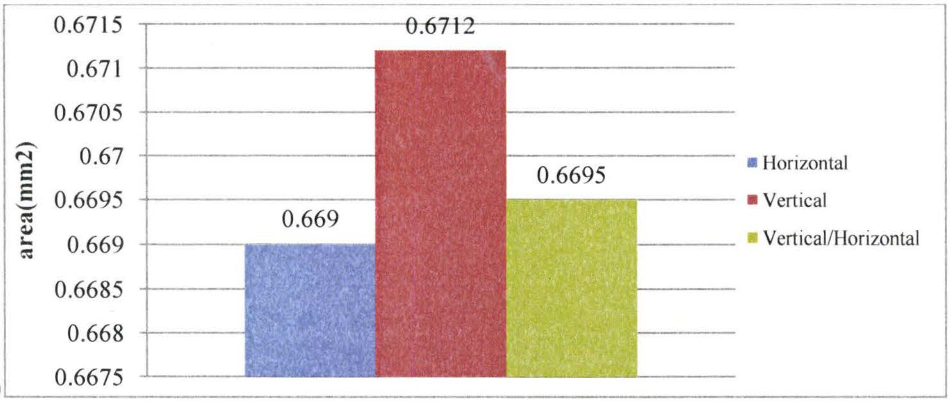

Figure A-5 - Predicted value of a) axial force and b) area at 12750 rpm, f=0.081mm/tooth and 7.5 mm width of cut.

a) 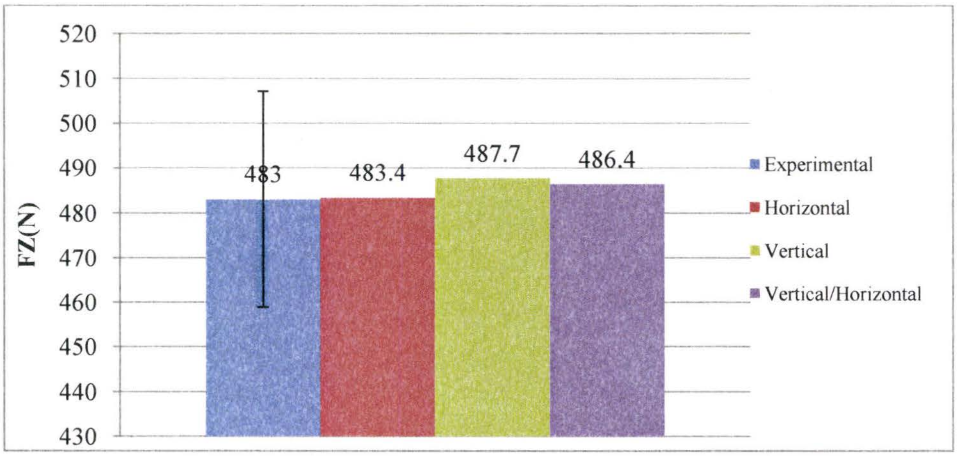

b) 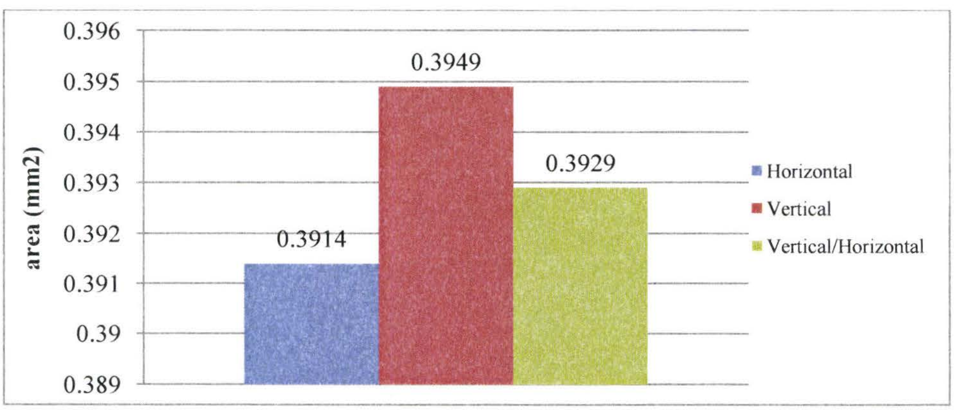

Figure A-6 - Predicted value of a) axial force and b) area at 14750 rpm, f=0.07mm/tooth and 5 mm width of cut

It can be noticed from the force and area prediction by each approach, that the vertical approach is not recommended for modeling inserts with entering angle as explained previously. This is mainly due to the over prediction of the area cut by each insert which leads to higher level of predicted axial force. The effect of over prediction of area increases with the decrease of width of cut due to the fact that the over predicted area presents a higher percentage of the total area as the width of cut decreases. However, the differences between the predicted and measured cutting forces are not big for the three approaches with the results from the horizontal approach are closer to the measured data. The sensitivity of the studied approaches to system vibration in lateral and axial directions was studied for systems with rigid workpiece, Figure A-7 as well as for system with flexible workpiece in Figure A-8. This aims to check the ability of each approach to correctly predict the cutting forces as well as to sense the system vibration in lateral and axial directions.

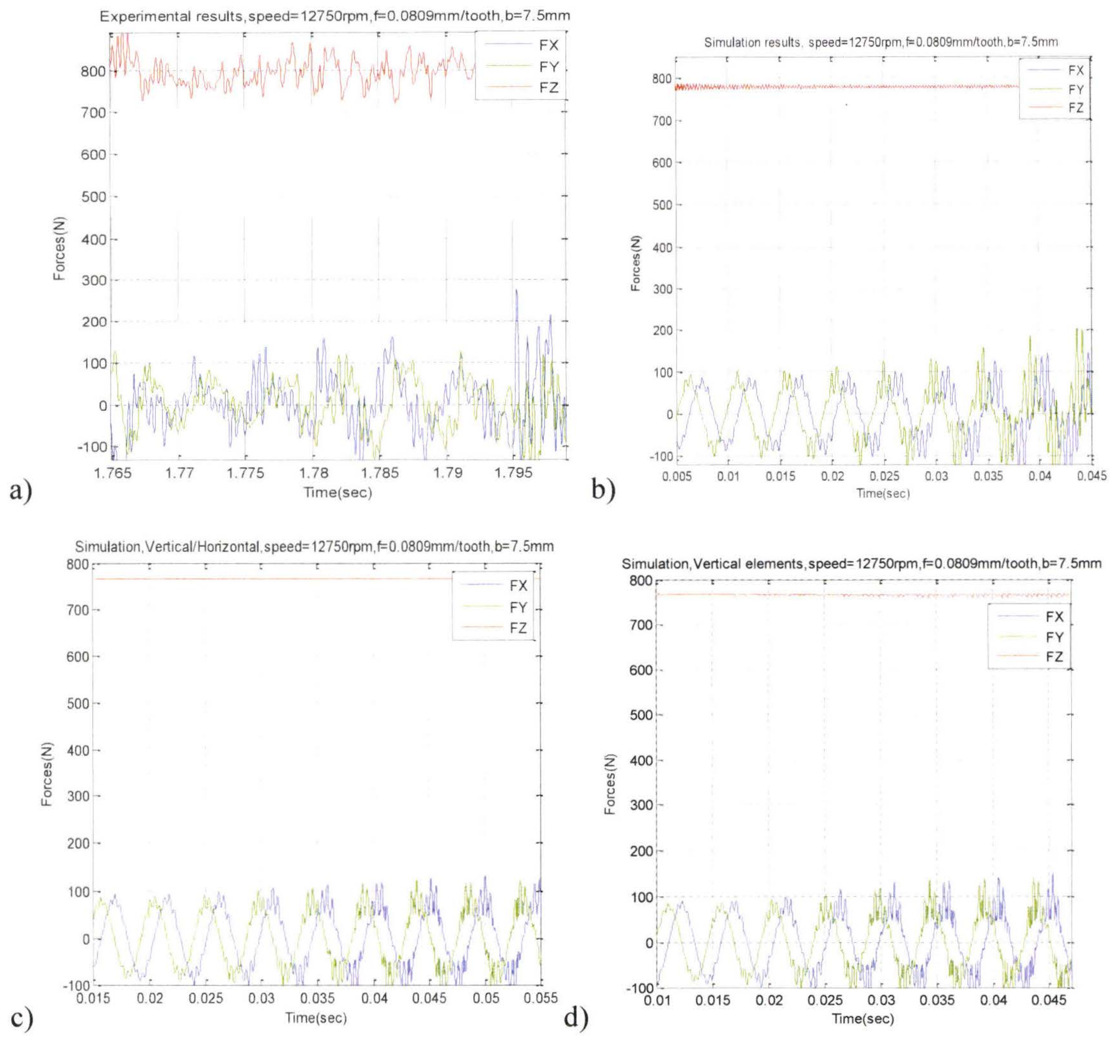

Figure A-7 – a) Measured and predicted cutting forces using b)Horizontal, c)Vertical/horizontal, d)Vertical elements for plunge milling at 12750 rpm, f=0.0809mm/tooth, b=7.5mm (rigid workpiece)

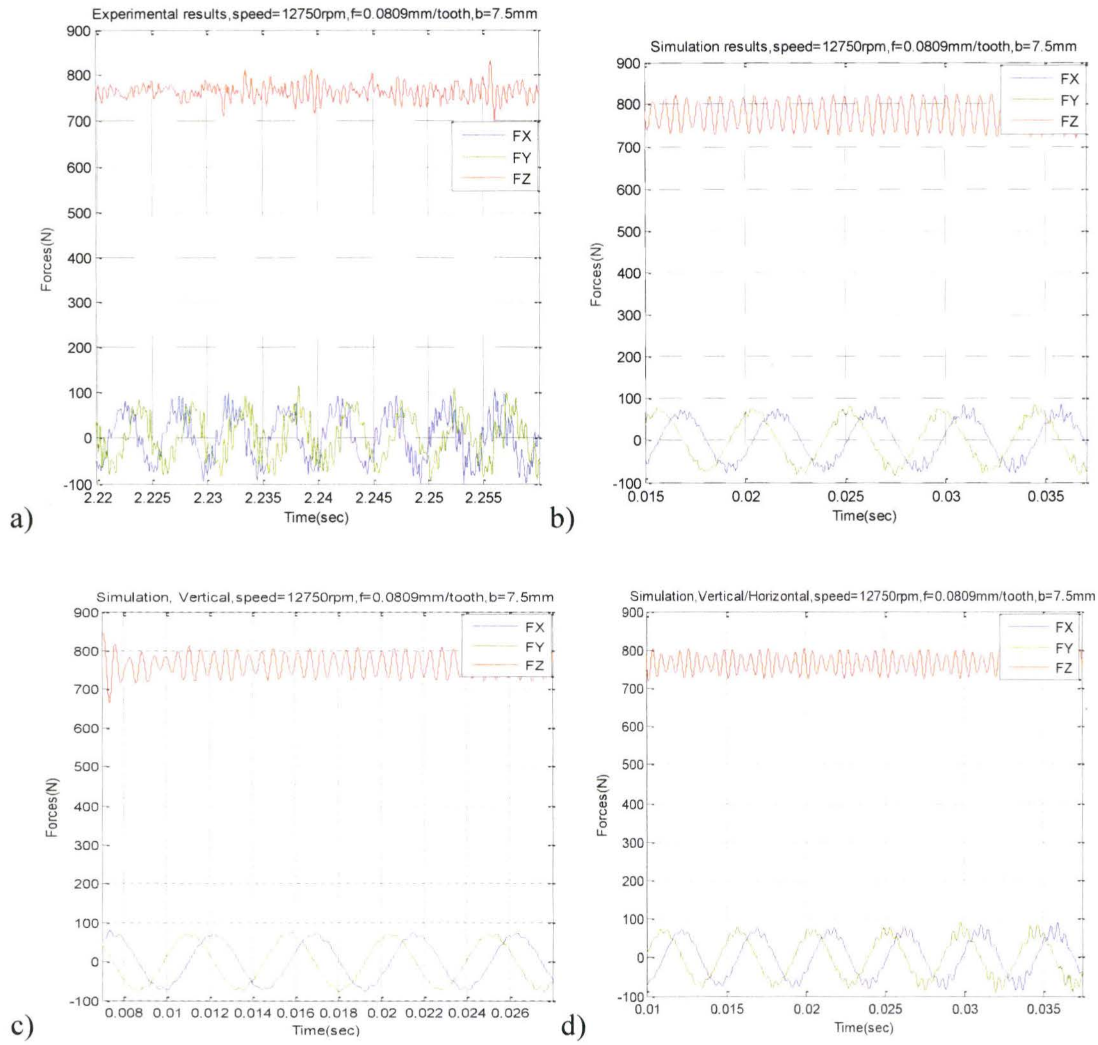

Figure A-8 – a) Measured and predicted cutting forces using b)Horizontal, c)Vertical, d)Vertical/horizontal elements for plunge milling at 12750 rpm, f=0.0809mm/tooth, b=7.5mm (Flexible workpiece)

It can be noticed that all the three approaches (Horizontal, Vertical and Vertical/horizontal) shows good agreement with the trend and magnitude measured cutting forces for both stable and unstable cutting for cases of rigid and flexible workpiece with the horizontal approach showing better results. The three approaches were found to be sensitive to lateral and axial vibration of the cutting system (i.e. tool and workpiece) as shown by the variation of lateral and axial forces in response to corresponding system vibrations. The horizontal approach was shown to be more sensitive to lateral and axial vibrations more than the other two approaches as illustrated in case of rigid and flexible workpiece. Table A-1 summarizes the advantages and limitations of each approach.

Table A-1 Advantages and limitations of approaches used for area modeling.

	Horizontal	*Vertical*	*Vertical/Horizontal*
Illustration	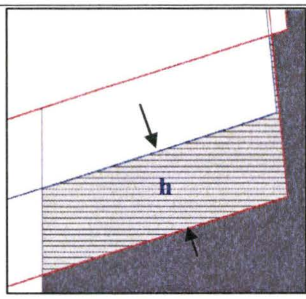	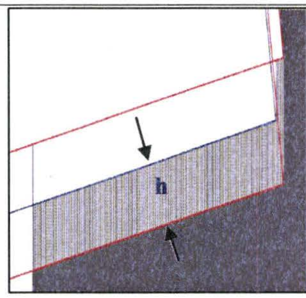	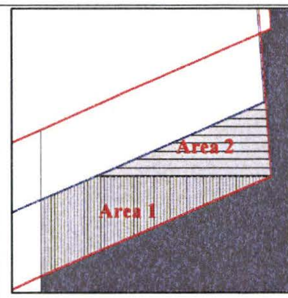
Concept	• Both main and side edges are divided in axial elements. • Area cut by each insert is evaluated as the area enclosed between the main and side edges of present insert and the main and side edges of the previous insert. • Chip thickness is evaluated in the normal direction to the main edge as a	• Insert is modeled by dividing the main edge into radial element. • Area cut is evaluated as the area enclosed between the main edge of the present insert and the main edge of the previous insert. No effect of side edge is considered. • Chip thickness is evaluated in the	• Combine both the vertical and horizontal approaches. • Main edge is modeled using radial elements while the side edge is divided by axial elements. • Chip thickness is evaluated in the normal direction to the main edge as a function of the position of

	function of the position of main edge of the present insert with respect to the main edge of previous insert.	normal direction to the main edge as a function of the position of main edge of the present insert with respect to the main edge of previous insert.	main edge of the present insert with respect to the main edge of previous insert.
Comments	• Efficient in modeling inserts with entering angle as well as it can be used for inserts with zero entering angle. • Consider the contribution of main and side edges in cutting. • Can be used to predict surface profile. • Interpolation is used to minimize effect of number of elements on area and force prediction. • Running time is similar to vertical	• Efficient in modeling inserts with zero entering angle. • Inaccurate prediction of the area cut by each insert, which leads to higher predicted cutting forces can limit its use for inserts with entering angle. • The contribution of side edge in cutting is not considered. • Area prediction is sensitive to the number of radial elements. • Cannot be used to	• Efficient in modeling inserts with entering angle. • Consider the contribution of both main and side edges in cutting. • Can be used to predict surface profile. • Problem may occur in modeling the transition between radial and axial elements. • Longer running time as compared to vertical and horizontal approach.

	approach • Sensitive to lateral and axial vibrations of the tool and the workpiece. • Shows better sensitivity to lateral vibration as compared to other approaches. • Shows good agreement with experimental results.	predict surface roughness. • Running time is similar to Horizontal approach. • Sensitive to lateral and axial vibrations of the tool and the workpiece. • Shows good agreement with experimental results.	• Sensitive to lateral and axial vibrations of the tool and the workpiece. • Shows good agreement with experimental results.

Based on the study of different approaches which can be used to model the geometry of the insert to evaluate the dynamic chip area and chip thickness used in force prediction, the horizontal approach is used in the proposed simulation model. This is mainly due to the efficiency of the selected approach to model inserts with entering angle, which is the case of the inserts used in experiments, as well as its reasonable running time and agreement with experimental results. Additionally, the horizontal approach is easier to be in modeling inserts of any geometrically defined shape (e.g. circular edge).